بسم الله الرحمن الرحيم

Sudan University of Science and Technology

College of Graduate Studies

A COMPARATIVE STUDY BETWEEN WATER SATURATION MODELS in RESERVOIR EVALUATION FROM HEGLIG OIL FIELD, MUGLAD BASIN, SUDAN

دراسة مقارنة بين نماذج تشبع المياه فى تقييم المكمن لحقل هجليج النفطى

حوض المجلد - السودان

A thesis Submitted in Fulfillment for the Requirements

of PhD degree in Petroleum Geology

By:

Awad Karamalla Gaiballa

(M.Sc. Geology, Juba University, 2003)

Supervisor:

Prof. Rashid Ahmed Mohammed Hussien

Co – Supervisor:

Dr. Mohammed Zayed Awad

February 2017

Declaration

I declare that this thesis is a presentation of my original research work. Whenever contributions of others are involved, every effort is made to indicate this clearly, with due reference to the literature, and acknowledgment of collaborative research and discussions.

This work was done under the guidance of Prof. Rashid Ahmed Mohammed Hussein, and Dr. Mohammed Zayed Awad.

Awad Karamalla Gaiballa

الآيـــــــــــة

بسم الله الرحمن الرحيم

(وَسَخَّرَ لَكُم مَّا فِي السَّمَاوَاتِ وَمَا فِي الْأَرْضِ جَمِيعًا مِّنْهُ ۚ إِنَّ فِي ذَٰلِكَ لَآيَاتٍ لِّقَوْمٍ يَتَفَكَّرُونَ) [الجاثية:13]

Dedication

This thesis is dedicated to my deceased father and to my mother and my wife Hanan who supported me throughout this way

Acknowledgements

I would like to gratefully acknowledge the supervision of Prof. Rashid Ahmed Mohammed Hussein, for his advice and help to achieve my goal, and for his observation and comments which helped me to pursue the right trend of this research. Iam thank to Dr. Mohammed Zayed for his continuous help and heavy work in this study.

My thank extend to Mr. Mohammed Hammed, Mr. Ibrahim Ahmed, Mr. Ibrahim Kamel, Mr. Kamel Idris, and Mr. Mohamed Abdelgader for their support I received during this study.

My thank also extended to my deceased father and my wife for their moral support throughout this study.

Special thank, go to Mr. Mohmmed Alameen for his help in the preparation of the data and his useful directioning.

Table of content

LIST OF FIGURES

LIST OF TABLES

Abstract

The Muglad Basin is a large rift basin located in south Sudan. This basin is characterized by sedimentary section of non-marine clastic sequences of Jurassic (?)-Cretaceous and Tertiary age.

A high numbered of drilled wells and geophysical work is located in this basin, where the most significant oil discoveries, Unity and Heglig filed. This study has been carried out in Heglig Field.

This study explains the values of formation evaluation on Heglig Field, and explains its important in reserve estimation of oil in this area.

Petrophysical interpretations have been done on the previous log data of selected productive wells drilled in the study area, focusing on Bentiu Formation. From interpretations, reservoir properties such as porosity, permeability and water saturation have been determined.

Archie, Indonesian, Dual water, and Simandoux equations were used to calculate water saturation, which influence oil reserve estimation.

Comparisons between the values of water saturations have been done. Different models illustrate those differences. The comparison shows differences in oil content found in the same formation and shows that Dual water equation for water

saturation calculation is the best equation to be used in shaly-sand oil bearing formation as Bentiu Formation in this study filed.

الملخص

يمثل حوض المجلد اكبر حوض إخدودى يقع فى جنوب غرب السودان، حيث يتميز بروسوبيات غير بحرية تكونت منذ نهاية العصر الجيوراسى الى العصر الثالث . هنالك نسبة عالية من الأبار التى تم حفرها فى هذا الحوض لأن اهم الاكتشافات النفطية تم اكتشافها فى حقلى هجليج و الوحدة ، الا ان هذه الدراسة قد تمت فى حقل هجليج فقط.

ان الهدف الاساسى لهذه الدراسة هو توضيح قيمة التقييم التكوينى لحوض هجليج وتوضيح اهميته فى تقدير احتياطى البترول فى منطقة الدراسة. لذا فى هذا البحث تم اجراء تفسير للخواص الفيزيائية لسجلات أبار منتجة تم اختيارها من ضمن ابار حفرت فى هذه المنطقة مع التركيز على تكوين بانتيو, ومن هذا التفسير فإن خواص الخزان مثل المسامية, والنفاذية, ودرجة التشبع المائى, قد تم تقديرها.

أن معادلات أرشى, واندونسيان, ودول ووتر, وسموناكس, والتى تستخدم فى تقدير درجة التشبع المائى قد تم استخدامها لايجاد مقدار التشبع المائى حيث ان هذا التشبع المائى يؤثر على تحديد كمية احتياطى البترول

لقد تم اجراء مقارنات بين مقادير التشبع المائى التى تم حسابها بواسطة هذه النماذج المختلفة, حيث اظهرت هذه المقارنات اختلافا فى كمية البترول المحسوب فى التكوين الواحد, كما اظهرت بان معادلة دول ووتر هى المعادلة الانسب للإستخدام فى التكوين الطينى الرملى المحمل بالبترول مثل تكوين بانتيو الواقع فى الحوض المدروس.

Chapter I

Introduction

1-1. Location:

The study area is located in Southern Kordofan State, Muglad basin. It is between longitude 29 20' - 29 30' and latitudes 9^{o} $45^{'}$ - 10^{o} $5^{'}$, and it is cover an area of approximately 500 km^{2}. Figure (1).

1-2. Objectives of the study:

The objectives of this study are:

1-2-1. To maximize the understanding of oil bearing formation in Heglig field.

1-2-2. To calculate the porosity, permeability, and water saturation.

1-2-3. To correlate between the different values of water saturation of different equations and their influence in oil reserve estimation in the same field.

1-3. Methodology:

Using well log data in Heglig field belong to Greater Nile Company, these data analyzed in workstation by GeoFrame software (IESX) at College of Petroleum Engineering & Technology, Sudan University of Science and Technology, and models from Archie, Indonesian, Dual water, and Simandoux

equations in interpretation of these logs in this field focusing on Bentiu Formation.

Therefore; the materials used as follows:

1- Four wells data set including well logs and well reports are available.

2- Interpretation of wells data

3- Comparison between four wells logs

4- Application data of geological and structural information collected from various studies of the sedimentary basins in south of Sudan, which were done by companies working in the oil fields, such as Chevron, Greater Nile, and Petrodar who drilled several wells on those basins, Muglad and Melut basins.

All these data and information were integrated with each other to attain the desired objectives.

1-3-1. the present data

Well reports and log data have been obtained from the petroleum data centre (PDC) of Oil Exploration and production Authority (OEPA), Ministry of Energy& Mining, Sudanese Petroleum Corporation. The studies have been done by Chevron Company and Greater Nile Company.

Well data from wells drilled in the study area, part of them are hard copies and the others are soft copies. These wells locations cover most of the study area.

1-4. Physiography

1-4-1. Topography

Most of the study area is covered by alluvial plain deposit, overlain the Mesozoic sedimentary deposits. This area has low elevations comparing to the surrounding area, and consists mostly of black cotton soil cover, with fan delta of gravels, sands, silts, and small areas of laterite deposits.

The high area is located north-east, showing elevation varies from 500-600 m; where as other areas reach more than 1000 m in elevations, near the Nuba Mountains. In the south of the study area the high areas represented by few mountains of, approximately, 700m high along Sudan, central African borders.

The study area is dipping south east direction, therefore; most of the drainages flow from the north to the south direction towards Bahr El Arab River, which drains towards the White Nile River.

1.4.2 Climate

The area lies in the rich Savanna climatic region with rainfall ranging from 800 mm to 1000 mm. The wet season

generally starts in late April and lasts until October. There is considerable variation from year to year in the start and end of the rain fall. The average temperature reaches approximately 40 C^{o} at the hottest months in May and September. In winter from December to March the temperature reaches 25 C^{o}.

1-4-3. Vegetation

The vegetation covers are composed of dominant shrub savanna with scattered acacias trees, where the woody lands increase towards the south direction.

1-4-4. Population

The density of population in the study area is moderate, and influenced by the migration from villages to towns, during the last years.

The northern part of this area was inhabited by Meseria tribe which is scattered throughout the area. Most of these tribes are cattle herder, and live as nomadic tribes. The tribe moves from north to the south towards Bahr Elarab area, during the dry months, for water and grass.

In the south Sudan south the study area live the Nelotic tribes Dinka, Shulalk and Nower. They are depend on the cattle herding, and on fishing, they migrate north towards the Sudan during heavy rainy season.

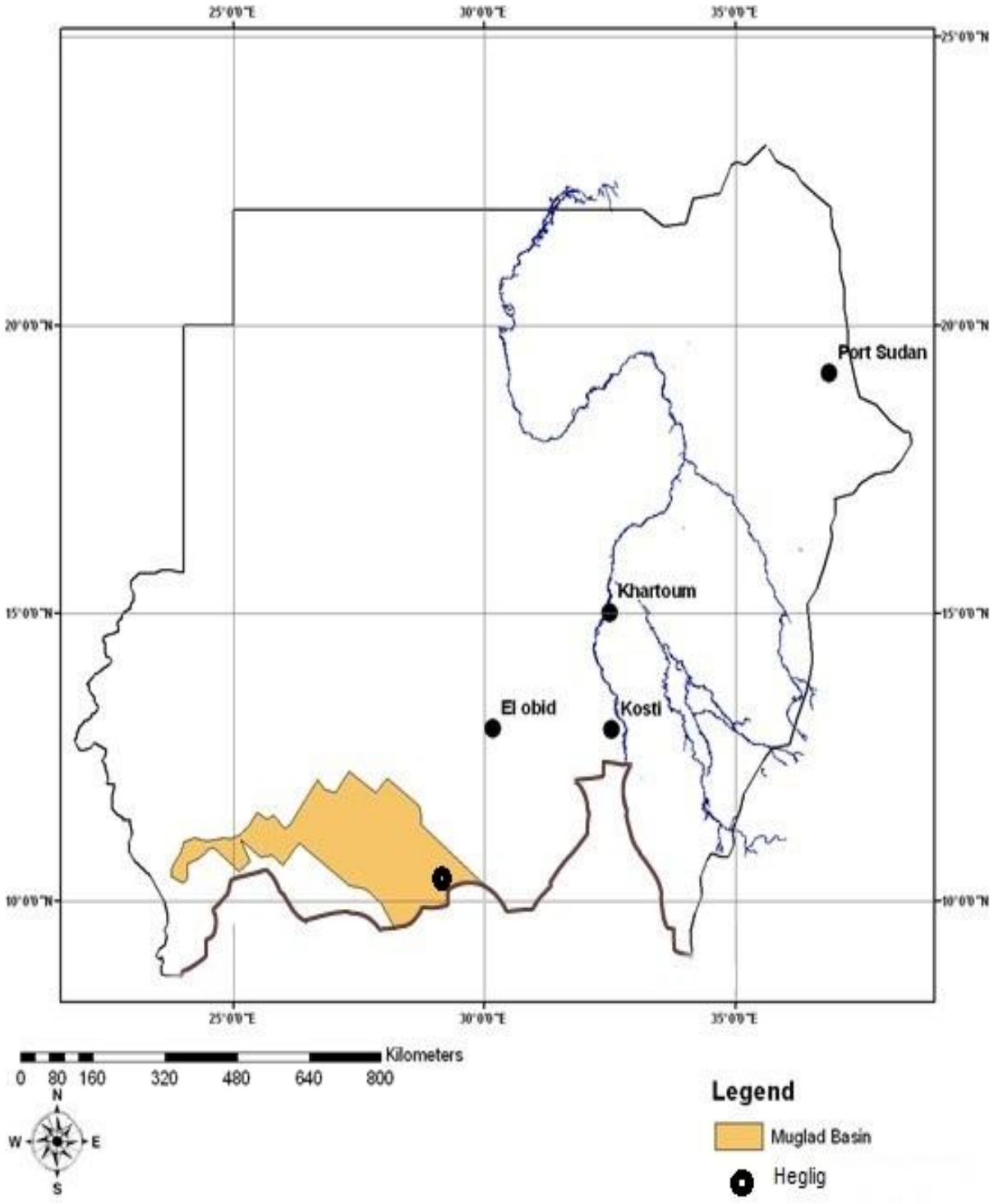

Fig (1) Location Map

1-5. Pervious work

The first work in the surrounding area was on the basement rocks. This work focused on exploration of mineral deposits. The area under study was visited through frequent tours to examine the outcrops in the northern and eastern parts. Russegger (1838), studied Nuba Mountain, and Hofrat el Nahas area.

A photogeological study and mineral exploration study carried out in the study area and its neighborhoods areas, by Andrew. & Yanni. (1945), and Hunting Geology and Geophysics (1969), & Hunting (1980).

Vail (1970,1971,1973,1974), and Whiteman (1971) produced an outline of the geology of the surrounding area and the Nuba Mountain, which included a geological map of major rock types and some structural information. Vail (1978) published his 1:2,000,000 geological map of the Sudan which shows a series of the Basement Complex Formations.

Curtis and Brinlemann (1985) carryout a reconnaissance trips in order to map, and analyze igneous rocks east of the study area.

Sadig and Vail (1985) constructed a geological sketch map using gravity traverses. Brown et al (1985), Jorgenson and

Bosworth (1989) carried out gravity studies about White Nile Rift and Central African Rift.

A geological study of Sandstones deposits in Sudan, and adjacent areas, was done by Sanford (1935), and Bead Nell (1909). Geophysical investigation of ground water in the central and northern of Upper Nile Province southeast of the area has been done by Strojexport works (1977), who described sandstone as detrital sediments derived from the erosion of basement rocks of Cretaceous age, and unconformable Cambrian -Precambrian basement complex.

Other works on basins sediments, Khartoum Basin, Kosti Basin, EL Gadaref Basin, were carried by Kherialla (1966), Omer (1975, 1983), Omer and Priaux (1976), Chialvo (1975), Moawia (1983), Barazi (1985), Abdel Salam (1966).

Studies in the area N-E Kordofan Province, and facies interpretation, and stratigraphy of the central Darfur, and stratigraphic and tectonic signature of late Craterous of Bagbag Basin sediment, were carried out by Khattab (1975), and distribution of the Kordofan sand by Edmonds (1942). Studies of palynostratigraphy and palynofacies of non-marine sediment in Blue Nile rift basin, has been carried out by Awad and Schrank (1992). Also stratigraphic works in Gezira area, carried out by Awad and Breir (1993).

A paleoecolgy studies of late Jurassic to mid Cretaceous of central and western Sudan, was carried out by Awad (1994). Also, a geological and petroleum potential studies of southern, central and eastern Sudan have been done by RRI (1991).

Studies of stratigraphic updated of the non-marine Cretaceous sediments, and facies of shallow marine sequences in NW Sudan, were carried by Klitzsch (a) &(b) (1984), Klitzsch and Lejal-Nicol (1984), Klitzsch and Wycisk (1987), Wycisk (1987), Schrank (1987b), Schrank (1990).

A Palynology and micro fossils studies in the Sudan basins have been carried out by Hassan (1973) and Awad (1987, 1994).

The works of regional tectonics and sedimentation related to the rift basin in western and eastern Africa was carried out by Fairhead (1986), Schandelmeir et al. (1987), Schandelmeir (1988), and Schull (1988). Bosworth and Marley (1994), El Shafie (1980), Birmingham et al. (1983).

A sedimentological works on White Nile, and Melut Rift Basin have been carried out by Ahmed (1983), and depositional models of Mugld Basin carried out by Ahmed (1993 & 1996), Abdullatif (1992), Bakr (1995), El Tayib (1993), Mohammed (1997), and Hussien (1997).

Geophysical, sedimentological and tectonic stratigraphic studies on Muglad basin have been carried out by Elamin (1993), Salama (1997), Amir (2000), and Idriss (2001), and study on reservoir geology of Omdurman formation carried out by Elamin (2001).

Studies of geochemical analyses of hydrocarbon in the Muglad basin, (unpublished) carried out by Mohamed (1996), and Mohamed et al, (1999), which in these works models of petroleum generation have been constructed.

Works on interpretation of shaly-sand log data have been done by Worthington (1985), Worthington and Johnston (1991), Silva and Bassiouni (1985), Silva and Bassiouni (1987), Smits (1968), Thomas (1976), Lau and Bassiouni (a) & (b) (1990), Hamada (1996), Poupon et al (1970,1971), Fertl and Hammack (1971), Gadallah (1994), and a comparison of shaly sand models has been done by Bussian (1984).

Study by Kurniawan (2002), on field in Indonesia on reservoir formation which is characterized by shaly sand and low salinity formation water.

Other study in log interpretation done by Crain et.al (2000), who analyzed log data of 150 wells in the Western flank Reservoirs of shore in Lake Maracaibo. They developed

technique to determine accurate values of porosity, permeability and water saturation, from old logs. A depositional environment of complicated sequence of superimposed fluvial channels, in this area, where these wells drilled, in which a quantitative reservoir description for all these well had been done by calculation with traditional log analysis methods and from which a highly detailed reservoir properties were calculated.

Chapter 2

Geological Setting of the Study Area

2-1.General geology.

2-1-1. Introduction.

Muglad basin is a large rift basin located in south Sudan. (Fig 2). It is bordered largely by basement rocks in the North West and South West sides.

The Nubian Sandstone crops out near the northern edge of the Muglad basin, but most of the study area is covered by surficial deposit of sands, silts, clays, black cotton soil, and latritic soil.

2-1-2.basement rocks

The Basement Rocks adjacent to the Muglad basin are predominantly Precambrian and Cambrian metamorphic rocks with limited occurrences of intrusive igneous rocks. The rock types are granitic gneiss, and granodioritic gneiss, which overlain by quartzite of Paleozoic age.

The oldest sedimentary rocks are non-marine of lower Jurassic salt, and siltstones. Figure (3).

2-1-3. Nubian sandstone

This type of rocks cover most of the Sudan and confined to the northern part except the isolated outliers in the eastern of the Sudan

This type of rocks outcrops North-East and North of the area of Heglig filed. It is composed of undifferentiated fluviatile sandstone, siltstone, and minor conglomerates of Cretaceous age. These sediments have been deposited by currents flowing generally towards North direction, (Amir, 2000).

2-1-4. lateritic deposits

The lateritic soil in Sudan covers most of the southern region, and South Sudan North of Juba Town. It is composed of thick and extensive sandy soils outcrops, (Vail, 1978).

The lateritic deposits are yellow to reddish brown or black in colour, spongy and more massive hydrated iron oxides with scattered silicate grains, and big angular rock fragments. (Vail, 1978).

In the study area these deposits cover the area between Heglig and Lake Keilak 90 km North of Heglig. Their thickness varies from few centimeters to more than 30 meters. It was deposited by seasonal streams of water rich in iron, and alluvial

minerals. It is occur as massive beds, and it is often show oolitic and pisolitic texture, (Idriss, 2001).

2-1-5. Superficial Deposits (recent deposits)

2-1-5-1. Wind Deposits

The superficial deposits in the study area are composed of wind-blown sands. It is composed of small, rounded grains of quartz, usually well sorted, and may be mixed with lighter fraction of dust, mica flakes, feldspar fragments and clay. The top layers of the older deposit, (qoz) are reddened by iron stains, and they are white or grey in colour. It is vary in thickness, and it is reach up to 50 meter thick.

These sands originated from the underlying bed rocks, and the rework of products of fluvial process from previously wetter climatic period, (Vail 1978).

In Kordofan Province found north of the study area, these sand dunes are referred to as Goz.

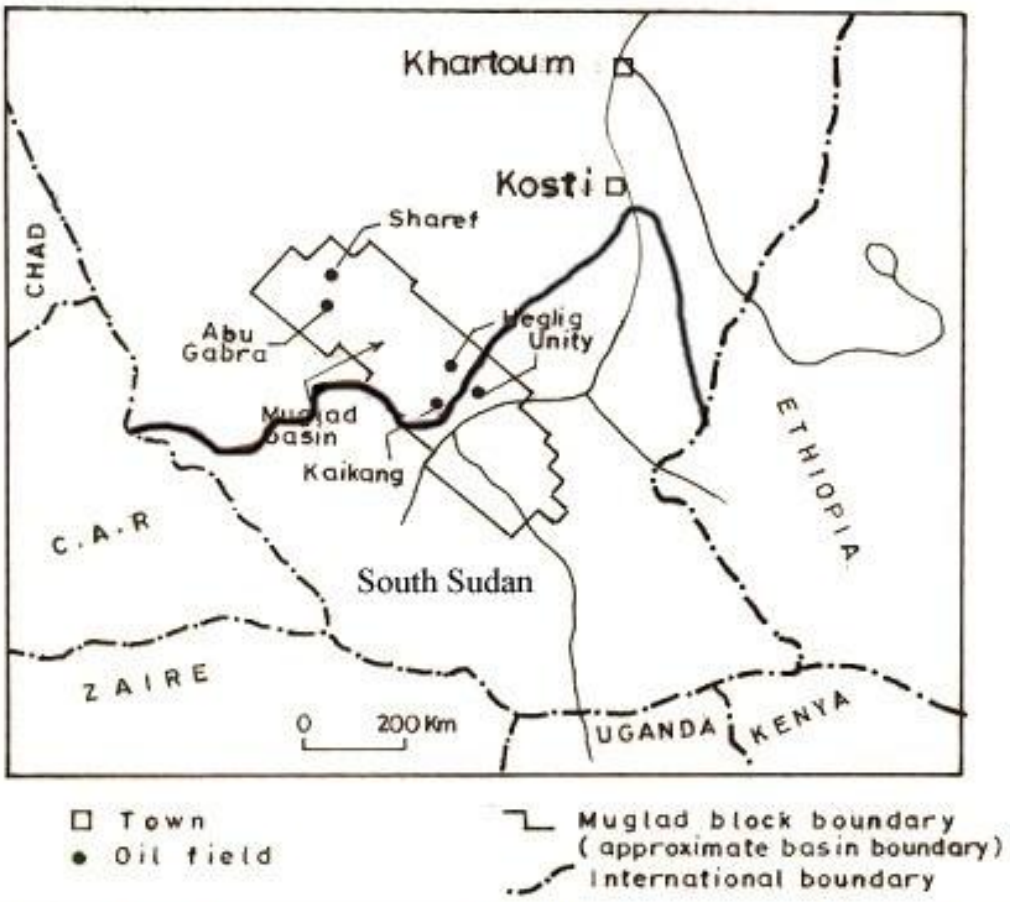

Figure (2) Map of Sudan & South-Sudan shows Muglad Basin boundry (Mohamed et al, 1999)

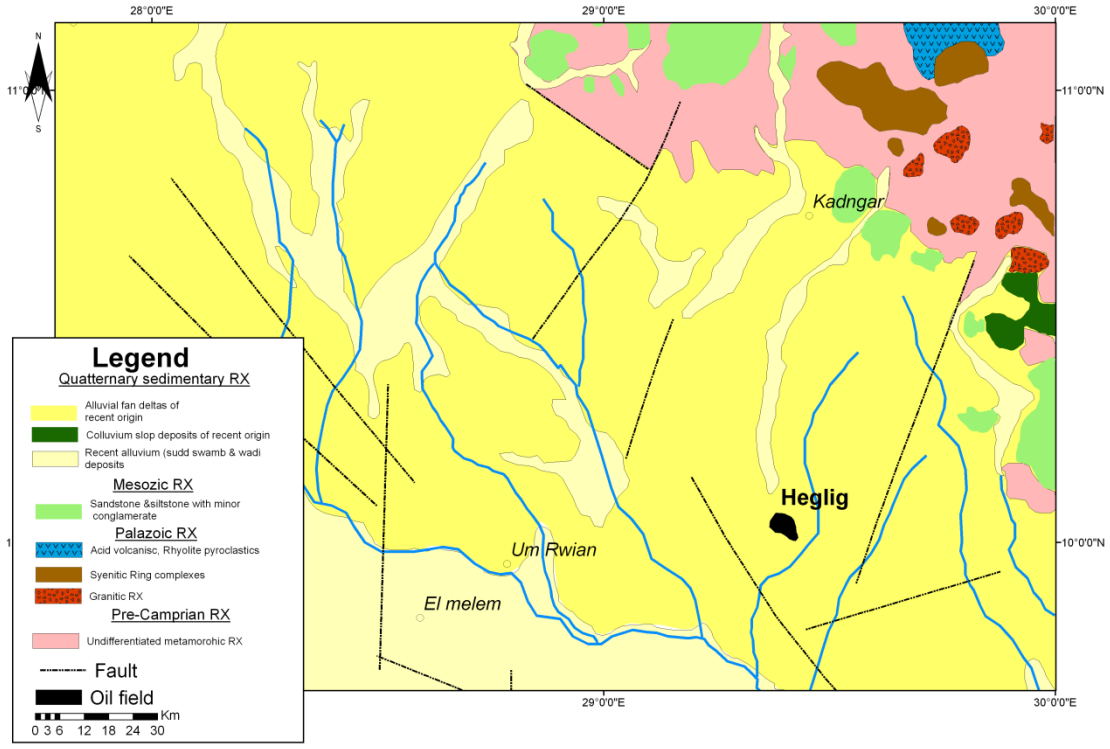

Figure (3) Geological map of the studies and adjacent area (GRAS & RRI, 1995)

2-1-5-2. alluvial deposits

Alluvial deposits are mainly confined to stream beds and flood plains. Many of the smaller river systems have well developed alluvial deposits, and some of the large rivers especially those draining from well watered interiors have developed large delta fans on the plains.

Alluvial is composed of sand constituents, gravel and humus–rich deposits.

In the study area alluvial deposits are confined to drainage system, streams and wadies. They consist of loams, clays, and fine grained sands and other coarse-grained sands. Those deposits covered mostly by this alluvial deposit. At the South direction, at Bahr El Arab flood plain and at the west direction include fan deposit of Khor Wirral, and alluvial deposit along Khor Shellengo in the east direction, at Khor Kir, (Figure, 3).

2-1-5-3. Residual Deposits

Weathering products have been found in the study area at the foot hills of the Nuba Mountains north of the study area. They consist of rock fragments and wash out deposits these fragment of angular and rounded shapes, they are the product of igneous and metamorphic rocks.

2-2. Muglad stratigraphy

2-2-1. Introduction

The knowledge of the stratigraphy of this basin is limited to well control and the inferences made from the seismic data; therefore, the depositional environments were determined by integrating data from wells, seismic data and basin geometry. This integration reflects the geology of the Muglad basin, and the generalized stratigraphic column. (Fig 4).

2-2-2. Precambrian-Jurassic Rocks

The basement has been penetrated and cored in some wells. At these locations rock of granitic or granodioritic gneiss has been recorded. The oldest sedimentary rocks have been penetrated are nonmarine Jurassic (?) salts, siltstone, and claystones. Quartzite of unknown age overlying gneissic basement has been penetrated in one well. (Schull, 1988).

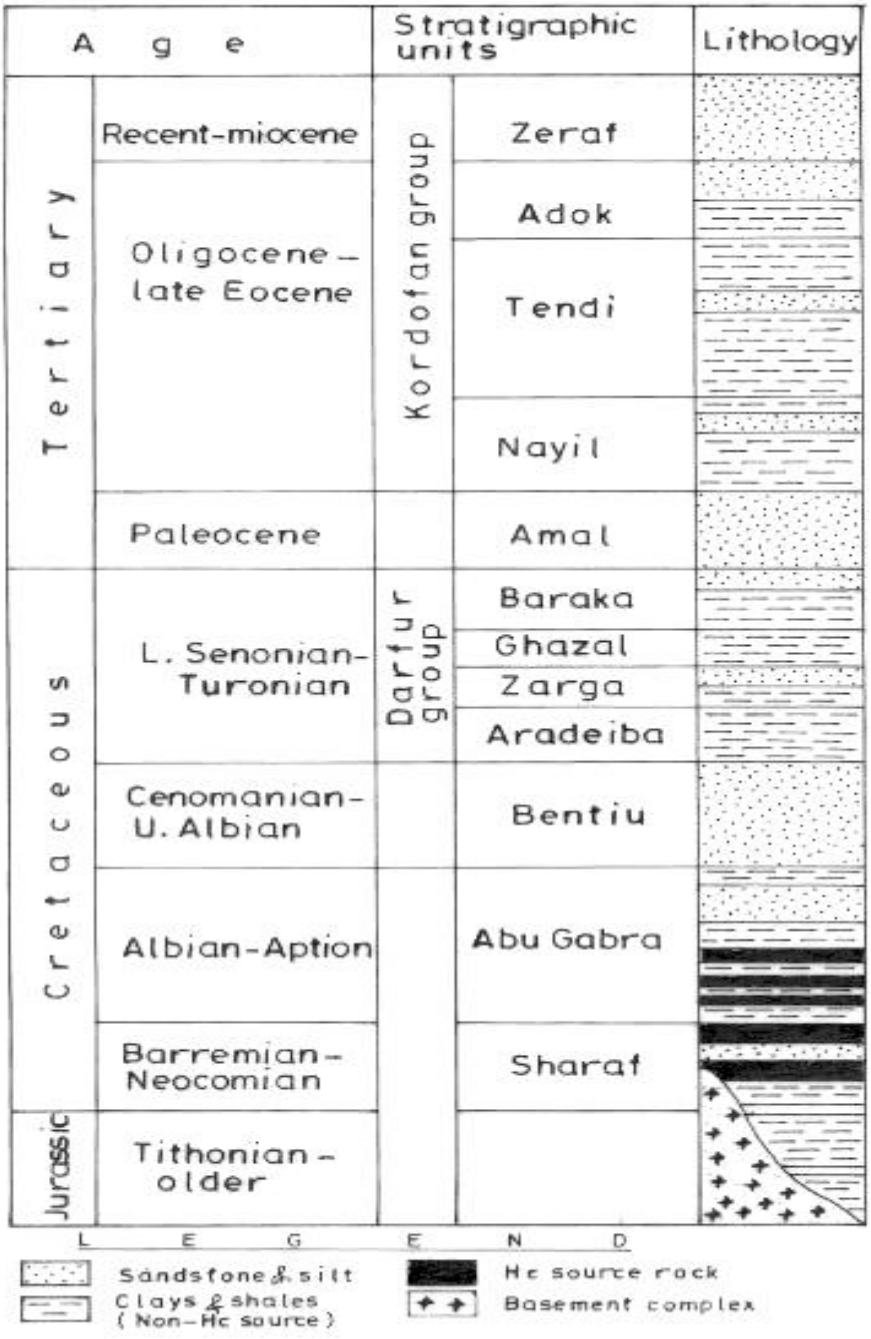

Figure (4) Stratigraphic column of the interior Sudan basin with generalized lithology (Schull, 1988)

2-2-3. Cretaceous Rocks

Thick sequences of Cretaceous sediments have been penetrated at the subsurface of the Muglad basin. This sequence is time equivalent to the Nubian outcrop. From seismic and well data an estimated 6096 meters of Cretaceous sediments have been deposited in the deepest troughs. (Fairhead, 1986).

Cretaceous-Paleocene sediments reflect two cycles of deposition, each represented by a coarsening-upward sequence. These cycles are correlatable basin wide and are directly related to the African rifting and basin infilling. The first cycle is represented by the Sharaf, Abu Gabra, and Bentiu Formations. The second cycle presents in the Cretaceous Darfur Group and the Paleocene Amal Formation. (Figure, 4).

2-2-3-1. Sharaf and Abu Gabra Formations

They are considered as the early cycle of sediments derived from the gneissic basement complex. During the early phases of rifting, Neocomian and Barremian claystones, siltstone, and fine-grained sandstones of the Sharaf Formation were deposited in fluvial-floodplain and lacustrine environments.

The maximum penetration of this unit is approximately 366 meters in the northwest Muglad basin.

The Aptian-early Albian Abu Gabra Formation represents the period of greatest lacustrine development. Several thousand feet of organic-rich lacustrine claystones and shales were deposited with interbedded fine-grained sands and silts.

The nature of this deposit was probably the result of a humid climate and lack of external drainage, indicating that the basins were tectonically silled. The Abu Gabra Formation is estimated to be up to 1829m thick. In the northwestern Muglad block, several wells have recovered oil from sands within this sequence. These sands were deposited in a lacustrine-deltaic environment. The lacustrine claystones and shales of this unit are the primary source rock of the interior basins. (Schull, 88).

2-2-3-2. Bentiu Formation

During the late Albian-Cenomanian a predominantly sand sequence of Bentiu Formation was deposited (Figure 4). The alluvial and fluvial-floodplain environments expanded, probably due to a change from internal to external drainage. The regional base level, which was created by the earlier rifting and subsidence, no longer existed. These thick sandstone sequences were deposited in braided and meandering streams. This unit, which is up to 1524m thick, typically shows good reservoir

quality. Sandstones of the Bentiu Formation are the primary reservoir of the Heglig area, (Schull, 88).

2-2-3-3. Darfour Group:

This group of fine to coarse-grained sediments was deposited during Turonian-late Senonian period. The lower portion of this group, Aradeiba, and Zarga Formations, are characterized by the predominance of claystone, shale, and siltstone. These initial deposits followed the second rifting phase. The excellent regional correlation of this unit verifies the strong tectonic influence on sedimentation. Floodplain and lacustrine deposits were widespread. The low organic carbon content indicates deposition in shallow and well oxygenated waters. These units may represent a time when the basins were partially silled. Throughout the basins, the Aradeiba and Zarga Formation are an important seal. Interbedded with the floodplain and lacustrine claystones, shales, and siltstones, are several fluvial/deltaic channel sands generally 321m thick. These sands are significant reservoirs in the Unity area. (Figure, 4).

The Cretaceous ended with the deposition of increasingly coarser grained sediments in the higher sand percentage of the Ghazal and Baraka Formations. (Figure, 4). These units were deposited in sand-rich fluvial and alluvial fan environments,

which prograded from the basin margins. The Ghazal Formation is also an important reservoir in Unity field. The Darfour group is up to 1829 m thick.

2-2-4. Tertiary deposit

In outcrop, the Tertiary deposit is represented by sequences of unconsolidated sands, gravels, silts and clays deposited in alluvial, fluvial and shallow lacustrine environments, (Vail, 1978). These sedimentary rocks are difficult to be distinguied from the overlain Pleistocene and Holocene alluvium.

In the subsurface, a thick sequence of Tertiary sediments has been penetrated (Figure 4). The initial deposits of the Tertiary were medium to coarse-grained sedimentation associated with the final rifting phase. Based on well control and seismic data, over 5486m of Tertiary rock is present in the deepest troughs (Fairhead, 1986).

2-2-4-1. Amal Formation

These massive sandstones of the Paleocene, which are up to 762m thick, are composed dominantly of coarse to medium-grained quartz arenites. This formation represents high energy deposition in a regionally extensive alluvial-plain environment with coalescing braided streams and alluvial fans. These sandstones are potentially excellent reservoirs. (Schull 1988).

2-2-4-2. Kordofan Group

These sediments represent a coarsening upward depositional cycle that occurred from the late Eocene to Middle Miocene. The lower portion of this cycle, the Nayil and Tendi Formation, is characterized by fine-grained sediment related to the final rifting phase. The deposits represent an extensive fluvial-floodplain and lacustrine environment. The lake deposits of this interval appear to have only minor oil source potential; however, they offer excellent potential as a seal overlying the massive sandstones of the Amal Formation.

Upward, this unit is generally characterized by interbedded sandstone and claystone with an increasing sand content. The fluvial-floodplain and limited lacustrine environments gave way to the increasing of alluvial input which reflected in the sand-rich braided stream and fan deposits of the Adok and Zeraf Formations. An exception occurs in the area of the Sudd Swamp where approximately 610 m of late Tertiary claystone were deposited.

2-3. Tectonic Evolution of Muglad Basin

The tectonic evolution of Muglad basin can be divided into a pre-rift phase, three rift phase, and sag phase (Fairhead, 1986).

i- pre-rifting phase

By the end of the Pan-African orogeny (550 My), this region had become a consolidated platform. (Figure 5 and Figure 6). During the remainder of the Paleozoic and Early Mesozoic time, this highland platform provided sediments to adjacent subsiding areas. The nearest preserved Paleozoic rocks are continental sediments in northwestern Sudan, near Chad and Libyan borders.

ii- rifting phase

Three stages rifting phase have occurred in response to crustal extension, which provided the isostatic mechanism for subsidence. Rifting is thought to have started in the Early Cretaceous. Seismic and well data indicate that this initial and strongest rift phase lasted until near the end of the Albian. The termination of the early rift is stratigraphically marked by the basin wide deposition of the thick sandstones of the Bentiu Formation.

The second rifting phase occurred during the Turonian-Late Senonian. Stratigraphically, this phase is seen in the widespread deposition of lacustrine and floodplain claystone and siltstones, which abruptly terminated the Bentiu Formation. This phase was characterized by minor volcanism. The end of this phase is marked by the deposition of the thick sandstone of the Paleocene Amal Formation.

The final rifting phase began in the Late Eocene-Oligocene, and is reflected in the sediments by a thick sequence of lacustrine and floodplain claystones and siltstones. The only evidence of volcanism in wells is the occurrence of thin Late Eocene basalt flows in the southern Melut Basin, near Ethiopia. After this period of rifting, deposition became more sand-rich throughout the Late Oligocene-Miocene.

iii- sag phase

In the Middle Miocene, the basinal areas entered an intracratonic sag phase of very gentle subsidence accompanied by little or no faulting.

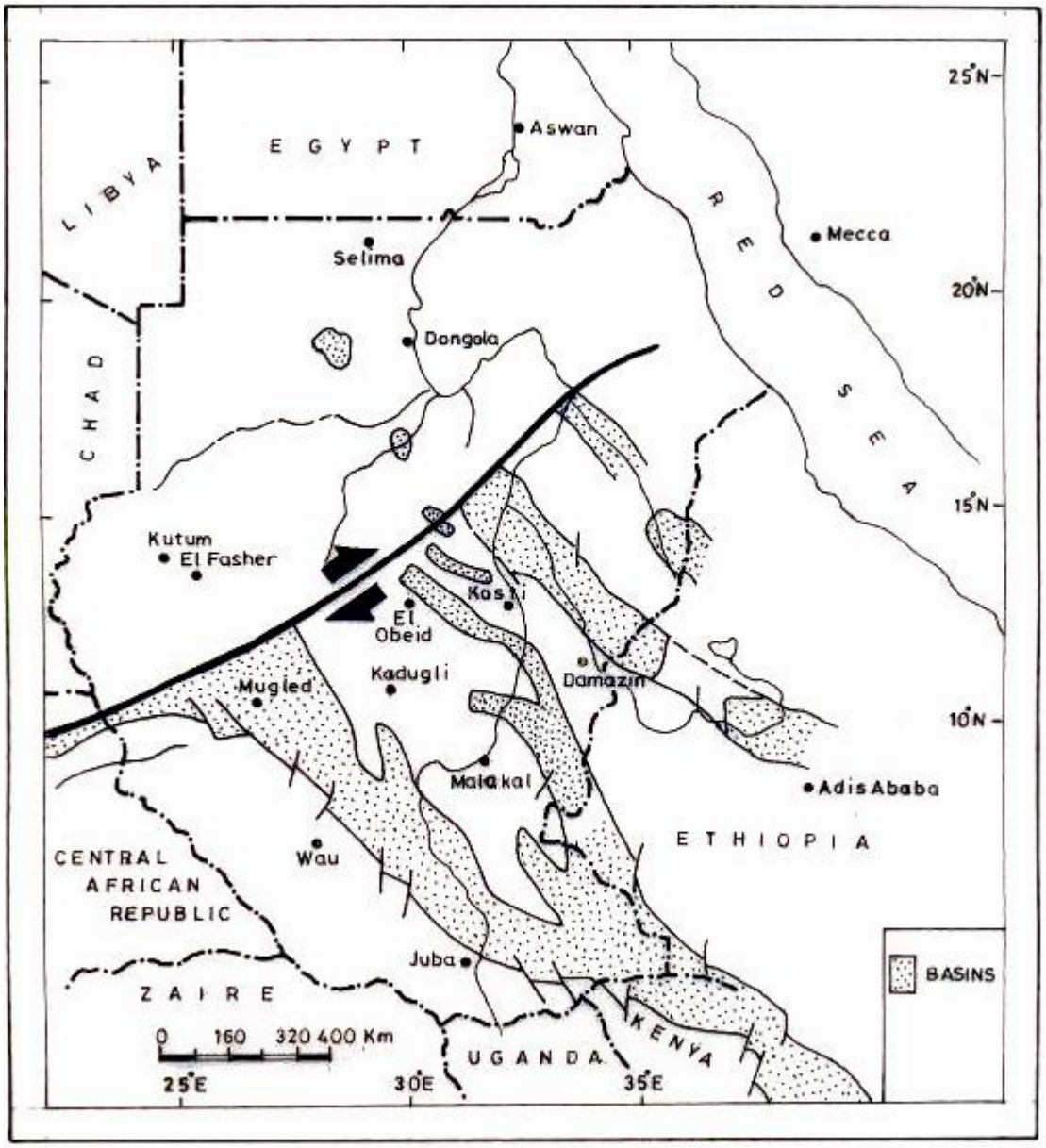

Figure (5) Structural setting of the rift basins in the Sudan and Neighbouring countries (Awad 1994)

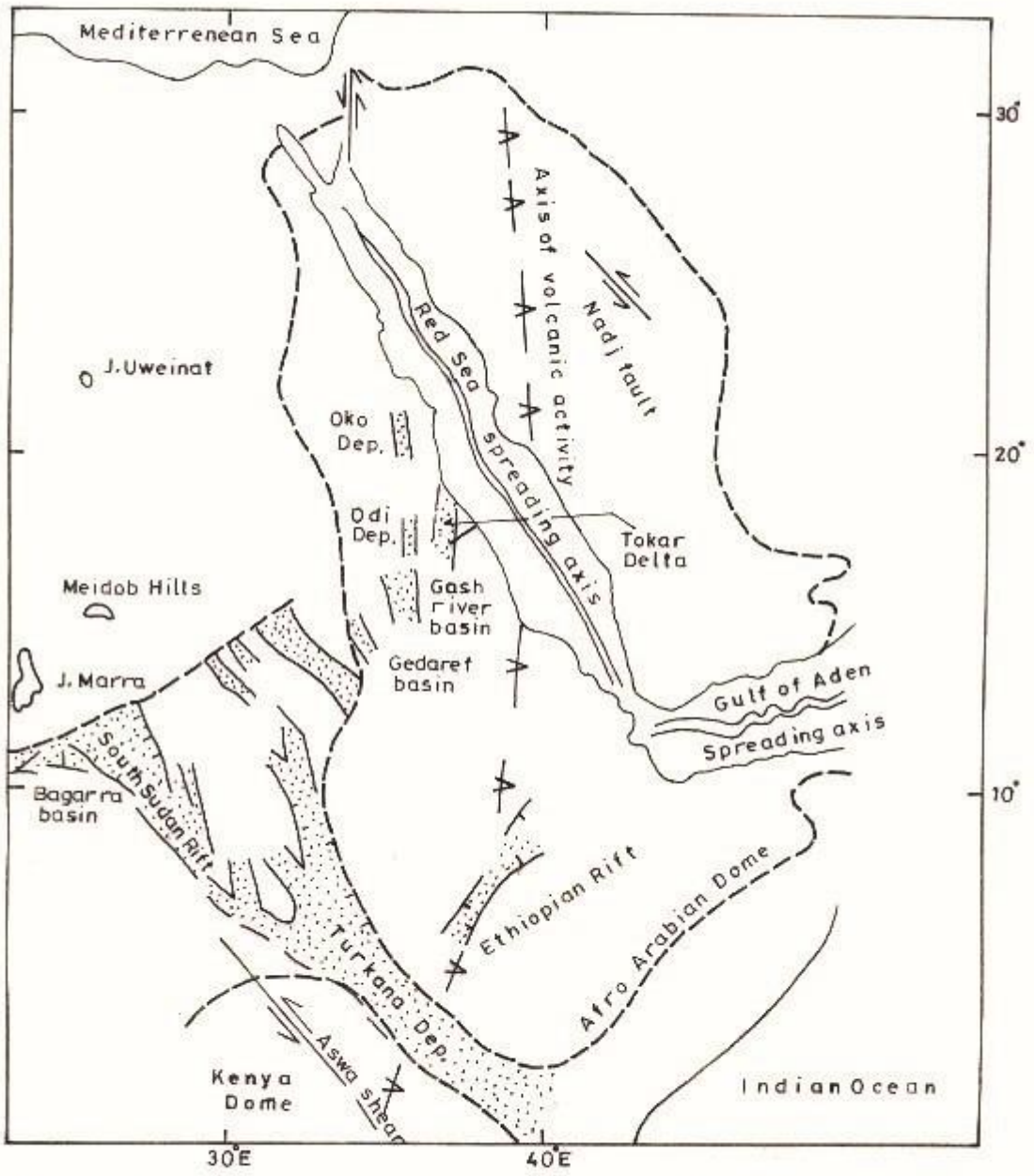

Figure (6) Tectonic evolution of North-East Africa, Late jurassic-recent (After RRI, 1991)

2-4. Structural style

Structurally, the Muglad Basin is dominated by dip-slip normal faults. The predominant fault orientation is parallel or sub-parallel to the strike of the primary grabens and basin margins. These longitudinal faults mainly strike N40°- 50°W throughout the basin.

In the central and southern Muglad Basin, an apparently older north-northwest trend also exists. The general structure of the Muglad Basin is shown in figure (7). Common structure are faults oblique to the primary trends. Relatively few major transverse faults occur. The faulting exhibits great variety in displacement, geometry, and growth history. Representative structural profiles (Figure 8) and (Figure 9) reflect this variety and provide a cross-sectional view of the structural style of the Muglad Basin. Along the basin flanks, the faults clearly, involve basement; however, in the deeper troughs, many faults appear to sole into the fine-grained early rift sequence.

The Muglad Basin has been essentially subjected to extensional stresses, where the good evidence for compressional structure and strike-slip movement is confined to the Baggara Graben in the northwest of the study area. The data from this area suggested that structures associated with the major basin-

bounding faults were formed by Cretaceous and Tertiary compressive forces related to strike-slip movement. These structures are generally en echelon folds associated with reverse faults. The basins of this area are narrow and have a trend similar to basinal area in eastern Chad and Central African Republic where dextral strike-slip movement is still documented (Schull, 1988).

The productive and prospective structures resulting from this complex extensional history in the Muglad Basin have been categorized as rotated fault blocks, drape folds and reverse drag folds. This were formed during the first rift phase (Berriasian-Cenomanian), second rift phase (Turonian-Paleocene), and the third rift phase (Eocene-Early Miocene).

Rotated fault blocks are formed by simple block rotation along a normal fault plane. This type of structure is common throughout the basin and can be seen in seismic lines (Figure 10) and (Figure 11). They are important producing traps. They are also among the most elusive as their effectiveness is highly dependent on an adequate lateral seal across the faults for the reservoirs, which become the more doubtful as shale/sand ratios precisely decrease towards the edges (Schull, 1988).

Drape folds result from differential subsidence and/or compaction over buried basement or fault blocks. Their closure may be significantly accentuated over host-like basement blocks bounded by oppositely dipping faults through “relative growth” on the block when compared to the subsidence on both of its flanks. When they result in 4-way dip closures, these folds provide structural petroleum traps which are much more dependable than straight fault traps as almost any sealing bed above the potential reservoirs may be sufficient to ensure the preservation of hydrocarbons. The potentially productive Sharaf structure is an example for this type of closure.

There are numerous examples of rollover anticlines resulting from rotation of fault blocks on the down-thrown side of large faults, principally listric in nature. These anticlinal structures may even be accentuated by a similar rollover into the antithetic faults associated with the earlier listric faults resulting into a larger anticlinal closure. The Unity field is an example of such a relatively large trap (Schull, 1988).

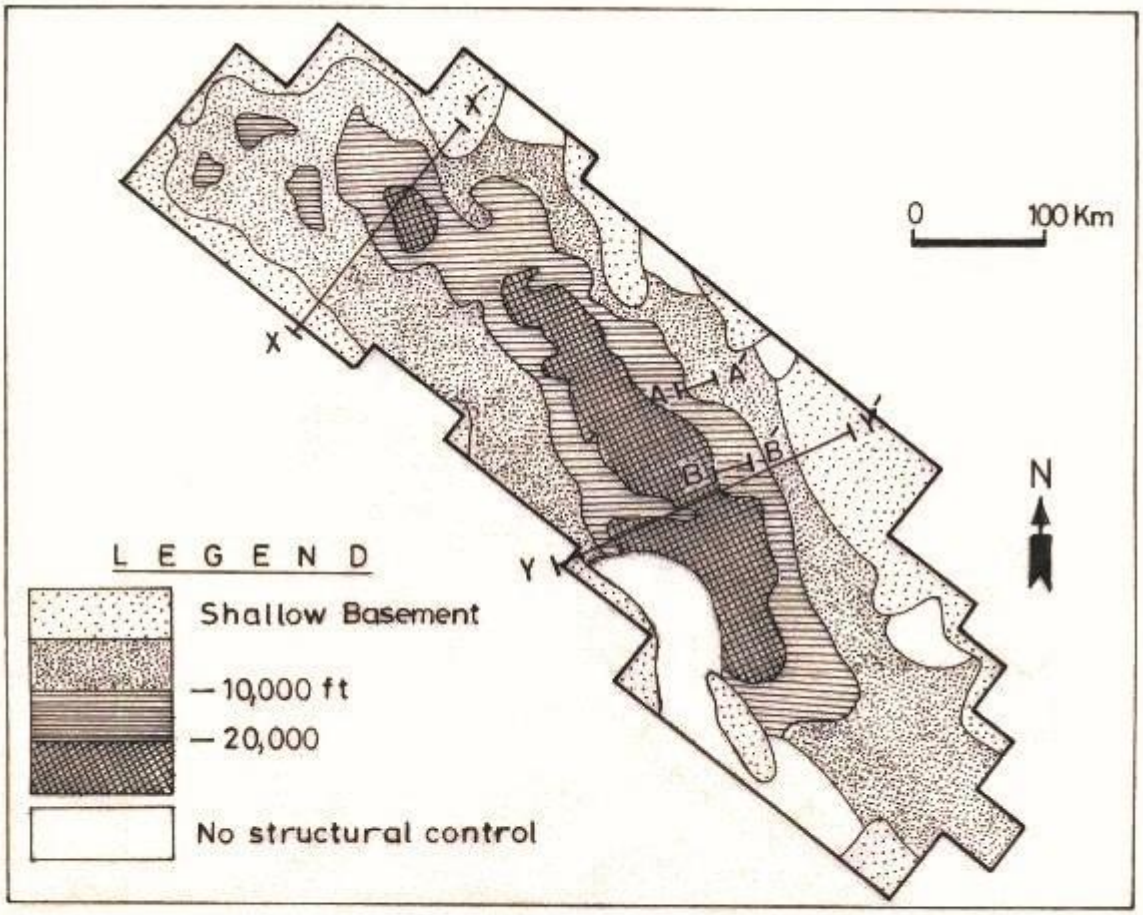

Figure (7) General structure map of depth top Abu Gabra formation of the Muglad basin, showing line of cross section A-A', B-B' and seismic line X-X', Y-Y'. Faulting is omitted. (After Schull 1988)

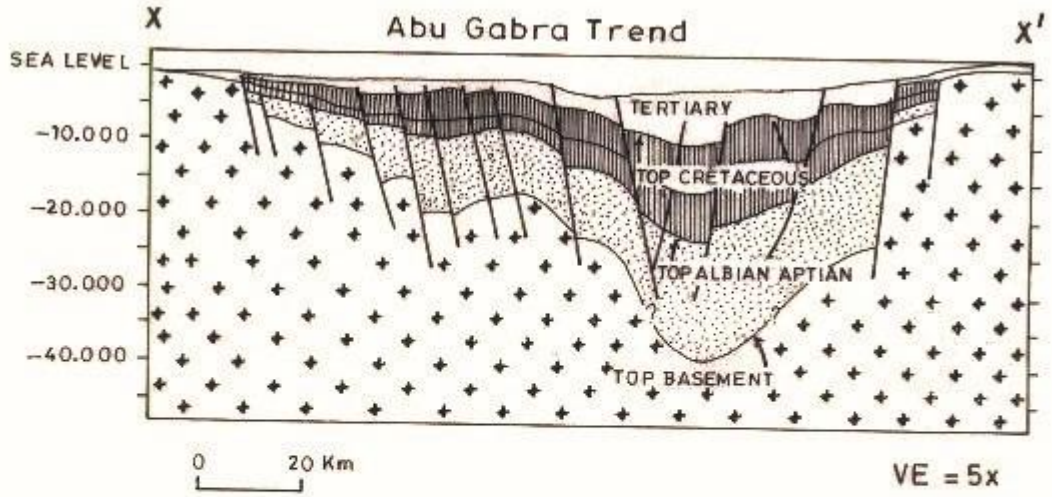

Figure (8) Structural cross section across Abu Gabra trend of Southern Muglad Basin (After Schull, 1988)

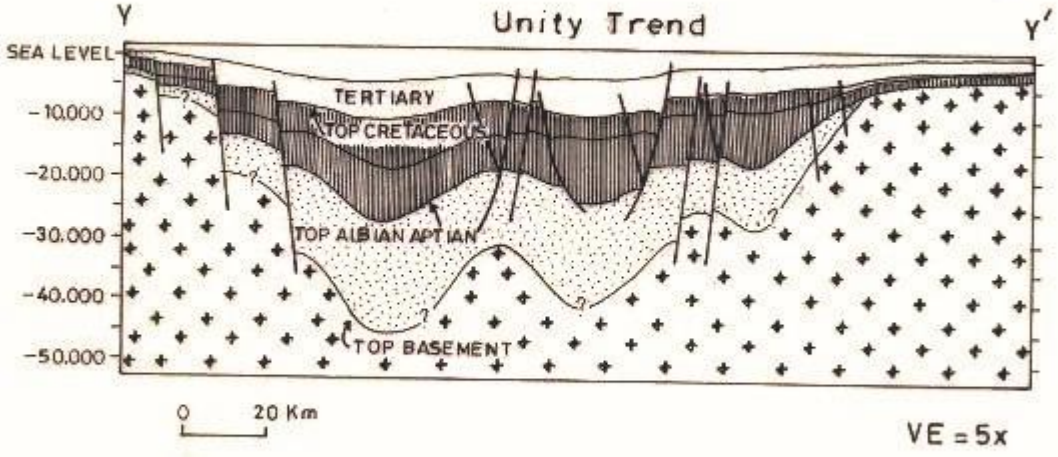

Figure (9) Strucural cross section across Unity trend of Muglad Basin in South Sudan (After Schull, 1988)

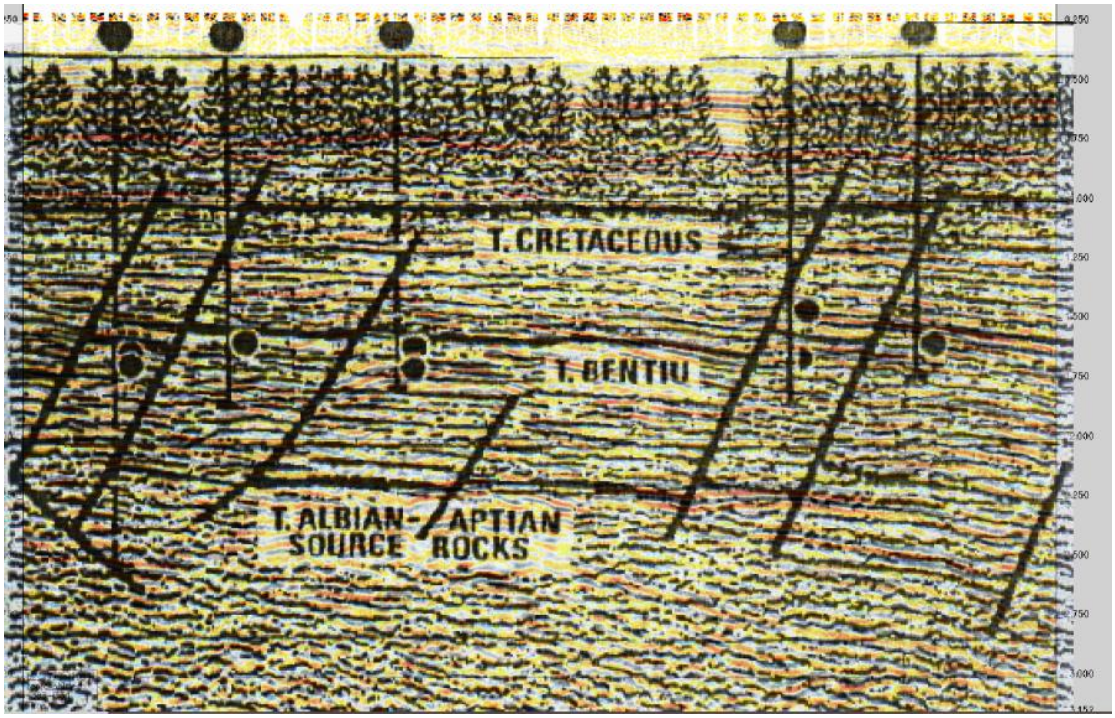

Figure (10) Seismic section across Heglig area of southern Muglad Basin. Times shown are two-ways travel time in second, (after Schull 1988)

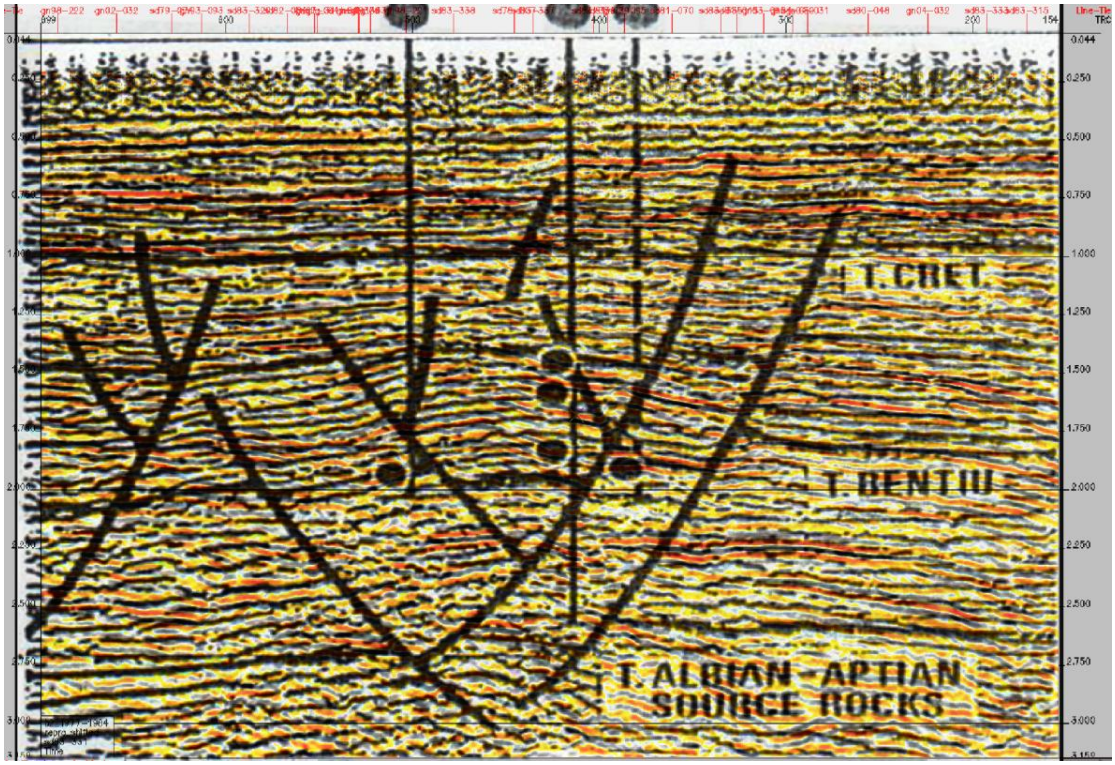

Figure (11) Seismic section across Unity area of southern Muglad Basin. Times shows are two-ways travel time in seconds. (After Schull 1988)

2-5. Petroleum Geology

2-5-1. Source Rocks

2-5-1-1. Proven Source Rocks

Sharaf Formation and Abu Gabra Formation are the very best source rocks in the Muglad Basin, where the organic-rich shales deposited in half-grabens during the first rifting phase. These lacustrine distal dysoxic-anoxic shaly facies were deposited in stratified lakes during times of greater rifting and subsidence. Shales over the entire section consistently yield Hydrocarbon Potential in excess of 5 mg HC/g rock, with a high proportion in excess of 10 mg HC/g rock. In general, the Total Organic Carbon (TOC) values range from 1% to 5% with an average of 1.3% (Schull, 1988).

The richest section of Abu Gabra Formation in the north-western Muglad has a TOC range from 3% to more than 7%, and Hydrogen Index (HI) from 400 to 900 mg HC/g TOC. Mohamed et al. (2001) stated that the average kerogen composition in this formation is 45% vitrinite, 35% alginate, 10% inertinite , 5% liptinite and amorphous. Over the entire Abu Gabra Formation, the average HI and TOC are 280 mg HC/g TOC and 1.3%, respectively. The Sharaf Formation in the northwest Muglad has a reported average kerogen content of 50% alginate, 20% exinite, 5% vitrinite and 25% inertinite, with

average HI of 270 mg HC/g TOC and TOC of 1.0% (Mohamed et al. 1999).

Mohamed et al. (2001) divides the Abu Gabra Formation into an upper unit with good source potential, and a lower unit of relatively low potential. The typical well illustrated by Schull (1988) shows an upward decline in TOC from around 2% (at a vitrinite reflectance of 0.6-0.8) to 0.5%. In this well, the HIs were also reported to decrease upwards from around 500mg HC/g TOC (oil-prone) to 100mg HC/g TOC (gas-prone), with a mean of 280 mg HC/g TOC reported by Mohamed et al. (2001).

The nonmarine oils derived from these source rocks are typically paraffinic and of low sulfur content. The organic matter is dominantly oil prone and oils are paraffinic, low sulfur, 18° to 45° API gravities with high pour-points of 26° C to 59° C. None of the oils have been heavily biodegraded, but slight biodegradation is seen in some of the Ghazal and Zarga intervals. In the Unity field, oils are chemically similar, suggesting that they were derived from the same or environmentally similar lacustrine source.

2-5-1-2. Possible Source Rocks

Source rocks of apparently lesser importance than the Abu Gabra-Sharaf formations are occasionally found in the Upper Cretaceous Darfur Group, Maastrichitan-Paleocene Amal (lower

member), and Eocene-Oligocene Nayil and Tendi formation in some parts of the northwest Muglad Basin and Kaikang trough.

2-5-2. Reservoirs

The reservoirs in the Muglad Basin consist of sandstones deposited in fluvial-channel, lacustrine-delta plain-distributary's channel, and delta-front environments. The distribution and qualities of the sandstones bodies show large variations with respect to the age, depth and depositional environment. Generally, the best reservoirs were deposited in the more proximal alluvial and fluvial environments. The more distal lacustrine environment generally lacked the energy necessary to rework and clean up the potential reservoir sands. Typical Cretaceous reservoirs are very-fine to medium-grained, moderately sorted, and subrounded to subangular sandstones. Coarser-grained, more poorly sorted sandstones are common in alluvial intervals.

2-5-2-1. Proven Reservoirs

a- Abu Gabra Formation (Aptian-Lower Albian)

The sandstones of the Aptian-Lower Albian Abu Gabra Formations are the oldest reservoirs in the basin. They were deposited during the first rifting phase in a shaly sequence of lacustrine environment. They are the most problematic producers as they are associated with a low energy distal

lacustrine environment and are consequently fine-grained with a mud matrix. This reservoir is present in the Abu Gabra-Sharaf area in the northwestern part of the basin. In this reservoir porosity values between 5% and 35% have been recorded.

b- Bentiu Formation (Upper Albian-Cenomanian)

Upper Albian-Cenomanian Bentiu Formation is thick sand – stone sequence deposited during the first rifting phase in alluvial, floodplain, braided and meandering stream environments. The Bentiu Formation forms very good reservoirs in fields including the Heglig, Unity. Porosity values range from 3.6% to 29%, averaging above 20%. The lowest permeability value reported is 0.1 mD and the highest value is 8,250 mD in the Unity field. Test results from wells at Unity and Heglig fields show flow rates as high as 3,100 bo/d (Unity 14) and 2,538 bo/d (Heglig), (IHS, 2006).

c- Darfur Group (Turonian-Senonian)

The Upper Cretaceous Darfur Group (Aradeiba, Zarga and Ghazal formations) was characterized by a cycle of fine to coarse-grained deposition.

The lower part of the group, Aradeiba and Zarga formation, is characterized by the predominantly shales and siltstone. Interbedded with the floodplain and lacustrine shales are several fluvial/deltaic channel sands generally from 3m to 21m thick,

which form important reservoirs in the Unity, Heglig, Thar Jath and Talih West fields/discoveries. The porosity and permeability values in the Aradeiba sandstone range from 12% to 38.7% and from 0.1 mD to 9,800 mD, respectively. The extreme values are recorded in the Unity field. In this field, the porosity values averaged more than 25%. The Zarga Formation has porosity values ranging from 10% to 30%, and permeabilities from 0.1 to 6,070 mD.

The overlying Ghazal Formation was deposited in sand-rich fluvial and alluvial fan environment, and consists of increasingly coarser grained sediments. The Ghazal Formation is an important reservoir in the Unity field. The maximum and minimum porosity and permeability values recorded in the Ghazal sandstones in the Unity field are, respectively: 5-42% and 0.1-9,050 mD, (IHS, 2006).

d- Tendi Formation (? Upper Eocene)

Tertiary non-marine clastic reservoirs are restricted to the? Eocene lacustrine and fluvial-floodplain sandstone of the Tendi Formation, which, however, assume only minor importance.
The Tertiary sandstones generally have good reservoir qualities and include some quartz arenite units. They maintain their reservoir qualities at greater depth than the Cretaceous reservoirs. An average porosity value of 25% is recorded at

Kaikang (Southwest of the study area). Sandstones of the Tendi Formation are oil-bearing reservoirs only in the Kaikang field located to the southwest of the Unity field. The Kaikang oil well is the first and the only well recorded a substantial oil flow from a Tertiary reservoir. The well tested 1,359 b/d of 34.5° API crude. There was no identification of water in the reservoir.

The Nayil Formation, which underlies the Tendi Formation, is reported to form a reservoir (non-commercial) at El Mahafir (1). This reservoir levels might be located in the upper part of the formation, where the sandstones are inderbedded with shales, deposited in fluvial and lacustrine environments. The Mahafir (1), is the well recovered swab oil with sand production and no water.

2-5-2-2. Potential Reservoirs

Potential reservoirs include the thick sandstone of the Paleocene Amal Formation, which have excellent reservoir properties. However, their significant thickness makes them vulnerable to leakage through the faults as they require thick seal beds to prevent it. The Amal Formation represents high energy deposition in a regionally extensive alluvial-plain environment with coalescing braided streams and alluvial fans.

2-5-3. Seals

Efficient sealing is the most critical factor for the preservation of hydrocarbons in a severely faulted basin like the Muglad Basin. Whereas the sealing of an unfaulted 4-way dip closure may require only a limited thickness of sealing material, it does require thicker sealing beds for fault traps.

Most seals in the Muglad Basin are intraformational shales interbedded with the reservoirs. Major Cretaceous seals of the Abu Gabra, Bentiu, Aradeiba, Zarqa and Ghazal formations, with minor intraformational seals in the Tendi Formation. Eocene shales of the Nayil Formation may form local seals.

Chapter 3

Formation evaluation

3-1. **Introduction**

Formation evaluation is the analysis and interpretation of well log data, in terms of the nature of the formation and their fluid content. Appendix (B) illustrates notes on logging.

The objectives of formation evaluation are:

a- To ascertain the presence of commercial hydrocarbons.

b- To determine the best means for their recovery.

c- To derive lithology and other information on formation characteristics for use in further exploration and development.

The main information which can be obtained from well logs can be summarized as follows:

a- Lithology boundaries of rock formation and stratigraphic correlation (e.g. gamma-ray for shale identification).

b- Density (ρ) determination.

c- Porosity (ϕ) determination.

d- Water and hydrocarbon saturation

3-2. Formation evaluation & shale effect.

The formation evaluation studies in the study area started by Chevron Oil Company, after an extensive geophysical survey have been carried, concentrated on seismic method which includes, processing and interpretation from 1975 to 1985, followed by observations drilled wells. Other studies of seismic reflection and gravity methods have been integrated with well data to construct a geological model, done by Mohamed et al. (2001) for Muglad Basin. A thermal maturity evaluation study of the Muglad Basin has been done by Abdullatif (2002).

Hamada (1996) suggested an accurate determination of formation porosity and fluid saturation in shaly sand, where that shale caused some problems in formation evaluation. This study presents a comprehensive approach in the problem of shaly sand. Therefore, effective porosity and water saturation have been determined for different shaly models. In this study a comparison of the various water saturation in shaly sand shown

that the clean sand equation Archi equation shows very high water saturation but Simandoux or Indonesia equation is applicable to laminated clay models, where Dual water model is essentially designed for dispersed or structural clay models, therefore, it provides lower water saturation values than of laminated clay models i.e. Indonesian equation. Studied in water saturation models in clean and shaly layers which show an accurate determination of initial oil in place in the early life of reservoir or evaluation of developed reservoir in required to well estimate, the hydrocarbon volume either in place or left in the reservoir, by (Hamada, 2003). This study appears a modified Archi formula $\left(s_w = \left(aR_w / \phi^m R_t \right)^{\frac{1}{n}} \right)$ as a basic equation to computes water saturation in clean formation or suitable shaly water saturation models in shaly formation, where the water saturation value for given reservoir conditions depends on the accuracy of Archi parameters a, m and n. This study presents a new technique to determine Archi parameters a, m and n. The developed technique is based on the concept of three dimensional- regression (3-D) plot of water saturation, formation resistivity and porosity. This 3D technique provides simultaneous values of Archie Parameters.

This study builds a comprehensive interpretation algorithm to evaluate the shaly- sand reservoir in this formation using limited well log data. Dual Water, Simandoux and Indonesian models were used for comparison in this study and Archie clean sand model were also discussed. Therefore, Archie formula gives a misleading result because Archie formula assumes that the formation water is the only electrically conductive material in the formation, and neglects the present of shale. The effect of shale on various log responses depends on the type, the amount, and the way that it is distributed in the formation. Shale distributed in sand stone reservoirs in three possible ways. The laminar shale occurs between layers of clean sand, structural shale which exists as nodules within the formation matrix, dispersed shale which dispersed throughout the sand, partially filling the intergranular interstices or coating the sand grains. Therefore this study discusses that each of those form can affect the amount of rock porosity and water saturation.

The most controversial problems in formation evaluation is the shale effect in reservoir rocks, because the accurate determination of formation porosity, and fluid saturation in shale-sand is subjected to many uncertain parameters, which are induced by the existence of shale in pay formation.

The occurrence of shale reservoir rocks can result in erroneous values of water saturation and porosity as calculated from well logs. Aside from shale effect on porosity and permeability, the electrical properties of reservoir rocks, consequently their fluid saturation are sensitively affected by the existence of shale, the physical properties of shale, and the way that distributed in the host layer.

Shale material can be distributed in the host layer in three ways (laminar, structural and dispersed). All of these forms may occur simultaneously in the same formation. However shale in only one form is predominant and simplified models can provide reasonable porosity and water saturation, e.g. (Archie, 1942, Dresser Atlas, 1982, Simandoux, 1982, Smits, 1968, Clavier et al, 1984, Fertl, and Hammack, 1971, Waxman, and Smits, 1968, Poupon et al, 1970; Bussian, 1984 and Schlumberger, (1987).

All models are reduced to the clean sand model when the volume of shale is insignificant. For relatively small shale volumes, most shale models might yield quite similar results.

3-3. Reservoir Character of Bentiu Formation

This formation has a rock of fine to medium grained, and moderately sorted, sub-angular, of coarser grained in texture and more poorly sorted sandstone. They composed of dominant quartz, feldspar, low heavy mineral content, and matrix of clay and mica minerals, with lesser amounts of calcite, and chlorite.

This sandstone interbedded with claystone of dark brown, greenish grey, sub blocky, silty, sticky, of kaolinite, and mica trace.

Schull (1988) concludes some remarks from the study of a number of thirty wells, in this study region focusing on Bentiu Formation, (Figures 12 and 13). These remarks as follows:

i- Reservoir quality decreases with depth due to compaction.

ii- Reservoir quality decreases with decreasing size, the coarser grained sandstones are better in quality than the finer grained sandstones.

iii- Reservoir quality decreases with increasing amount of feldspar and lithic grains.

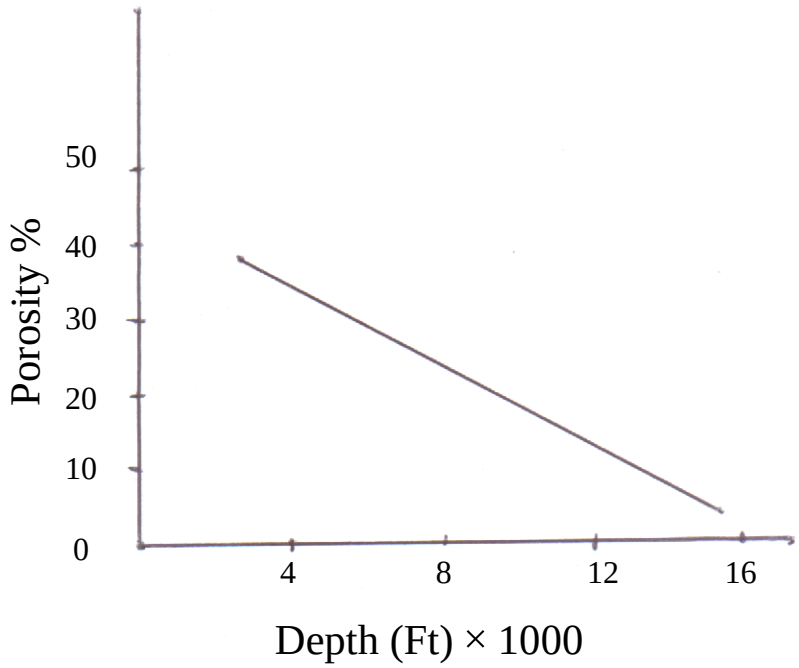

Fig (12) Porosity vs Depth Illustrate Reservoir Character.
(From Schull 1988)

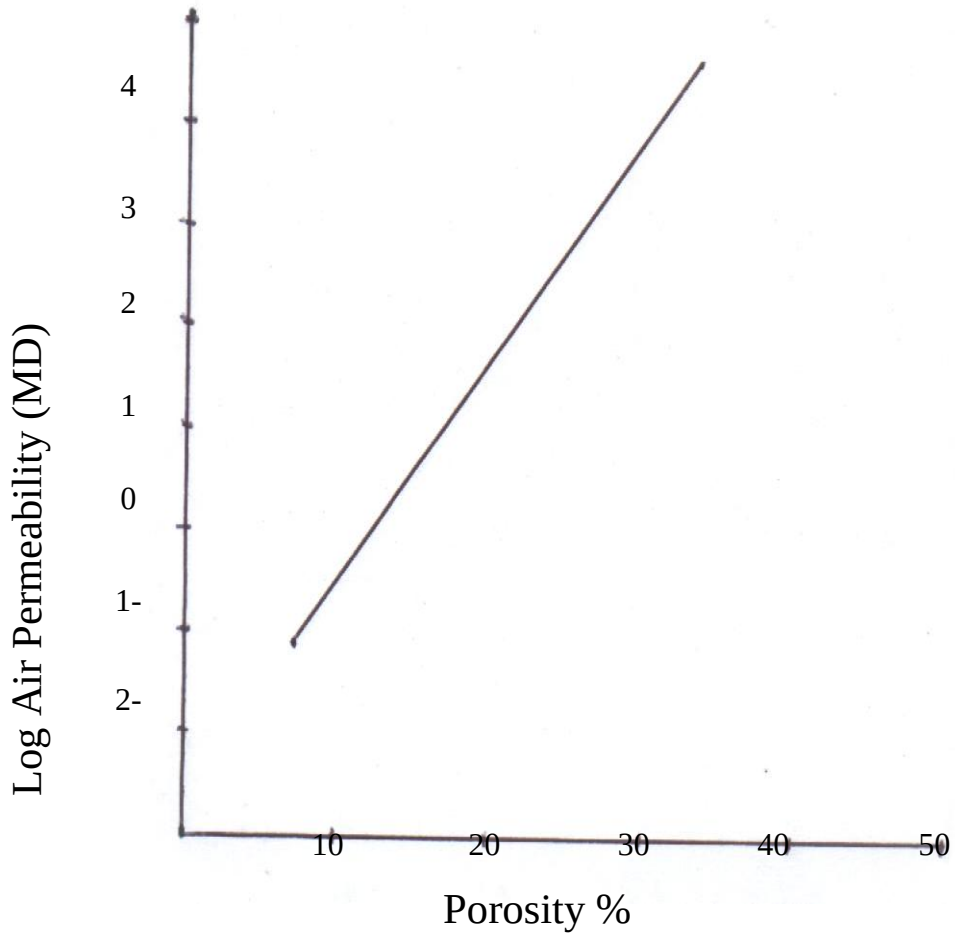

Figure (13) porosity vs. permeability illustrates reservoir character. (From Schull 1988)

3-4. Log Interpretation.

Log analysis has been used for determination of reservoir parameters by calculation of porosity, water saturation, and hydrocarbon saturation from the log data of well number 15, well number 16, well number 22, and well number 35, these wells have been drilled in the study area. Figure (1).

There are many softwares and different techniques used in determination of physical properties of reservoir formation.

1- The softwares:

a- Pfeffer V.1 & V.2

b- Petris Winds

c- Rock works

d- Easy log

e- J log® version 4

f- Log Dig-Automated well log Digitizing software

g- Petra Seis

h- Petro log. etc

2- The techniques:

a- OBM core analysis (Woodhouse & Warner 2004)

b- EXXON technique (Passey et.al. 1990)

c- Archi equation (Archi 1942)

d- Selly equation (Selly 1998)

e- Dual water model (Waxman and Smits 1968)

f- Simandoux model (1963)

g- Indonesia model (Poupon and Leveaux 1971)

3-5. Interpretation method

All the different types of models used in log interpretation must consider the following:

a. Sand has low density, and shale has high density.

b. Shale has high gamma ray, and sand has low gamma ray.

c. Fresh water has high resistivity, and oil has high resistivity.

3-5-1. Archie equation

This method used in determination of reservoir parameters in this study, because it is work well as long as salinity very low and there is no presence of trace amount of clay i.e. in pure sand.

3-5-1-1. Porosity

The density porosity of the zone of interest has been determined by the following equation:

i. *Porosity (ϕD)* $= \dfrac{\rho_{ma} - \rho_{\log}}{\rho_{ma} - \rho_{flu}}$ ---------- (X_1)

Where:

ρ_{ma} = Density of matrix.

$\rho_{\log}$ = Density from log data.

ρ_{flu} = Density of fluid

ii.Average Porosity $= \dfrac{\phi N + \phi D}{2} \rightarrow (X_2)$

Where:

ϕ_N = Neutron porosity

ϕ_D = Density porosity

iii.Effective Porosity ϕe

$$\phi_e = \phi D - V_{sh} \times \phi D_{sH} \qquad \rightarrow (X_3)$$

Where:

ϕD = porosity of density

V_{sh} = volume of shale

The volume of the shale (V_{sh}) determined by the equation

$$V_{sh} = \frac{GR_{\log} - GR_{ma}}{GR_{sh} - GR_{ma}} \qquad \rightarrow (X_4)$$

Where:

GR_{log} = gamma Ray from log data

GR_{ma} = gamma Ray of matrix

GR_{sh} = gamma Ray shale

ϕD_{sH} = porosity of shale.

3-5-1-2. Water saturation.

The water saturation (SW) determined by the following equation:

$$S_w = n\sqrt{\frac{aR_w}{\phi_e^{\,m} R_t}} \qquad \rightarrow (X_5)$$

(Archi equation)

Where:

R_w = water resistivity

R_t = deep resistivity

ϕ_e = effective porosity

a = cementation factor

n = saturation exponent

3-6. **Interpretation of log well number 22**

Bentiu Formation at this well consist of mainly fine sandstone of translucent off white, un consolidated, medium to fine grained , trace coarse grained, sub angular to sub rounded, moderately sorted , quartz, common kaolinitic cement, interbedded with claystone of dark brown, greenish grey, soft to firm, sub blocky, silty, sticky, trace kaolinite, trace mica.

The oil shows in this well is of trace to common light brown oil stain, minor spotty to abundant even dull-bright yellow direct fluorescence, minor very slow streaming to abundant fast blooming dull-bright yellowish white cut fluorescence and rare to abundant light brown residual oil were observed, (table 1).

Table (1) Oil Show of Bentiu Formation at well 22

No	Internal (m)	Shows Degree	Cut Flour	TG ppm
1	1645.0 -1675.0	Patchy – Even	B/mg	591-1988
2	1683.0 -1689.0	Spotty	Streaming B/mg	604 -800

3-6-1. selected zones of well number 22

Three Productive zones have been selected from log data of this well on Bentiu Formation, (Figures 14), according to the oil show as on table (1), these zones:

a. From 1644 m to 1661 m
b. From 1662 m to 1672 m
c. From 1528 m to 1538 m

3-6-2. zone (a) from 1644 m to 1661 m

a.Thickness of the zone = 17 m

b. The gamma ray:

- Gamma ray reading = 60 API
- Gamma Ray sand = 45 API
- Gamma Ray shale = 105 API

C. Resistivity deep reading average 600 Ohm/m

d. average Density = 2.35 g/cc

e. average Neutron porosity = 33%

f. average (Self Potential) S.P = 20 mV

g. average Porosity (ϕD)

Substitute in equation X_1

$$Porosity\ (\phi D) = \frac{\rho_{ma} - \rho_{\log}}{\rho_{ma} - \rho_{flui}}$$

$$\phi D = \frac{2.65 - 2.35}{2.65 - 1.1} = \frac{0.3}{1.55} = 0.19 = 19\%$$

Therefore porosity from density = 19%

h. Average porosity

From equation (X_2), average porosity =

$$Average\ porosity = \frac{19 + 33}{2} = \frac{52}{2} = 26\%$$

i. Effective Porosity (ϕe)

Substitute in equation X_3

$\phi e = \phi D - Vsh * \phi Dsh$

$\phi D = 19\%$

$V_{sh} = ?$

$\phi D_{sh} = ?$

For V_{sh} used gamma ray and using equation X_1

$$V_{sh} = \frac{GR_{\log} - GR_{ma}}{GR_{sh} - GR_{ma}}$$

(GR = gamma ray)

$$V_{sh} = \frac{60 - 45}{105 - 45} = \frac{15}{60} = 0.25 = 25\%$$

$\therefore$ 25% shale and 75% sand.

For ϕDsh (from any shale we read ρ_{log} and Substitute in equation X_1).

$$Porosity\ (\phi D) = \frac{\rho_{ma} - \rho_{\log}}{\rho_{ma} - \rho_{flui}}$$

ρ_{ma} shale= 2.67 (constant)

ρ_{log} shale= 2.65 (from log)

By Substitution in equation (X_1)

$$\phi \text{ D shale} = \frac{2.67 - 2.65}{2.67 - 1.1} = \frac{.02}{1.57} = 0.13 = 13\% \ (const.)$$

(Porosity of the mud taken, 1.1 because it is saline)

$\therefore$ We Substitute in equation – X_3

The effective porosity:

$$\phi e = \phi D - V_{sh} * \phi D_{sh}$$

$$= 0.19 - 0.25 \text{ x } 0.13 = 0.19 - 0.033 = 0.16 = 16\ \%$$

g. For water Saturation (SW):

We substitute in equation X_3

$$S_w = \sqrt[n]{\frac{aR_w}{\phi_e^{\ m} Rt}}$$

ϕe = 16% (from equation X_3)

R_w (from Archi equation in consider S_w = 1 in water zone)

$\therefore$ if S_w=1. The Equation be. $R_w = Rt \times \phi e^2$

(R_t = 9 ohm/m from pure water zone, fig. (14))

$$R_w = 9 \times (0.16)^2 = = 9 \times 0.256 = 0.23 \ ohm/m \ (const.)$$

$\therefore$ always R_w = 0.23 ohm/m constant

by substitute in equation X_4

$$S_w = \sqrt{\frac{1 \times 0.23}{(0.16)^2 \times 600}} = \sqrt{\frac{0.23}{15.36}} = \sqrt{0.02} = 0.12 = 12\%$$

Therefore water saturation =12%

Oil saturation = (100 – 12) % = 88%

Therefore in zone 1644 m to 1661 m, oil saturation equal 88%

3-6-3. Zone (b) from 1662 m. to 1672 m.

a. Thickness of the zone = 10 m

b. Gamma ray

- Gamma ray reading. = 60 API
- Gamma ray sand = 45 API
- Gamma ray shale = 150 API

c. Resistivity (deep reading) =150 ohm.m

d. Density = 2.35 g/cc

e. Neutron porosity = 39 %

f. S.P = 70 mV

G. Porosity (ϕD)

$$Porosity\ (\phi D) = \frac{\rho_{ma} - \rho_{\log}}{\rho_{ma} - \rho_{flui}}$$

$$\phi D = \frac{2.65 - 2.35}{2.65 - 1.1} = \frac{0.3}{1.55} = 0.19 = 19\%$$

$\therefore$ Porosity from density = 19%

. Average porosity = $\frac{porosiydensity + Neutronporosity}{2}$

$= \frac{19 + 39}{2} = 29\%$

. Effective porosity (ϕe) using equation X_3

$\phi e = \phi D - Vsh \times \phi Dsh$

We have

$\Phi D = 19\%$

For V_{sh} , from equation X_1 :

$$V sh = \frac{GR_{\log} - GR_{ma}}{GR_{sh} - GR_{ma}} = \frac{60 - 45}{150 - 45} = \frac{15}{105} = 0.14 = 14\%$$

$\therefore$ 14% shale and 86% sand.

For ϕD_{sh} ρ log from any shale zone = 13% (constant).

Therefore by using X_3

$$\phi e = \phi D - vsh \times \phi Dsh$$
$$= 0.19 - 0.14 \times 0.13 = 0.19 - 0.018 = 0.17 = 17\%$$

For calculation of water saturation (S_W), by using equation X_4

$$S_W = n\sqrt{\frac{aR_w}{\phi_e{}^m Rt}}$$

Where:

$\phi e = 0.17$

$R_W = 0.23$ ohm.m (constant)

Rt = 150 ohm.m

$$SW = \sqrt{\frac{1\times 0.23}{(0.17)^2 \times 150}} = \sqrt{\frac{0.23}{4.335}} = \sqrt{0.053} = 0.23$$

Therefore the water saturation 23%

Oil saturation = 77%

3-6-4. Zone (C), from 1528 m. to 1538 m.

a. thickness of the zone = 10 m

b. Gamma ray

- Gamma ray reading = 60 API
- Gamma ray sand = 145 API
- Gamma ray shale = 150 API

C. Resistivity (deep) = 110 ohm.m

d. density = 2.25 g/cc

e. Neutron Porosity = 33%

f. S.P = 18%

g. Porosity (ϕD)

Using equation (X_1)

$$Porosity\ (\phi D) = \frac{\rho_{ma} - \rho_{\log}}{\rho_{ma} - \rho_{flui}}$$

$$\phi D = \frac{2.65 - 2.25}{2.65 - 1.1} = \frac{0.4}{1.55} = 0.26 = 26\%$$

Therefore porosity from density = 26%

Average porosity

$$= \frac{porosiy\ density\ +\ Neutron\ porosity}{2} = \frac{26 + 33}{2} = 29.5\% = 30\%$$

. Effective porosity (ϕe), by using equation X_2

ϕe = ϕD – Vsh * ϕDsh

ϕD = 26%

For V_{sh} , used equation X_1

$$= \frac{60 - 45}{150\,45} = \frac{15}{105} = 0.14 = 14\%$$

$\therefore$ 14% shale and 86% sand.

ϕDsh = 13% (constant)

By using equation X_3

ϕe = ϕD – Vsh * ϕDsh

= 0.26 – 0.14 * 0.13 = 0.26 -0.018 = 0.24 = 24 %

For calculation of water saturation (S_W), using equation X_4

$$S_w = n\sqrt{\frac{aR_w}{\phi_e{}^m Rt}}$$

Where:

$\phi e = 0.24$.

$R_W = 0.23$ ohm/m (constant)

Rt = 150 ohm/m

$$SW = \sqrt{\frac{1\times 0.23}{(0.24)^2 \times 150}} = \sqrt{\frac{0.23}{8.64}} = \sqrt{0.027} = 0.16 = 16\%$$

$\therefore S_W = 16\%$, and oil saturation = 84%.

Table (2) illustrates the formation evaluation of well number 22.

Table (2): Formation evaluation of well 22

Zone	Top	Bottom	Gross (m)	VSH	Net Sand	Porosity	Neutron	Average Porosity	ϕe %	Water Saturation
a	1645	1659	14.5	0.25	14.5	19%	33%	0.26	16%	12%
b	1662	1672	10	0.14	10	19%	39%	0.29	17%	23%
c	1528	1538	10	0.14	10	26 %	33%	0.3	26%	16%

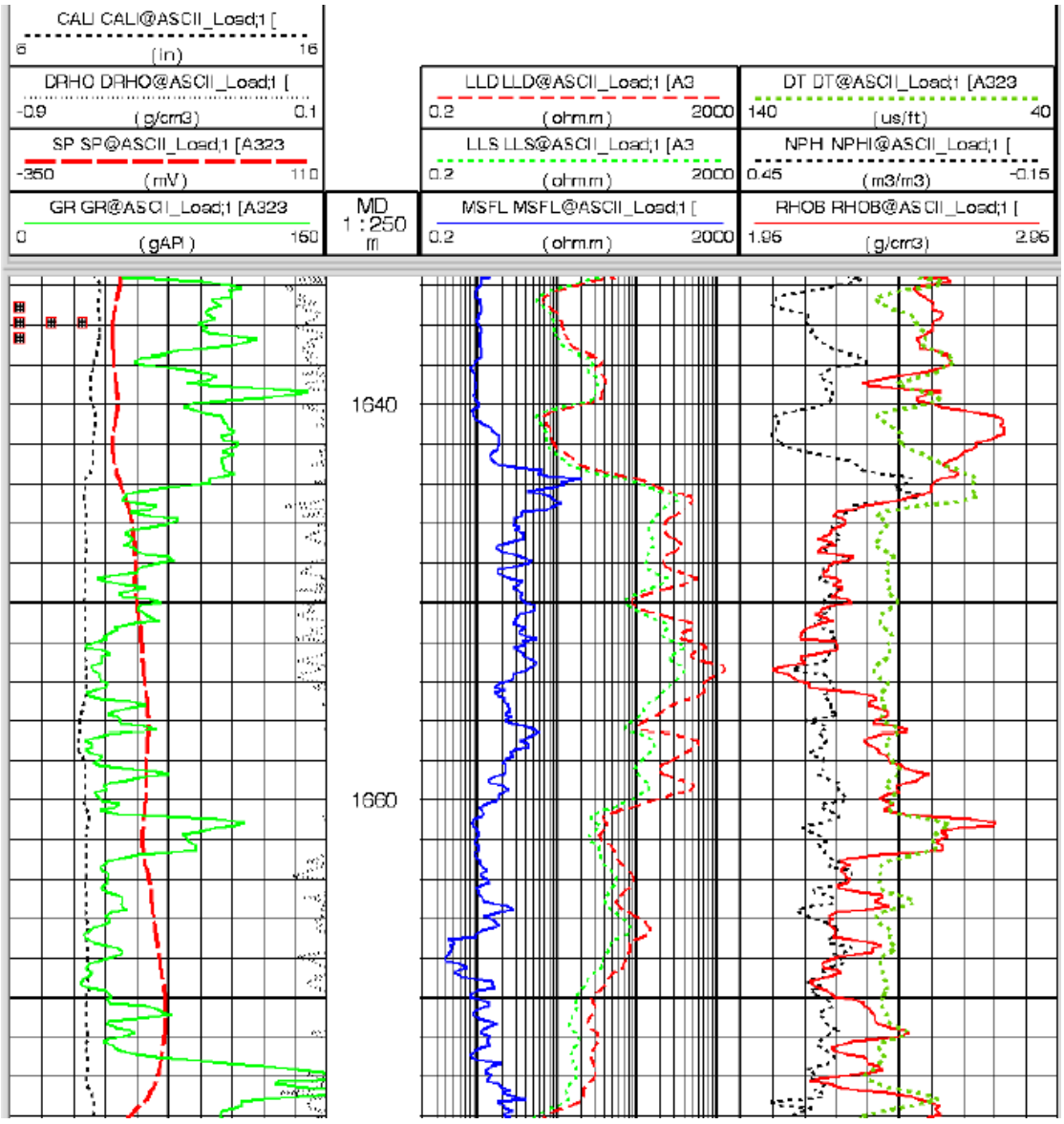

Figure (14) Log of well 22 shows the interested zones

3-7. Interpretation of Log of well number 16

Bentiu Formation in this well shows sandstone of clear to light brown, buff occasional translucent, desegregated, un-consolidated, fine to coarse grain, sub angular to sub rounded, poor to moderate sorted poor to good intergranular porosity, kaolinite cement, occasional quartz over growth, traces of graphite & pyrite. This sandstone interbedded with claystone of reddish brown, grey to dark grey, soft to firm, sub blocky in part crumbly, abundant kaolinite, and non-calcareous.

The oil show in this well is spotty light brown oil stain, spotty dull yellow direct fluorescence, moderate streaming dull milky yellow cut, faint light brown residual ring.

3-7-1. The selected zones

The selected zone (a), shows in figures (15) from 1646 m. to 1658 m, and the other zone (b), from 1873 m. to 1880 m. (not in figure).

3-7-2. Zone (a) from 1646 to 1658m.

a. thickness of the zone 12 m

b. Gamma ray

- Gamma ray reading 60 API
- Gamma ray sand 30 API
- Gamma ray shale 132 API

c. Resistivity (deep reading) = 900 ohm.m

d. Density = 2.25 g/cc

e. Neutron porosity = 24%

f. S.P = 10 mv

g. Porosity (ϕD):

By substitute in equation X_1

$$(\phi D) \quad = \frac{\rho_{ma} - \rho_{\log}}{\rho_{ma} - \rho_{flui}} \quad = \frac{2.65 - 2.25}{2.65 - 1.1} = \frac{0.4}{1.55} = 0.26 \ 26\%$$

There Porosity from density = 26 %

Average porosity = $\frac{26 + 24}{2} = 25\%$

Effective (ϕe) by using equation X_3

ϕe = ϕD – Vsh * Ø Dsh

ϕD = 0.26

V_{sh} by equation (X_1)

$$V sh = \frac{GR_{\log} - GR_{ma}}{GR_{sh} - GR_{ma}} \quad , \ v_{sh} = \frac{60 - 30}{132 - 30} = \frac{30}{102} = 0.29 = 29\%$$

Therefore volume of shale 29% and volume of sand 71%

For ϕDsh (read of ρ_{log} from any shale zone), by equation (X_1)

$$(\phi D) \quad = \frac{\rho_{ma} - \rho_{\log}}{\rho_{ma} - \rho_{flui}}$$

ρ_{ma} shale = 2.67 (constant)

ρ_{log} (from any shale zone = 2.45)

$$= \frac{2.67 - 2.45}{2.67 - 1.1}$$

$$= \frac{0.22}{1.57} = 0.14 = 14\%$$

By substitute in equation (X_3)

$$\phi e = 0.26 - 0.29 \times 0.14 = 0.26 - 0.04 = 0.22 = 22\%$$

For water saturation (S_W). By substitute in equation (X_4)

$$S_W = n\sqrt{\frac{aR_w}{\phi_e^{\,m} Rt}}$$

Where:

R_w = 0.23 ohm (constant)

ϕe = 0.22

Rt = deep resistivity reading from log

$$SW = \sqrt{\frac{1 * 0.23}{(0.22)^2 * 900}} = = \sqrt{\frac{0.23}{43.56}} = \sqrt{0.005} = 0.07 = 7\%$$

Therefore water saturation = 7%

Oil saturation = 93%

3-7-3. Zone (b). From 1873 m. to 1880 m.

a. Thickness of the zone 7m.

b. Gamma ray

- Gamma ray reading 52 API
- G.R sand 30 API
- G.R shale 123 API

c. Resistivity (R_t) deep reading = 250 ohm.m

d. Density 2.25 g/cc

e. Neutron porosity 21%

f. S.P 8mv

g. Porosity (ϕD).

Using equation X_1

$$(\phi D) = \frac{\rho_{ma} - \rho_{\log}}{\rho_{ma} - \rho_{flui}}$$

$$= \frac{2.65 - 2.25}{2.65 - 1.1} = 0.26 = 26\%$$

Average porosity = $\frac{26 + 21}{2} = 23.5\%$

Effective porosity (ϕe).

By using equation X_3

$\phi e = \phi D - Vsh * \phi Dsh$

Where:

$\phi D = 26\%$

For V_{sh} , by using equation X_1

$$Vsh = \frac{GR_{\log} - GR_{ma}}{GR_{sh} - GR_{ma}} = \frac{52 - 30}{132 - 30} = \frac{22}{102} = 0.215 = 0.22 = 22\%$$

Therefore volume of shale 22% and volume of sand 78%.

By substitute in X_3

$\phi e = 0.26 - 0.22 \times 0.14$

$= 0.26 - 0.03 = 0.23$

$= 23\%$

For calculation of water saturation (S_W), using equation X_5

$$S_w = n\sqrt{\frac{aR_w}{\phi_e^{\,m} Rt}}$$

Where:

R_w = 0.23 ohm (constant)

ϕe = 0.23

R_t = deep resistivity from log = 250 ohm.m

$$SW = \sqrt{\frac{1*0.23}{(0.23)^2 *250}} = \sqrt{\frac{0.23}{13.22}} = \sqrt{0.017} = 0.13 = 13\%$$

$\therefore S_W$ = 13% and oil saturation = 87%

Table (3) illustrate the formation evaluation of well number 16.

Table (3): Formation evaluation of well 16

Zone	Top	Bottom	Gross (m)	VSH	Net Sand	Porosity	Neutron	Average Porosity	ϕe %	Water Saturation
a	1646	1658	12	0.29	12	26%	0.24%	0.25%	22%	7%
b	1873	1880	7	0.22	7	26%	0.21%	0.235%	23%	13%

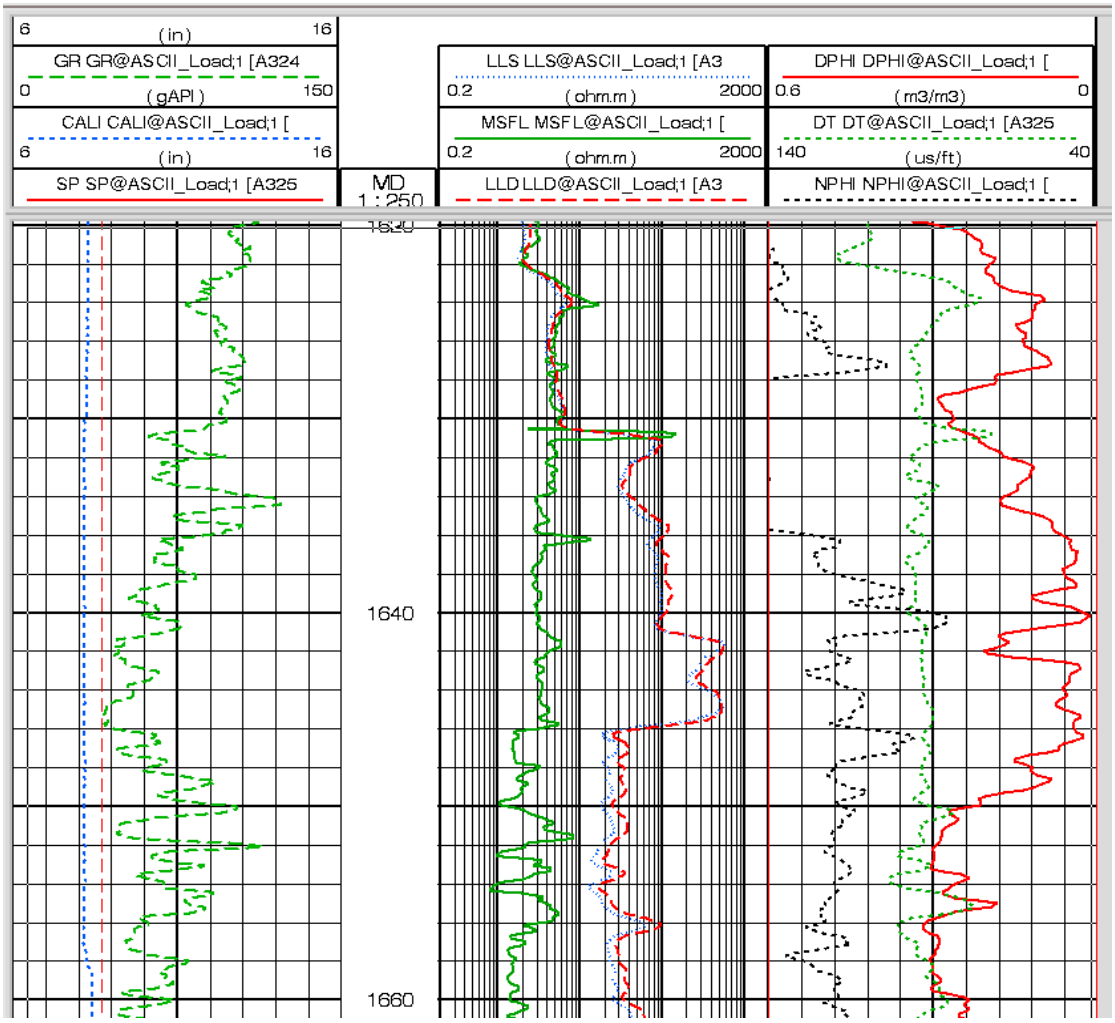

Figure (15) Log of well 16 shows the interested zone

3-8. Interpretation of Log of well number 15

Bentiu Formation in this well composed of sandstone of transparent to translucent un-consolidated, common poorly fine grain, sub angular to sub rounded, moderate sorted, quartz, common kaolinite cement occasional calcareous cement, traces mica, rare chlorite, and poor porosity.

This sandstone interbedded with claystone, reddish brown in color, occasional grey to dark grey, occasional moderate hard trace, silty, and slightly calcareous.

The oil show is common light brown oil stain, abundant even bright yellow fluorescence, abundant fast blooming bright milky white cut fluorescence, common light brown residual oil.

3-8-1. Selected zone

There is only one zone selected from log data which is between 1640 m to 1659 m. Figures (16).

a. thickness of zone is 19m

b. Gamma Ray

- Gamma Ray from log = 75 API
- Gamma Ray sand = 30 API
- Gamma Ray shale = 142 API

c. Resistivity (R_t) deep reading = 550 ohm/m

d. Density = 2.25 g/cc

e. Neutron porosity.

f. S.P 10 mv

g. porosity (ϕD), by using equation X_1

$$Porosity\ (\phi D) \quad = \frac{\rho_{ma} - \rho_{\log}}{\rho_{ma} - \rho_{flui}} \quad = \frac{2.65 - 2.25}{2.65 - 1.1} = \frac{0.4}{1.55} = 0.26 = 26\%$$

Effective (ϕe), by using equation X_3

$$\phi e = \phi D - Vsh * \phi Dsh$$

Where:

$$\phi D = 0.26$$

V_{sh} by equation X_1

$$V\,sh = \frac{GR_{\log} - GR_{ma}}{GR_{sh} - GR_{ma}} \quad = \quad \frac{75 - 30}{142 - 30} = \frac{45}{112} = 0.40 = 40\%$$

Therefore volume of shale 40% and volume of sand 60%

ϕD_{sh} equal 13% (constant)

$$\therefore \phi e = \phi e - Vsh * \phi Dsh$$

$$\phi e = 0.26 - 0.4x\ 0.13$$

$$= 0.26 - 0.05 = 0.21 = 21\%$$

For calculation of water saturation using equation X_4

$$S_w \ = \ n\sqrt{\frac{aR_w}{\phi_e{}^m\, Rt}}$$

Where:

R_W = 0.23 ohm.m (constant)

ϕe = 0.21

R_t = 550 ohm/ m. (deep resistivity-from log)

$$S_w = \sqrt{\frac{1 \times 0.23}{(0.21)^2 \times 550}} = \sqrt{\frac{0.23}{0.04 \times 550}} = \sqrt{\frac{0.23}{22}} = \sqrt{0.01} = 0.10 = 10\%$$

Therefore water saturation in this zone equal 10% and oil saturation equal 90%. Table (4) illustrated the petrophysical evaluation of well number 15. Appendix (C), shows the log of well 15 from 1725m to 1800m.

Table (4). Formation evaluation of well number 15

Top	Bottom	Gross (m)	VSH	Net Sand	Porosity	Neutron	Average Porosity	ϕe %	Water Saturation
1640	1659	19	0.4	11.5	26%	0.24%	0.21%	21%	10%

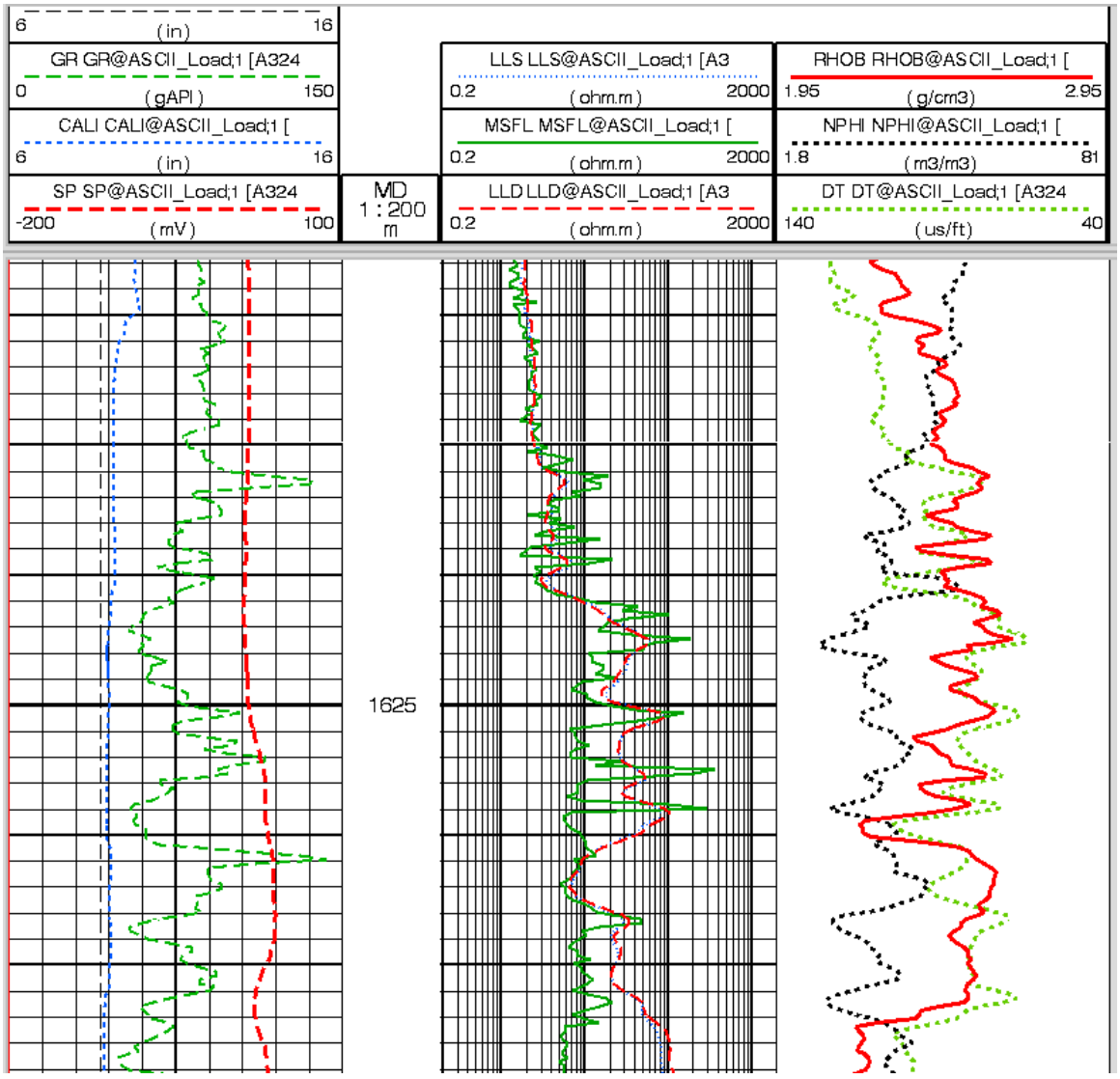

Figure (16) Log of well 15 shows the interested zone

3-9. Log interpretation of well number 35.

Bentiu Formation in this well composed of sandstone, translucent off white un- consolidated, medium to fine grained, sub angular to sub rounded, moderately sorted, quartz, common kaolinite cement.

This sandstone interbedded with claystone of medium grey, sub blocky, sticky, and non calcareous.

The oil show in this well is a yellow fluorescence, slow streaming to abundant fast blooming, yellowish white cut fluorescence, brown residual oil were observed.

From log interpretation the interesting oil zone on the log of well 35 appear at depth 1635 m, and depth 1665 m .Figure (17), where in this zone resistivity value high and gamma ray value very low.

In this interpretation of this well the interested zones as top Bentiu Formation appear at depth 1163m, Aradieba Formation at depth 1588m. Figure (18) and Zarga Formation at depth 1325m. Figure (19). Appendix (D) shows a calibrated log data of well (35).

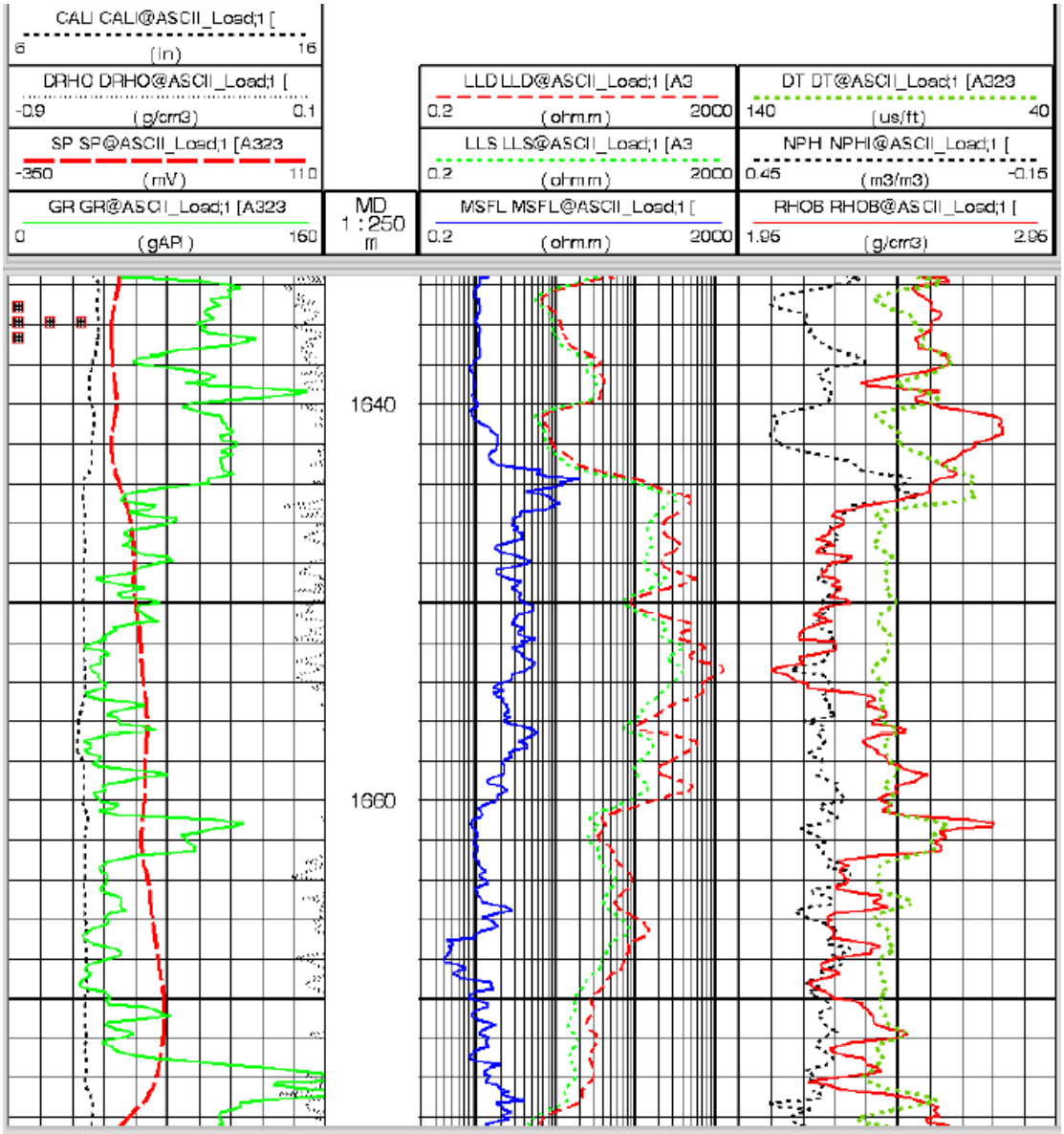

Figure (17) Log of well 35 shows the interested zones

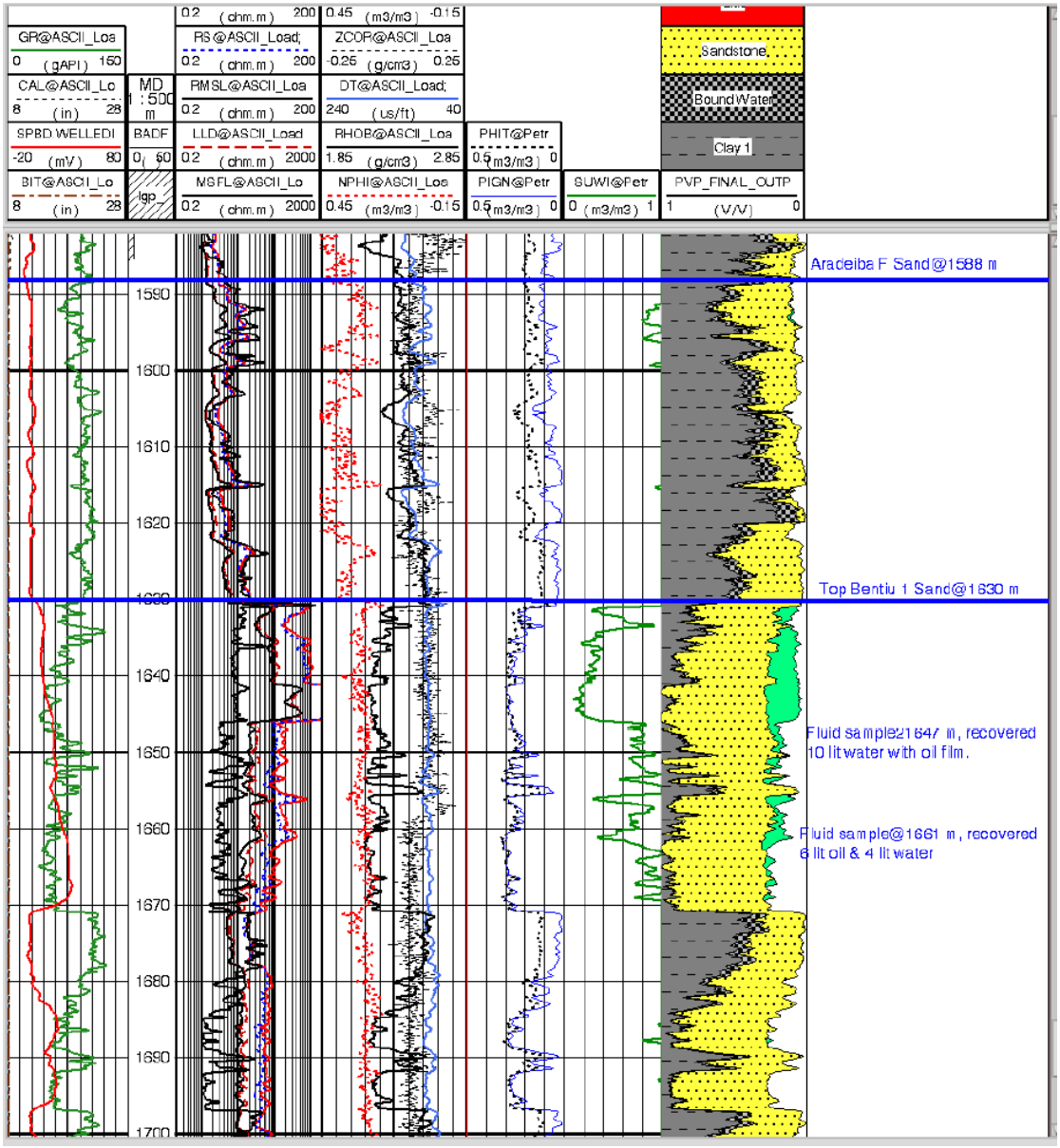

Figure (18) Interpreted log of well 35 show Top Bentiu Formation

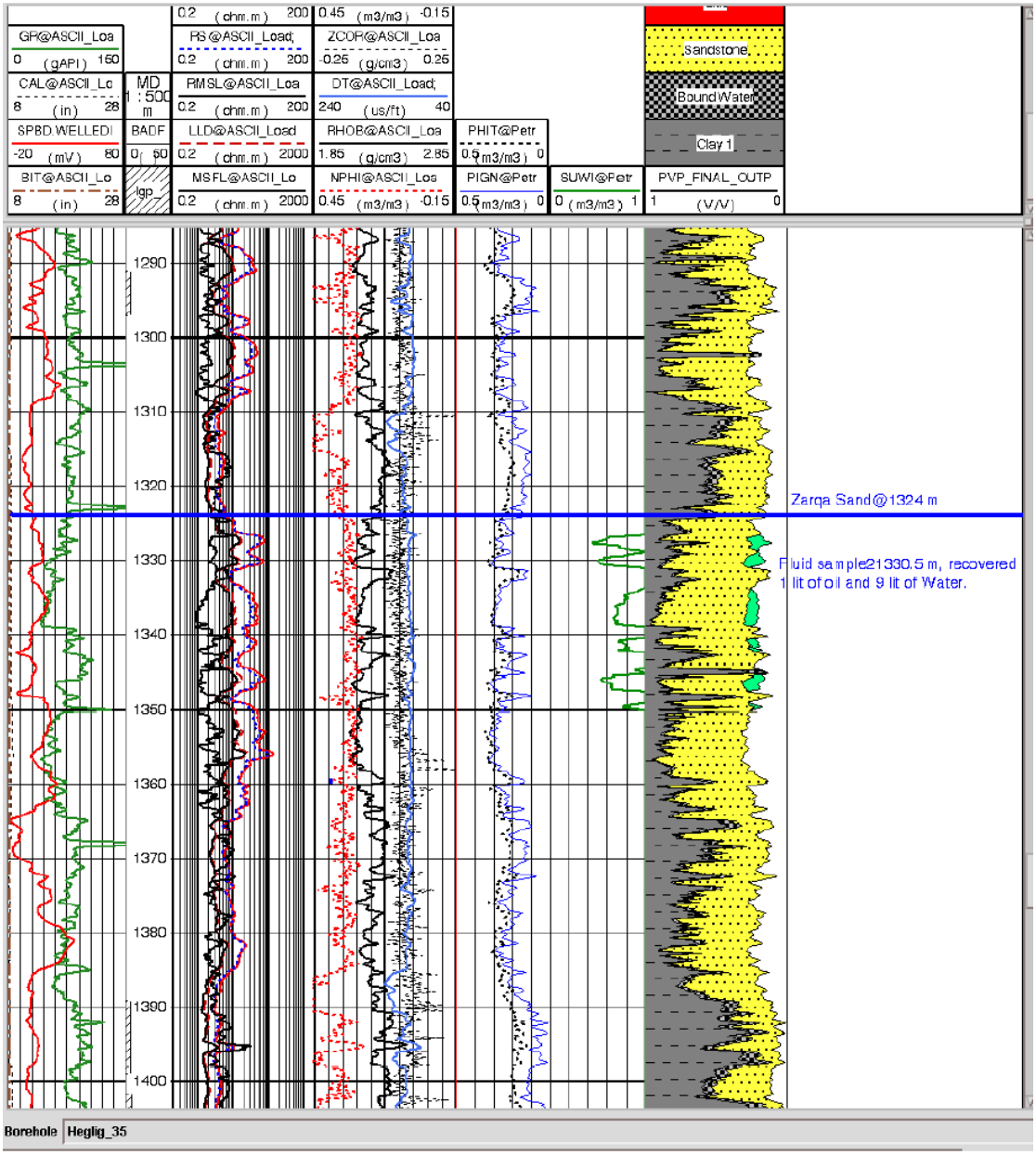

Figure (19) Interpreted log of well 35 shows Top Zarga Formation.

3-10. Indonesian equation

By Indonesian equation water saturation state that

$$Sw = \left[\frac{1}{\left(V_{sh}^{1-v_{sh/2}} / R_{sh}^{0.5} \right)} + \frac{\phi_e}{0.81 R_w^{0.5}} \right] x \frac{1}{R_t^{0.5}}$$

Where:

= Shale volume V_{sh}

= shale density 9/cc R_{sh}

= water saturation S_w

= formation resistivity - ohm/m R_t

= effective formation porosity % ϕ_e

= water resistivity - ohm/m R_w

3-10-1. Interpretation of log of well (22)

The same three productive zones in this well have been interpreted using this equation.

3-10-1-1. zone (a) from 1644m to 1661m.

The thickness of this zone equal 17m.

In substitute in Indonesian equation:

$$S_w = \left[\frac{1}{0.5^{1-0.2/2} / 2.35^{0.5}} + \frac{0.16}{0.81x\ 0.23^{0.5}} \right] x \frac{1}{600^{0.5}}$$

$= 6.21 \text{x} 0.04 S_w$

$= 0.24$

$= 24\%$

Water saturation equals 24% therefore oil saturation equals 76%

3-10-1-2. zone (b) from 1662m to 1672m.

The thickness of this zone = 10 m.
In substitute in Indonesian equation

$$S_w = \left[\frac{1}{0.14^{1-0.14} / 2.35^{0.5}} + \frac{0.19}{0.81x\ 0.23^{0.5}} \right] x\ \frac{1}{150^{0.5}}$$

= (4.084+0.489) x0.0816
= 4.573x 0.0816 = 0.37
= 37%
Water saturation equal 37%, therefore oil saturation equal 63%

3-10-1-3. zone (c) from 1528m to 1538

The thickness of the zone = 10m.
by substitute in equation:

$$S_w = \left[\frac{1}{0.14^{1-0.07/2} / 2.25^{0.5}} + \frac{0.24}{0.81x\ 0.23^{0.5}} \right] x\ \frac{1}{110^{0.5}}$$

= 4.784x 0.095
= 0.45 = 45%
Water saturation equal 45%. Therefore oil saturation 55%.

3-10-2. Interpretation of log of well (16)

The selected zones
a - From 1646 m to 1658 m
b – From 1873 m to 1880 m

3-10-2-1. Zone (a) from 1646 to 1658

The thickness of this zone equal 12m
In substitute in Indonesian equation

$$S_w = \left[\frac{1}{0.29^{1-0.29/2} / 2.25^{0.5}} + \frac{0.26}{0.81x\ 0.23^{0.5}} \right] x\ \frac{1}{900^{0.5}}$$

= 2.7x 0.0333 = 0.09 = 9%

Water saturation 9%, therefore oil saturation equal 91%

3-10-2-2. Zone (b) from 1873 m to 1880 m

The thickness of this zone 7m.

by substitute in Indonesian equation

$$S_w = \left[\frac{1}{0.22^{1-0.22/2} / 2.25^{0.5}} + \frac{0.23}{0.81x\,0.23^{0.5}} \right] x \frac{1}{250^{0.5}}$$

= 3.166 x 0.063 = 0.199 = 0.2

= 20%

Water saturation equal 20%, therefore oil saturation equal 80%.

3-10-2-3. Interpretation of log of well number (15).

The selected zone from 1640 m to 1659 m

The thickness of this zone 19 m

by substitute in Indonesian equation

$$S_w = \left[\frac{1}{0.4^{1-0.4/2} / 2.25^{0.5}} + \frac{0.21}{0.81x\,0.23^{0.5}} \right] x \frac{1}{550^{0.5}}$$

= 3x0.042 = 0.127 = 0.13 = 13%

Water saturation equal 13%, therefore oil saturation equal 87%.

3-11. Dual water equation

This equation state that:

$$S_w = \frac{1}{\phi_{sd}} x \left(\frac{R_w}{R_t} \right)^{\frac{1}{2}} - V_{sh} x \left(\frac{R_W}{R_c} \right)^{\frac{1}{2}}$$

Where:

= porosity of density ϕ_{sd}

= clay density R_c

= water resistivity R_w

= formation resistivity R_t

= shale volume V_{sh}

3-11-1. Interpretation of log of well (22)

i- Zone (a) from 1644 m to 1661m
by substitute in Dual equation:

$$S_w = \frac{1}{0.19} x \left(\frac{0.23}{600}\right)^{\frac{1}{2}} - 0.25x \left(\frac{0.23}{2.35}\right)^{\frac{1}{2}}$$

= 5.263 x 0.0195 – 0.078
= 0.02 = 2%
Water saturation equal 2%

ii – zone (b) from 1662m to 1672m.
by substitute in Dual equation:

$$S_w = \frac{1}{0.19} x \left(\frac{0.23}{150}\right)^{\frac{1}{2}} - 0.14x \left(\frac{0.23}{0.35}\right)^{\frac{1}{2}}$$

= 5.26 x 0.039 – 0.14 x 0.31
= 0.16 = 16%
Water saturation equal 16%.

iii – zone (c) from 1528m. to 1538m.
by substitute in Dual equation:

$$S_w = \frac{1}{0.26} x \left(\frac{0.23}{110}\right)^{\frac{1}{2}} - 0.14x \left(\frac{0.23}{2.25}\right)^{\frac{1}{2}}$$

= 3.846 x 0.045 – 0.14 x 0.319 = 0.13
= 13%
Water saturation equal 13%.

3-11-2. Interpretation of log of well (16)

i – Zone (a) from 1646m to 1658 m
by substitute in Dual equation:

$$S_w = \frac{1}{0.26} x \left(\frac{0.23}{250}\right)^{\frac{1}{2}} - 0.29x \left(\frac{0.23}{2.25}\right)^{\frac{1}{2}}$$

= 0.027 = 3%
Water saturation equal 3%.
ii – zone (b) from 1873m. to 1880m.
In substitute in Dual equation:

$$S_w = \frac{1}{0.26} x \left(\frac{0.23}{250}\right)^{\frac{1}{2}} - 0.22x \left(\frac{0.23}{2.25}\right)^{\frac{1}{2}}$$

= 0.115 – 0.07 = 0.045 = 4%
Water saturation equal 4%.

3-11-3. Interpretation of log of well (15)

The selected zone from 1640 m. to 1659 m
by substitute in Dual equation:

$$S_w = \frac{1}{0.26} x \left(\frac{0.23}{550}\right)^{\frac{1}{2}} - 0.4x \left(\frac{0.23}{2.25}\right)^{\frac{1}{2}}$$

= 0.76 – 0.127 = 0.048 = 0.05
= 5%
Water saturation equal 5%.

3-12. Simandoux equation

This equation state that:

$$S_w = \frac{0.4 x R_w}{\phi_e^{\,2}} x \left[\sqrt{\frac{5x\,\phi_e^2}{R_W X R_t} + \frac{V_{sh}}{R_{sh}}} - \frac{V_{sh}}{R_{sh}} \right]$$

Where:

Water resistivity $R_{w=}$

= effective porosity ϕ_e

= formation resistivity R_t

= shale volume V_{sh}

= shale resistivity R_{sh}

3-12-1. Interpretation of log of well (22)

i – Zone (a) from 1644m. to 1661m.

In substitute in Simandoux equation

$$S_w = \frac{0.4x\,0.23}{0.16^2} x \left[\sqrt{\frac{5x\,0.16^2}{0.23x\,600} + \frac{0.25}{600}} - \frac{0.25}{600} \right]$$

(There is small difference between formation resistivity and shale resistivity, therefore substitute as the same value)

= 3.593 x 0.036 = 0.13 S_w

= 13%

Water saturation is equal to 13%

ii – zone (b) from 1662m. to 1672m.

by substitute in Simandoux equation

$$S_w = \frac{0.4x\,0.23}{0.172} x \left[\sqrt{\frac{5x\,0.17^2}{0.23x\,150} + \frac{0.14}{150}} - \frac{0.14}{150} \right]$$

= 3.183 x (0.071 – 0.0009)

= 0.224 = 22%

Water saturation is equal 22%.

iii – zone (c) from 1528 m to 1538 m

In substitute in Simandoux equation

$$S_w = \frac{0.4x\,0.23}{0.24^2} x \left[\sqrt{\frac{5x\,0.24^2}{0.23x\,110} + \frac{0.14}{110}} - \frac{0.14}{110} \right]$$

= 1.59 x (0.111 – 0.001)

= 0.175 = 18%

Water saturation is equal 18%.

3-12-2. Interpretation of log of well (16)

i – Zone (a) from 1646m. to 1658m.

In substitute in Simandoux equation

$$S_w = \frac{0.4x\,0.23}{0.22^2} x \left[\sqrt{\frac{5x\,0.22^2}{0.23x\,600} + \frac{0.29}{600}} - \frac{0.29}{600} \right]$$

= 0.09 = 9%

Water saturation is equal 9%.

ii – zone (b) from 1873m. to 1880m.

by substitute in Simandoux equation

$$S_w = \frac{0.4x\,0.23}{0.23^2} x \left[\sqrt{\frac{5x\,0.23^2}{0.23x\,250} + \frac{0.22}{250}} - \frac{0.22}{250} \right]$$

= 1.739 x (0.0739 – 0.00088)

= 0.127 = 0.13

Water saturation is equal 13%.

3-12-3. Interpretation of log of well (15)

The selected zone from 1640 m to 1659 m

by substitute in Simandoux equation

$$S_w = \frac{0.4x\ 0.23}{0.21^2} x \left[\sqrt{\frac{5x\ 0.21^2}{0.23x\ 550} - \frac{0.4}{550}} - \frac{0.4}{550} \right]$$

= 2.09 x 0.0315 = 0.065

= 0.07 = 7%

Water saturation equal 7%.

Table (5), shows water saturation percentage of wells, 22, 16 and 15, by the four models.

Table (5) SW% of wells using application from models

Wells	Zones	Archie	Indonesia	Dual water	Simandoux
22	a (1644-1661)m	12%	24%	2%	13%
	b (1662-1672)m	23%	37%	16%	22%
	c (1528-1538)m	16%	45%	13%	18%
16	a (1646-1658)m	7%	9%	3%	9%
	b (1873-1880)m	13%	20%	4%	13%
15	(1640-1659)m	10%	13%	5%	7%

Chapter (4)

Results and Discussion

4-1. Characteristic of Reservoir Formation from well log analysis

The economic value of oil fields is determined to considerable extent, by the physical properties of the reservoir rocks, reservoir fluids, and reservoir capacity.

The main physical properties of rocks and fluids that characterize oil reservoirs from the production stand point are the following:

i- Total and effective porosity.

ii- Permeability.

iii- Saturation of rocks with oil, gas and water.

In the interpretation of log data of well number 16, well number 15, well number 22, and well number 35, the values of porosity for each sand layer of reservoir formation reveal decrease in it with depth, and this is due to the pressure of the weight of the upper formations. Figure (20), illustrate this fact when this porosity values plotted against depths.

In relation to the values of water saturation, the amounts of water vary in these wells, on which oil could not completely displace the water from the porous medium of this formation.

Therefore, in plotting the values of water saturation that determined by Archie equation against depths, (Figure 21), this plot shows the follows:

a- Water saturation increase with depth, and because the specific gravity which cause the water to occupy the lower structure of the oil trap of the reservoir formation.

b- Water saturation increases laterally to the south direction of the study area. (Schull 1988)

4-2. Comparisons of different models in determination of water saturation

Comparison between these different models lead to different idea can be gathered from this comparison. The Archie's formula used for calculating water saturation always has been used in a shale-free reservoir, therefore it has been widely used by many log analysts especially when dealing with clean sand reservoir, but in evaluating shale-sand reservoir; Archie formula may give a misleading result. This is because Archie formula assumes that the formation water is the only

electrically conductive material in the formation. The shale effect on various log responses depends on the type, the amount, and the way it is distributed in the formation.

Archie model was used to generate abase value. It is known that in a shaly sand formation, this technique over estimated the values of water saturation. Thus in a shaly formation, a shaly sand model should yield a saturation value less than that given by Archie model.

The Indonesia equation was developed based on the typical characteristic of fresh formation waters and high degrees of shaliness that presents in many oil reservoirs.

In the comparison of the result in calculation of water saturation between all models, Archie, Indonesia, Simandoux, and Dual water, in which all values are differ, the water saturation calculated from Dual water are approximately lower than the other values.

4-3. Results

From the analysis of log data of well number 15, well number 16, well number 22, and well number 35, depths of reservoir formation can be determined. Focusing in Bentiu Formation shows depth vary from 1625 m to 1948 m. In this depth the interpretation of well number 22, shows SP reading up

to 80 mv, gamma reading less than 90 API, low reading bluck density less than 2.25 g/cc, and high deep resistivity reading reach 750 ohm.m. Therefore value of these reading indicates a sandstone formation containing oil.

In the interpretation of log data of well (15), reveal a sand stone layer at Bentiu Formation between depths 1640 and 1659 on this layer oil saturation reach up to 95% (In Dual water model), and 90%. (In Archie model), and water fill the rest.

In well number 16, sandstone layers of Bentiu formation reveal at depth 1625 up to depth 1970 m., and the interpretation of this well log data reveal an interesting thickness between depths 1646 to 1658, where a high SP reading 10 mv, gamma reading 60 API, low density less than 2.25 g/cc, and high deep resistivity reach up to 1000 ohm.m, this sandstone layers shows 97% oil saturation. (In Dual water model), and 93%. (In Archie model).

In other zone of the same well, between depths 1873 m and 1880 m. a value of a high SP reach 8 mv, low gamma less than 60 API, and density of 2.25 g/cc, and resistivity 600 ohm.m, in this zone oil saturation reach 96%. (In Dual water model), and 87%. (In Archie model).

In well number 22, Bentiu Formation have a thickness from 1645 up to 1981 m, all these thickness composed of varying texture sandstone, interbeded by reddish brown to brown claystone. The interpretation of this well show interesting zones between 1645 to 1659 m, of SP reading 60 mv, density less than 2.25 g/cc, these reading indicate present of sand, and shallow and deep resistivity reach to 1500 ohm, which these indicate present of oil, of saturation reach 88 %. (In Archie model), and reach 98% (In Dual water model).

In the same well other zone between 1662 m to 1672 m, SP reading reach 80 API, gamma Ray less than 60 API and density less than 2.25 g/cc, therefore sand is dominant, and resistivity reach up to 200 ohm.m, the oil saturation is lower and water saturation reach up to 23%. (In Archie model), and reach 16%. (In Dual water model).

The interpretation of well number 35, show positive zone at depth 1635 to 1665, this zone show high resistivity value, low gamma ray, therefore this zone shows high saturation of oil.

The percentages of oil saturation which calculated from the interpretation logs data, shows the concentration of oil increase towards the north - west part of the study area and this saturation varies according to the variation of water saturation values. Therefore water saturation values vary in each calculated

equation, Archie, Indonesian, Dual water, or Simandoux model. In this case different oil estimations records one of them give an approximately true oil content i.e. true water saturation than the other equation. This variation is due to the present of clayey layer among sand formation i.e. oil bearing formation.

Archie is not good model for estimating water saturation in shaly sand formation as our study area; therefore it is not a proper equation to use for water saturation in this field, where as Dual water equation is the best for this study calculation. Because the shale and clay mineral has the bound water within, where this bound water decrease the resistivity value, therefore the log evaluation influence by the effects of shale and clay mineral in the result estimation of water saturation. Whereas the type and volume as well as the distributions of shale and clay with respect to the pay sand, in which the presence of bound water within clay minerals, that occur to the present of surface conductivity of the clay and clay water system.

In this study area shows laminated clays which a thin layers of clay between layers of sand, therefore when we used different models for calculation of water saturation we have different values, but the models that put in conceder clay minerals show the right result example, Dual Water model, that shows low water saturation value for the wells in this study area,

which the true value, and it's not influence by the present of additional conductivity value from the bound water clays minerals, and this lead to safe value of original oil in place or original gas in place in the study area.

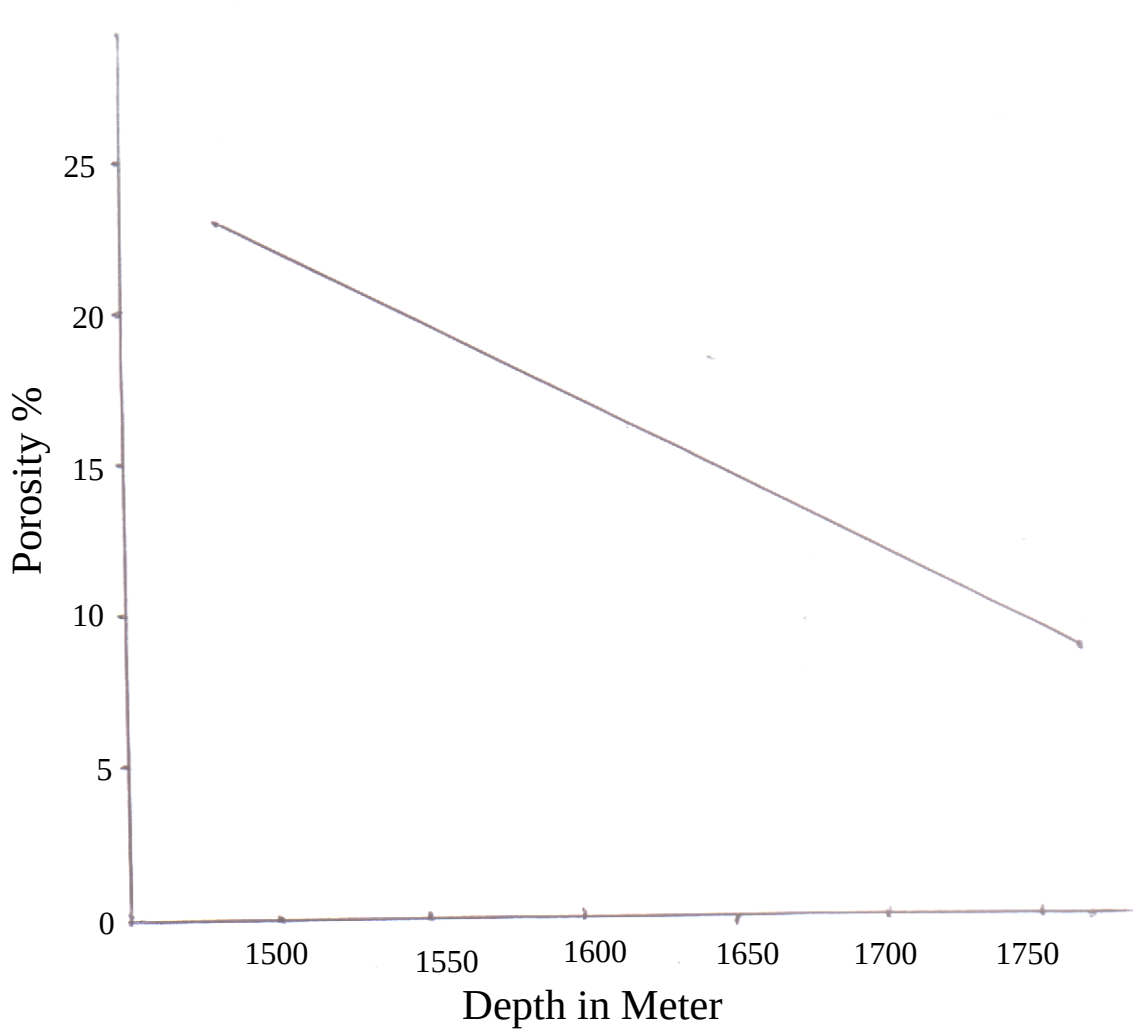

Figure (20) Porosity vs. depth from logs of wells in the study area

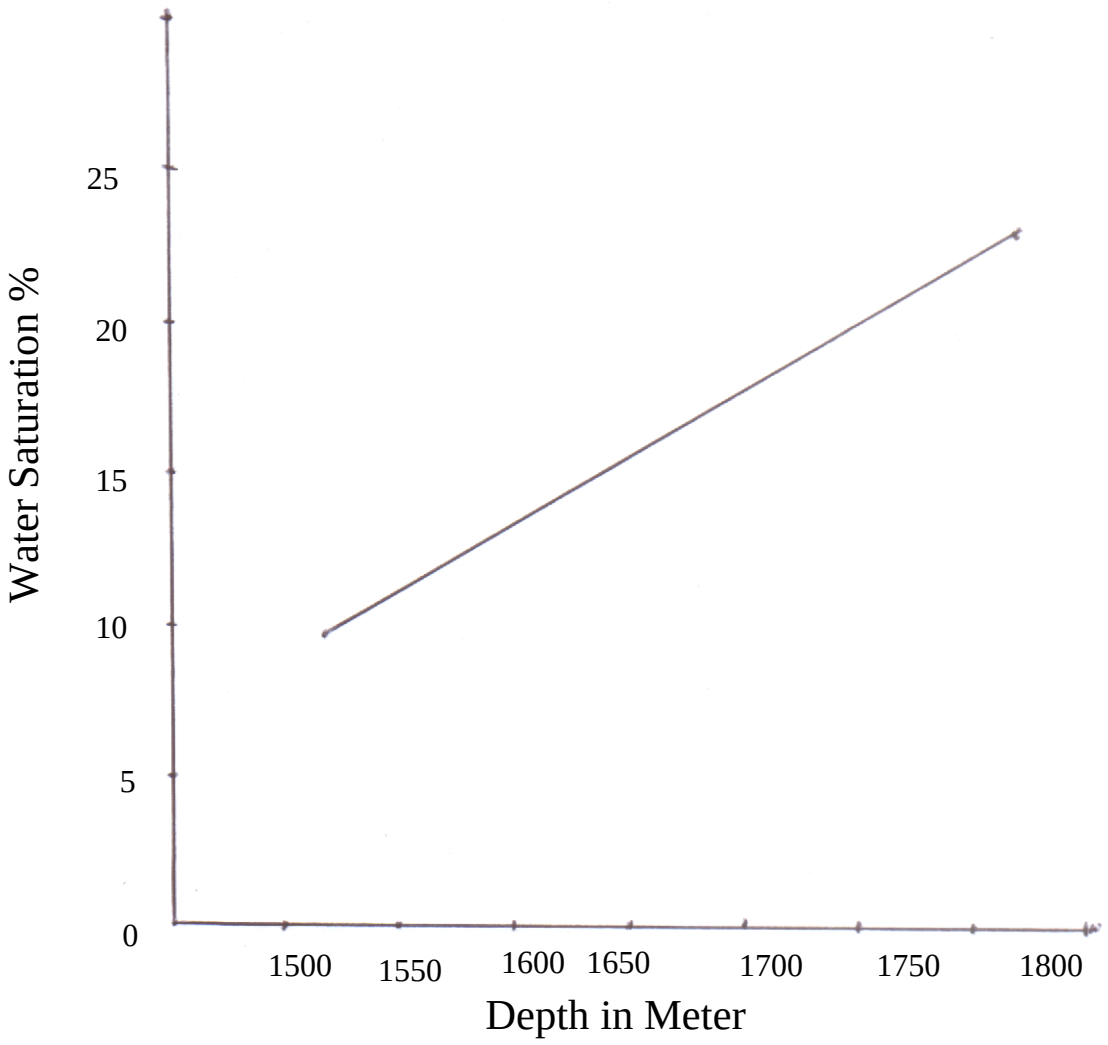

Figure (21) Water saturation vs. depth of wells data on the study area

Chapter (5)

Conclusion & Recommendations

5-1. General conclusions

The future of the oil industry in Sudan will depend on a more research than totally relays on discovered locations. Therefore; the geological, geophysical and engineering information have to be integrated to cover all possible potential from the ground.

The largest producer of oil field in the Muglad Basin is Unity Field in southern Sudan followed by the Heglig Field in the Sudan, but the significance of this study may make the Heglig Field, the largest producing field in the Muglad Basin and in Sudan in general.

The formation evaluation techniques plays a fundamental role in the hydrocarbon exploration and production process, it is being used in all the different phases of this process. Therefore in this study log application of current data has been done, and from these application the percentages of oil saturations, and water saturations, in this area, have been calculated.

Over the years, for shaly-sands a large number of models relating fluid saturation to resistivity have been developed

according to the geometric form of existing shale, (laminated, dispersed and structural).

In quantitative log interpretation accurate water saturation requires good values of parameters for being used either in Archie saturation equation in clean formation or in a shaly-sand water saturation model in shaly formation.

In this interpretation the value of water saturation is determined by using different equation, Archie, Indonesian, Dual water, and Simandoux equation. Variations on these values of water saturation have been detected by these calculations. These variations of water saturation lead to different values of oil saturation in the same oil bearing formation, and this due to the effect of shale content.

From this study the best equation to be used for water saturation and then oil content is Dual water equation.

5-2. Recommendations

All the petrophysical works of this study were dealt with the formation evaluation of oil reservoir in the study area in which the calculations of water saturation of a previous well data have been done by different models, Archie, Indonesian, Dual water, and Simandoux equation. Therefore, the author recommend more detailed study on the same area, using other

water saturation models in order to reach and accurate calculation of hydrocarbon content.

Also other reservoir development studies, for the most accurate determining of the amount of depletion, in specific producing layers of the large reservoir Bentiu Formation or Aradeiba Formation have to be considered.

Also the author recommends strongly the effective collection of data and adequate knowledge for resource management.

References

Abdel Salam, Y.1966: The Groundwater Geology of the Gezira. M.Sc. Thesis, University of Khartoum. (Unpubli).

Abdullatif, O.M., (1992): Sedimentology of late Jurassic/ Cretaceous/ Tertiary Strata of the NW Muglad and Nile rift basin, ph.D. Thesis, University of Khartoum.

Abdullatif, O.M (2002): Burial diagen and thermal maturity evaluation of the NW muglad rift basin, Sudan AAP

Cairo conference.

Ahmed Y.M., (1993): Depositional Models and Digenetic Events of the Sudan interior rift basins with Special Reference to Abu Gabra Formation, Muglad-Bentiu basin, Sudan. M.Sc. Thesis. University of Tokyo.

Ahmed Y.M., (1996): Organic matter Characterization and Environmental Control on Organic Facies and Lithofacies of Early Cretaceous Lake Assalam, north-west Muglad Basin, Sudan. Ph.D. Thesis, University of Tokyo.

Ahmed, A. S. (1983): Geology of South Central Sudan basins lithology and sedimentary evolution, Sudan .M.Sc. Thesis, University of Khartoum.

Amir, A.O, (2000): Sedimentology of the Cretaceous Outcropping Strata at the NE margin of the Muglad Rift Basin Western Kordofan State, Sudan, M.Sc. Thesis, University of Khartoum.

Andrew, G. and Yanni, K. G. (1945): Stratigraphic notes, Anglo-Egyptian Sudan. Sudan Notes and Records, v. 26, P. 157-166.

Archie, G.E. (1942): The Electrical Resistivity Log as An Aid in Determing Some Reservoir Characteristics. Trans. AIME 146, pp. 54-62.

Awad, M. Z. (1987): Facies interpretation and stratigraphy of the central Darfur region and some flora from north-western Sudan. M.sc. thesis, 120 pp., University of Khartoum.

Awad, M. Z. (1994): Stratigraphic, Palynological, and paleoeclogical studies in the east central Sudan (Khartoum and Kosti Basins) Late Juranic to Mid Tertiary. Berliner Genies. Abh. (A) 161.

Awad, M.Z. & Breir, F.E (1993): Oligo-Miocene to Quaternary Palaeoenvironment in Gezira area, central Sudan. In Thorweihe, U.&Schandelmeier, H (eds.).Geoscientific Research in Northeast Africa, 465-470, Rotterdam, Brookfiel (A.A.Balkema).

Awad, M.Z. & Schrank, E. (1992): Palynostratigraphy and Palynofacies of Late Jurassic to mid-Tertiary non-marine sediments, Blue Nile Rift Basin, Sudan. 8th Int. Palynol. Cong, Aix-en-Province. Abstr. 7, Aix-en-Province.

Bakr, I.M. (1995): Mesozoic and Cenozoic Sedimentary Facies of Muglad, Melut and Blue Nile Rift Basins. Ph.D. Thesis, University of Khartoum.

Ball, J. (1939): Contributions to the geography of Egypt (Cairo, Government Press) 30pp.

Barazi, N. (1985): Sedimentologie and Stratigraphic des Abyad-beckens (North-west Sudan). Berlinear Geowiss. Abh. A, V. 64, P. 85.

Bead Nell H.J.L. (1909): The Relation of the Nubian Sandstone and the crystalline rocks south of the Oasis of Kharga, Egypt. Geol. Soc. London 65, 41- 54.

Bermingham, P. M., Fairhead, J. D. and Stuart, G. W. (1983): Gravity study of the Central African Rift System: amodel of continental disruption, 2. Darfur domal uplift and associated Cainozoic volcanic rocks. Tectonophysics, v. 94, no. 1-4, P. 205-222.

Bosworth, W. and Marley, C.K. (1994): Structural and stratigrphyic evaluation OF Anza rift, Kenya. Tectonophysics. Vol. 236 P 93-115.

Brown, S. E. Fairhead, J. D. and Mohammed, I. I, (1985): Gravity study of the White Nile Rift, Sudan and its regional tectonic setting. Tectonophysics, v. 113, no. 1-2, P. 123-138.

Bussian, A.E., (1984): A comparison of shaly sand models, paper E, in 24th Annual Logging Symposium: Society of Professional Log Analysts

Chialvo, J. (1975): Contribution a la Geologie du confiuent Atbra-Setit. Etude des sites de barrage de Rumela et Burdana. Doctorate thesis, Univ. Grenoble, 203 P.

Clavier, C., Coates, G., and Dumanoir, J. (1984): Theoretical and Experimental Bases for the Dual Water Model For The Interpretation of Shaly Sands. SPEJ April 1984.

Crain, E.R., Manuel Garrido, Philip Mosher. (2000): Quantitative analysis of older logs for porosity and permeability. Lake Maracaibo, Western Flank Reservoirs, Venezuela. Geo Canada, Calgary, AB, May 2000.

Curtis, P.A.S. and Brinkmann, K. (1985): Geology of younger intrusive alkali complexes in the Southwestern Nuba Mountain, Sudan: results of reconnaissance mapping. Geol. Jahrb, Hannover, v. B 63, P. 3-41.

Dresser Atlas (1982): Well Logging and Interpretation Techniques, Dresser Ind. Inc.

Edmonds, J. M. (1942): The distribution of the Kordofan sand Anglo-Egyptian Sudan. Geol. Mag., V. 79, P. 18-30.

EL Amin, A.M. (2001): Depositional Environment Facies Architecture and Reservoir Geology of Omdurman Formation (Upper Cretaceous) around Khartoum, Sudan, M.Sc. Thesis, University of Khartoum.

EL Amin, M.B. (1993): Basin evolution and Sedimentary Facies with Special Reference to Oil Production in Muglad, Sudan. M.Sc. University of Portsmouth.

El Shafie, A. A. (1980): Contributions to the structure of central and southern Sudan. Proc. 5th Conf. Afr. Geol. Cairo, 1979, Ann. Geol. Surv. Egypt, v. 10, P. 1133-1137.

El Tayib, O. A. (1993): Sedimentology of Kordofan Group Sequences of the Melut Basin Southeastern Sudan. M.Sc. Thesis, University of Khartoum

Fairhead, J. D. (1986): Geophysical controls on sedimentation within the African Rift Systems. In Frostik. L. E. et al., (eds). Sedimentatation of the African Rift. Geological Society Special Publications No. 25 P. 10-18.

Fertl, W.H. and Hammack, C.W., (1971): A comparative look at Water Saturation in shaly pay Sand, in 12th Annual Logging Symposium Transaction: Society of Professional Logging Analysts.

Gadallah, R. (1994): "Reservoir Seismology" Geophysics in Non Technical Languages. Penn Well Publishng Company 1412 South Sberidan. Tulsa, Oklahoma741041.

GRAS & RRI. (1995): Accompanying geological notes to the 1:1,000,000 scale geological atlas of the Republic of the Sudan. Bulletin no. 40.130.

Hamada G.M. (1996): "An Integrated Approach to determine shale volume and Hydrocarbon Potential in shaly sand". Petroleum Engineering Dept. Faculty of Engineering, Cairo University, Giza, Egypt, SCA conference paper no. 9641.

Hamada G.M. (2003): Accuracy Analysis of Water Saturation Models in clean and shaly layers. Petroleum Engineering Department, Faculty of Engineering, Cairo University, Egypt. International symposium of the society. Core Analysts Presentation. Pau, France, 21- 24 September 2003.

Hassan, H.M. (1973): Fossil flora of Umm Badda, Omdurman-Sudan Notes and Records, 54, 153-167, Khartoum.

Hunting Geology and Geophysics LTD. (1969): Photo geological survey of the western Area: mineral Survey in three selected areas in Republic of the Sudan. Report to United Nations Development Programme, Khartoum. 58 pp. (Unpubl).

Hunting (1980): Mineral Exploration of Juba Area. (Regional Ministry of Finance, Industry and Economic Planning of Southern Regional Government, Democratic, Republic of Sudan).

Hussien, H.A. (1997): Sedimentology and Basin Analysis with Emphasis on Lithofacies and Reservoir Quality of Bentiu Formation, Sudan. M.Sc. Thesis, University of Khartoum.

Idriss, A. M. (2001): Depositional Environment and Reservoir Heterogeneity of Bentiu Formation (Albian-Cenomanian),

Muglad Rift Basin, Sudan. M.sc. Thesis, University of Khartoum.

IHS Energy (2006): An integrated database of petroleum exploration an production data for the Muglad Basin. GEPS reports. 1258 perly-Geneva Switzerland.

Jorgenson, J. G. and Bosworth, W. (1989): Gravity Modeling in the Central African Rift System, Sudan; Rift Geometries and Tectonic significance. J. of African Earth Sciences, V.8, 2/3/4, P. 283 -306.

Khattab, M. M. (1975): Sedimentary basins in North-east Kordofan, Sudan, indicated by a gravity survey. Egypt. J. Geol. 19, 1, 77- 85, Cairo.

Kheiralla, M.K. (1966): A study on the Nubian Sandstone Formation of the Nile Valley between Latitudes 14° N, and 17° 42' with reference to the Groundwater Geology. M.Sc. Thesis. University of Khartoum.

Klitzsch, E. (1984 (a)): Northwest Sudan and bordering areas: Geologic development since Cambrian time. In: Klitzsch, E., et al. (eds.), Berliner Geowiss. Abh. Reihe A/B and 50. Reimer-Veriag, Berlin, P. 23-45.

Klitzsch, E. (1984 (b)): Palaeozoic strata of southern Egypt and northern Sudan. J.Afr. Earth Sci., Abstr. V.1, no. 3-4, P. 363.

Klitzsch, E. and Lejal-Nicol, A. (1984): Flora and fauna from strata in southern Egypt and northern Sudan (Nubia and surrounding areas). Berliner Geowiss. Abh. Reih. A, V. 50, P. 47- 79.

Klitzsch, E., and Wycisk, P. (1987): Geology of the sedimentary basin of northern Sudan and bordering areas. In: Klitzsch, E., and Schrank, E. (eds.), Research in Egypt and Sudan. Berliner Geowiss. Abh. Reimer- Verlag, P. 97-137.

Kumiawan (2002): "Evaluation of the hydrocarbon potential in low salinity shaly sand" M.Sc. thesis Department of Petroleum engineering, Agricultural & Mechanical College, Louisiana state University.

Lau, M. N. and Bassiouni, Z., (1990 (a)): Development and Field Application of Shaly Sand Petrophysical Models Part 1: The Conductivity Model. SPE Publication, SPE 20386.

Lau, M. N. and Bassiouni, Z., (1990 (b)): Development and Field Application of Shaly Sand Petrophysical Models Part II: The Conductivity Model. SPE Publication, SPE 20387.

Moawia, K.O. (1983): The Geology of the Nubian Sandstone Formation in Sudan.

Mohamed, A.Y. (1996): Basin analysis and hydrocarbon maturation, Unity-Kaikang area, Muglad Basin, Sudan. PhD thesis (Un publ.). Aberdeen University, UK. 246p.

Mohamed, A.Y., Pearson, M.J., Ashcroft, W.A., Lliffe, J.E., Whiteman, A. J (1999): Modelling Petroleum generation in the southern Muglad Basin, Sudan. American Association Petroleum Geologists Bulletin, 83, 1943-1954.

Mohamed, A.Y, Ashcroft, W.A, Whiteman, A.J (2001): Structural development and crustal stretching in the Muglad Basin, southern Sudan. Aberdeen University, Kings College. J, Afr. Earth Sci. Vol. 32, No. 2, pp. 179-191.

Mohammed, A.S. (1997): The Sedimentology of the Lacustrine- Fluvial Sharaf and Abu Gabra Formation (lower Cretaceous). NW Muglad Rift Basin. Sudan. M.Sc. Thesis, University of Khartoum.

Omer, M. K. (1975): Genesis and diagenesis of the Nubian Sandstone Formation in Khartoum Province. Sudan Geol. Miner. Resour. Dep. Bull., 27 P.

Omer, M.K. (1983): The geology of the Nubian Sandstone Formation in Sudan, 209 pp. (Geol. Min. Resor. Dept., Ministry of Energy and Mining, Sudan), Khartoum.

Omer, M.K, and Perriaux (1976): La Formation Des Cre's de Nubie Dans La Prôvince de Khartoum – Sudan. Quatriéme réuion des Sciences de La temer, Paris, P.312.

Passey Q.R., Greaney J. B., Kulla, F.J., Moneti and Stroud, J.D. (1990). Apractical Model for Organic Richness from Porosity and Resistivity Logs. AAPG Bull. December. v. 74, p. 1777-1794.

Poupon, A., Clavier, C., Dumanoir, J., Gaymard, R. and Misk, A., (1970): Log Analyses of Sand-shale Sequences – Asystematic Approach: JPT (July 1970).

Poupon, A. and Leveaux, J. (1971): Evaluation of Water Saturation in Shaly Formation. Trans. SPWLA 12th Annual Logging Symposium, pp. 1-2.

RRI. (1991): The Geology and Petroleum Potential of Southern, Central and Eastern Sudan.Vol.1 Executive Summary.

Russegger, J. (1838): Ueber das Vorkommen Und die Verarbeitung des Raaseneisensteins augden Savannen des

nordlichen Kordofans-und uberdas Vorkommen des Goldes gebbel Tira im Lande Nuba (On the Occurrence and distribution of laterites on the Savannahs of northern Kordofan and on the occurrence of gold at jebel Tira in the Nuba district) Arch Mineral, v. 11, p. 315-331 (In German).

Sadig, A.A. and Vail, J.R. (1985): Geology and regional gravity traverses of the Nuba Mountains, Kordofan Province, Sudan. J.Afr. Earth Sci.

Salama, R.B. (1997): Rift Basins of the Sudan, (In Shelley, R.C: African Basin Elsevier Publications), PP.105- 148.

Sandford, K. S. (1935): Geological observation of the Northwest frontier of the Anglo_Egyptian and the adjoining part of the South Libyan Desert. Q. J. Geol. Soc. London, v. 91, no. 3, p. 323-381.

Schandelmeir, H., Klitzsch, E. F., and Wycisk, P. (1987): Structural Development of North East Africa since Precambrian times. Berliner Geowiss. Abh. A, S. 24

Schandelmeir, H. (1988): Pre-Cretaceous intraplate basins of NE. Africa. Episodes. 11, 4,270- 274 Ottawa.

Schlumberger. (1987): Log Interpretation Principle Application. New York.

Schrank, E (1987b): Paleozoic and Mesozoic Palynomorphs from north east Africa (Egypt and Sudan), with special reference to Late Cretaceous pollen and dinoflagellates. Berliner geowiss. Abh. A 75. 249-310. Berlin.

Schrank, E (1990): Palynology of the clastic Cretaceous sediments between Dongola and Wadi Mugaddam, northern Sudan. Berliner geowiss. Abh, A 120. 1, 149-168, Berlin.

Schull, T. (1988): Rift Basins of Interior Sudan, Petroleum Exploration and Discovery AAPG-V. 72, No. 10 P. 1128-114.7.

Selly R. C. (1998): Elements of Petroleum Geology (Second edition), New York, 470p

Silva, P. and Bassiouni, Z., (1985): A shaly Sand Conductivity Model Based on Variable Equivalent Counter-Ion Conductivity and Dual Water Concepts, SPWLA Trans., paper RR.

Silva, P. and Bassiouni, Z., (1987): Prediction of Membrane Potentials in Shales and Shaly Sands Using the S-B Conductivity Model. The log Analyst, March-April 1987, pp. 129-137.

Simandoux, P. (1982): Dielectric Measurements in Porous Media and Application to Shaly Formation. Revue del,Institut Fracais du Petrole, Supplementary Issue, 1963, pp.193-215. (Translated text in SPWLA Reprint Volume Shaly Sand, July 1982).

Smits L. J.M., (1968): SP Log Interpretation in Shaly Sands. J.P.T. June 1968, pp. 123-136.

Strojexport (1977): Geophysical investigation of groundwater structures, central and Northern Upper Nile Province. Fifth stage, (Khartoum: Ministry of Agriculture Food and Natural Resources Rural Water Corporation).

Thomas E.C. (1976): The Determination of Qv from Membrane Potential Measurements in Shaly Sand. Journal Pet. Tech., Sept 1976.

Vail, J.R (1970): Interpretation of satellite photographs of the Red Sea and Gulf of Aden. R.Soc. London, phil. Trans., Ser. A, V.267, P. 38-40.

Vail, J. R. (1971): Review of A. J. White man, 1971. The geology of the Sudan Republic. Sudan Notes and Records, v. 52, P. 120-123.

Vail, J.R. (1973): Outline of the geology of the Nuba Mountains and vicinity, S.Kordofan Province, Sudan. Geol. Min. Resour. Dep. Minist. Ind. Min. Bull., V. 23, P. 24.

Vail, J. R. (1974): Distribution of Nubian Sandstone Formation in Sudan and Vicinity. Bull. Am. Assoc. Pet. Geol., v. 58, no. 6, P.1025-1036.

Vail, J.R. (1978): Outline of the geology and Mineral Deposits of the Democratic Republic of the Sudan and Adjacent Areas. Over Seas Geol. Miner. Resources, 1 GS, London, Vol.49, P.68.

Waxman M.H. and Simits, L. J. (1968): Electrical Conductivities in Oil-Bearing Shaly-Sands, J.P.T., June 1968, pp.107-122.

Whiteman, A.J. (1971): The Geology of the Sudan Republic Calendon press. Oxford.

Woodhouse, R. Warner, H.R. Shell, **J., (2004):** Improved Log Analysis in Shaly-Sandstones-Based on S_w and Hydrocarbon Pore Volume Routine Measurements of Preserved Cores Cut in Oil-Based Mud, Journal Petrophysics, Volume 45, Number 3.

Worthington, P., (1985): The Evolution of Shaly-sand Concepts in Reservoir Evaluation. The Log Analyst, Jan-Feb. 1985, pp.23-40.

Worthington, P. F and Johnston, P.W. (1991): Quantitative Evaluation of Hydrocarbon Saturation in Shaly Freshwater Reservoir. The Log Analyst, v.32, no. 4, 1991, pp. 356-368.

Wycisk, P (1987): Contributions to the subsurface geology of the Misaha Trough and southern Dakhla basin (S.Egypt/ N.Sudan). Berliner Geowiss. Abh. A 75, 137-149, Berlin.

Appendix (A)

GeoFrame / IESX

IESX

Starting IESX

- One way to start IESX is to select in the 'Seismic' section of the product catalog in the **Process Manager** - and start it like any regular GeoFrame module. This will bring up the 'IESX Session Manager', from which you can start the various IESX applications.
- An other way to start the IESX Session manager is to choose the 'Seismic' icon in the 'Applications Manager': it will start the 'Seismic Catalog':

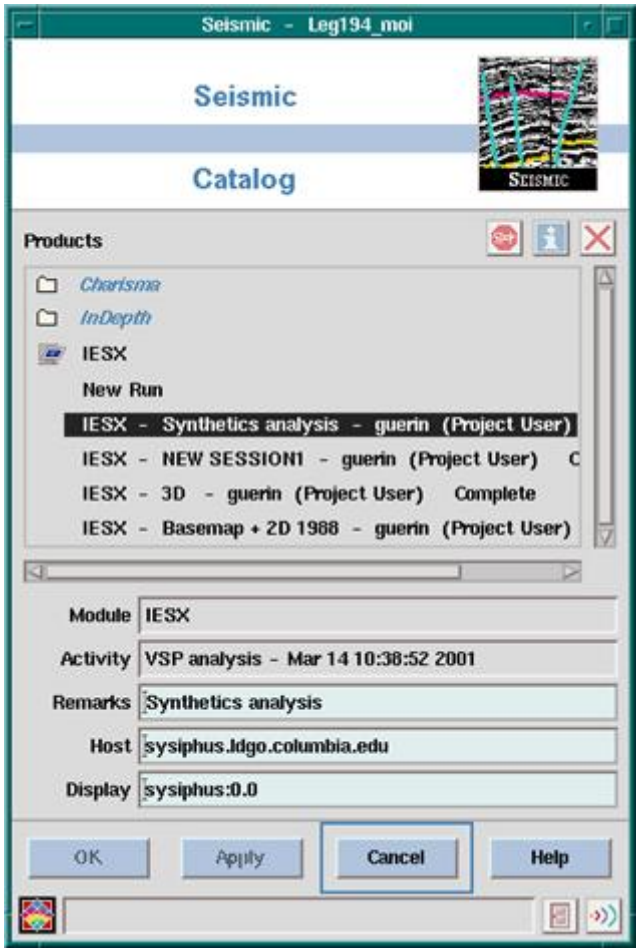

By clicking on the icon to the left of 'IESX', you can display previous sessions. A session can represent different kinds of data, different types of interpretations, different stages in a project, or only different ways to display things.

The IESX Session manager

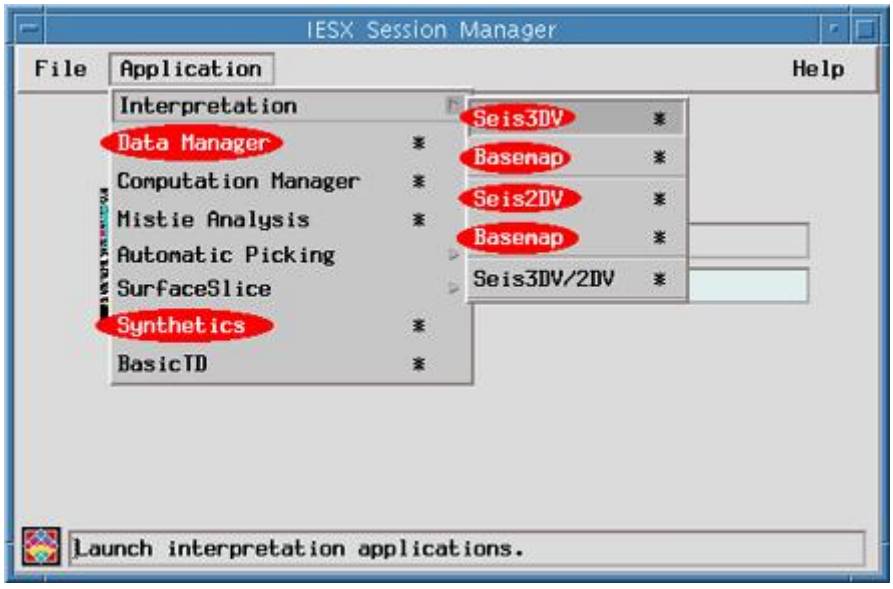

Pulling down the 'Application' menu displays all the IESX applications, among which the most commonly used are:
- *IESX Data Manager* (for loading, editing, sharing, deleting,... seismic data)
- *Basemap* (for viewing maps of the survey lines),
- *Seis2DV / Seis3DV* (for viewing and interpreting seismic data, and adding downhole log data),
- *Synthetics* (for generating synthetic seismograms).
Notes:

- GeoFrame applications - and IESX applications in particular - use up a lot of colors. Thus frequently, when starting any of the applications you may get the following error pop up (with some variations in the messages).

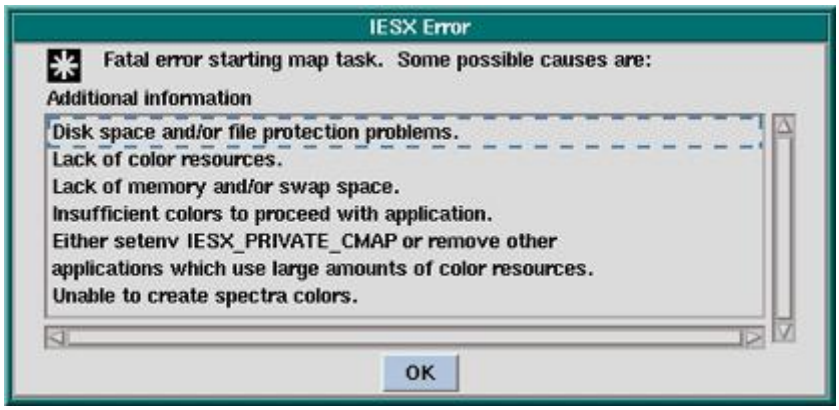

The 'Fatal' in the message is a gross overstatement...

If you have only one monitor, it is almost impossible to have two IESX windows opened simultaneously (i.e. Seis2DV/3DV and basemap - the data manager is not a big color sucker). If you iconify the already open window (press the second button from right in the upper right corner of the window), you should be able to open the application - and then you have to juggle between the icons and the windows, iconifying one before restoring the other. To save color memory, exit all unnecessary windows: the Geonet window, the Project Manager, and any non-GeoFrame window.

Closing IESX - saving sessions

A session will save not only what data were displayed when you saved it, but everything what was present in any IESX windows that were open when you saved it and the location/size of the windows in your screen. It is a convenient way to preserve particular configurations when working on a specific part of the survey, or on a specific type of interpretation or processing.

To save a session: select '**File/Save as...**' in the IESX Session Manager and enter the name of your session - or enter the name of your session in the area for this in the IESX Session Manager - and select '**File/Save**' .

When you exit IESX, you don't need to exit from the individual applications. Exit from the IESX Session Manager, and you will be given the option to save the session one last

time. The next time you open the IESX Session Manager, if you don't select a specific session, it will open the way you closed it the last time.

The IESX Data Manager

The IESX Data Manager allows you to import/export seismic data, to edit (delete, rename, copy...) seismic data, to share seismic data between projects and to export IESX-generated data such as synthetic seismogram, wavelets,....

To start it : **Application/Data Manager** in the IESX Session Manager:

Most command names are somewhat self explanatory, some are pretty obscure and not that useful - the most useful are:

'**Report...**' provides a general information summary for existing seismic volumes - the size, the sampling rate, number of samples, number of traces, some global statistics,... a quick way to check that all data were loaded.

'**Delete...**' - to delete classes of seismic data. A class is a version of seismic data, such as filtered, migrated, ...

'**Share...**' - to share seismic data between different projects and/or users - this can be very useful to save disk space, especially for large data sets.

'**Load Seismic...**' is the real piece of work to load SEG-Y seismic data.

'**2D surveys...**' - to move lines between 2D surveys.

'**Load 2D locations**' - to load navigation data which are necessary to locate your seismic data in space. In a perfect world, coordinates of the shot points should be in the headers of the SEG-Y files, and it would not be necessary to go through this step, but this is actually very rare. Navigation data should be in ASCII files made of columns with the line name, the shot point numbers and the coordinate of the shot points.

'**Edit 2D locations...**', '**Renumber 2D...**', '**Renumber 3D...**'

can turn out to be useful if navigation data and seismic data do not have the same 'conventions' in the shot point and CDP numbers. They allow you either to 'correct' some locations or to renumber the CDP and shot points.

In the '**Utilities**', the most useful are '**Delete...**' (seismic data can take a lot of disk space, and it can become necessary to remove unnecessary data - or data that were not loaded properly for some reason) and '**Export Synthetics**' to save to ASCII files synthetic seismograms calculated in IESX .

Loading SEG-Y seismic data

Start up `**Load Seismic**' from the IESX Data Manager:

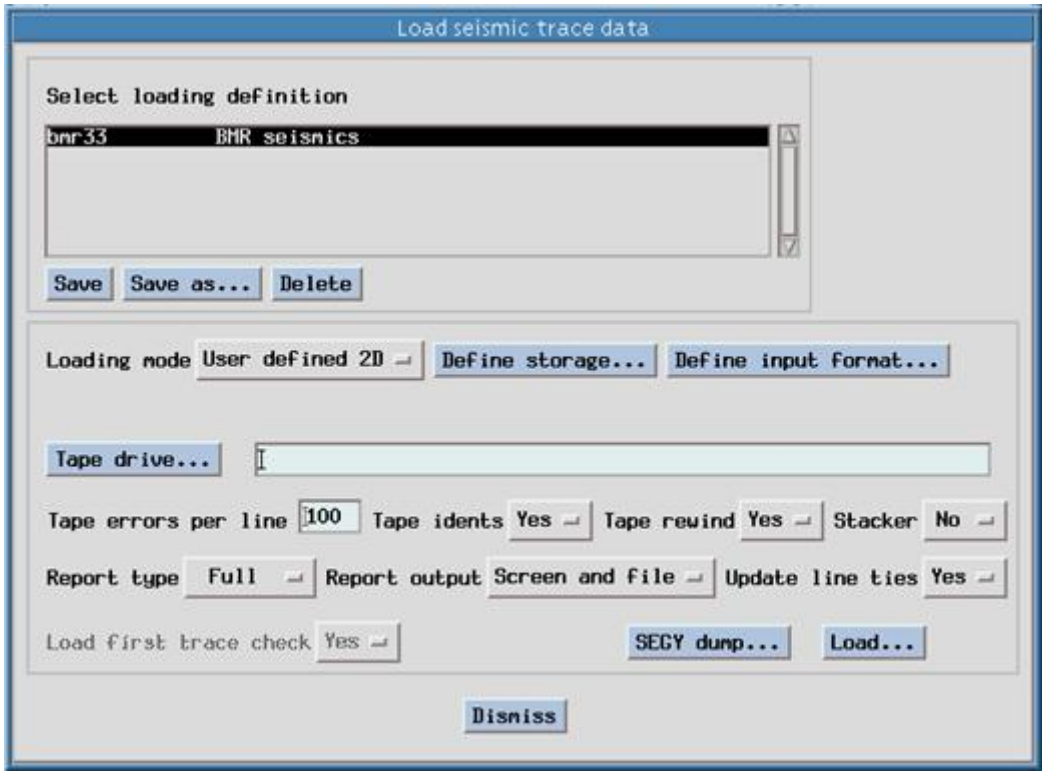

- Create a Loading Definition by using `**Save as...**', and entering a name and description. The loading definition will save all the parameters required to describe and load your data. It can be used later to import data coming from the same source or with

similar characteristics.
- Select the '**Loading Mode**' - usually 'User defined 2D' for 2D data or 'User defined 3D' for 3D data.
- Before getting any further, it is usually a good idea to get a preview listing of the contents of the SEG-Y file. To this, select '**SEG-Y Dump...**'

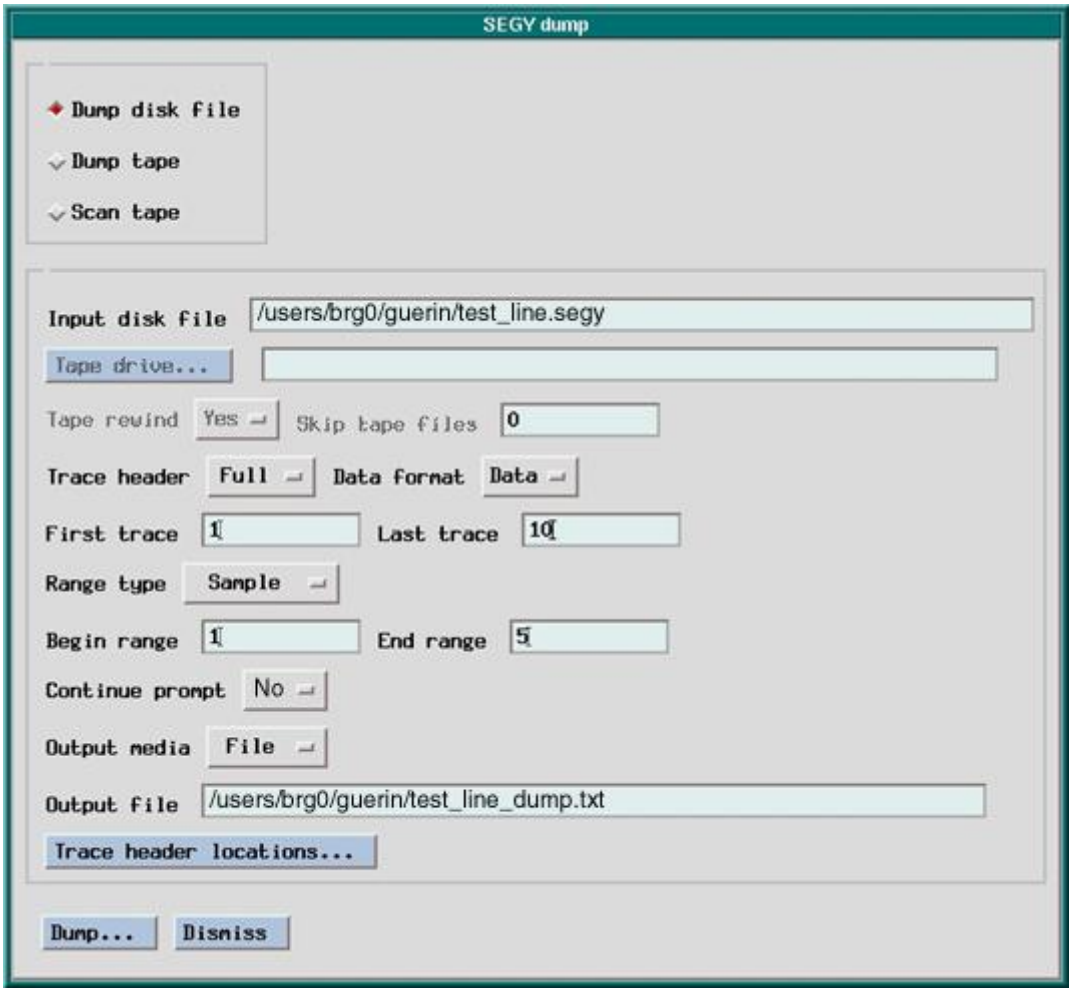

- Select the type of input storage (disk, tape,...)
- If it's a file on a drive or CD-ROM, enter the full path to the SEG-Y data file.
- Set **Trace Header** to '**Full**' to get the most complete overview of the headers.
- Limit the 'First trace' and 'Last trace' to a few traces (here 1 to 10) - you should get enough header information from the first

shots.
- Select 'Sample' for '**Range Type**' - and put a few samples only (here 1 to 5) - so it is going to list only the first 5 samples of each trace.
- Set '**Continue Prompt**' to No - so it is not going to bug you every page.
 -> 'Dismiss' to close

Loading 2D data

- Back in the 'Load seismic trace data' window, select '**User defined 2D**' and press `**Define Storage...**' to bring up the 'Define 2D seismic storage parameters' window:

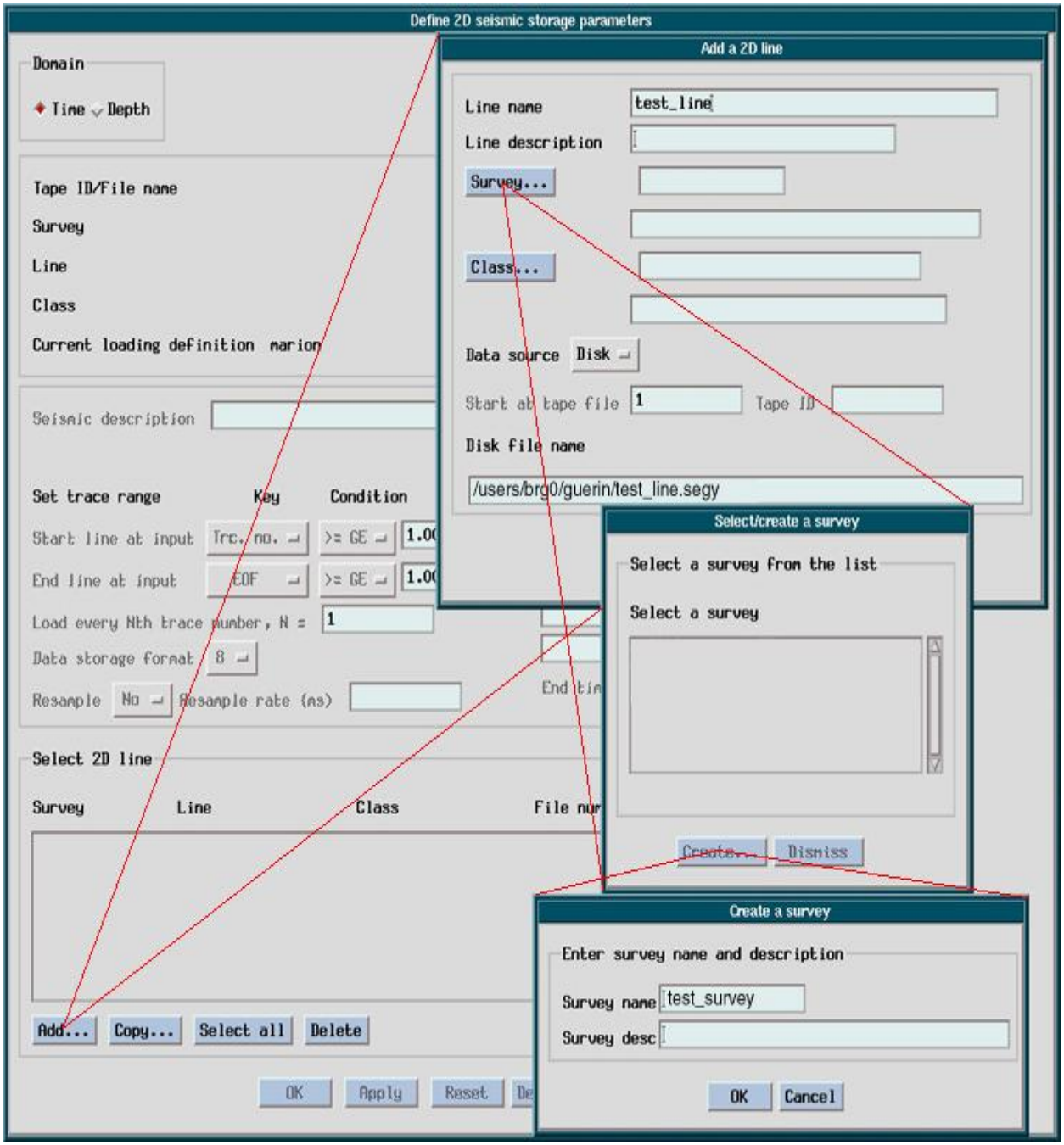

Note: this figure also illustrates that the different steps in this definition can bring up a lot of successive windows. It might happen that things appear frozen or that you can't dismiss one of these windows only because the latest small window is hidden behind some other one. This can happen here, or during the

'dumping' or in later steps - windows have to be closed in the reversed order they were open.

- Press `**Add...**' to bring up the `Add a 2D line' window.
- Enter the line name.
- As in the figure above select/create a **Survey...** and a **Class...**.
- Select the type of data storage (`Disk' or 'Tape') and enter the full path name or tape device name.
- Once the survey/class and file names are defined, they appear in the 'Define 2D Seismic storage parameters' window.
- In order to save space or to focus your data, you can also use this window to define the first and last trace(s) to load, a trace subsampling rate, and/or the times to end/stop trace loading (for instance to remove the water - or the deepest part).
- Click **OK** to close the window.
- Press `**Define Input Format'** in the 'Load Seismic Trace data' window to start to 'Define 2D input data format' - which is used to define the format of your SEG-Y file. Because the SEG-Y format is highly flexible, it is most likely that you will have to change some of the parameters in this window. To do this, it is useful to open the ASCII file with the results of your SEG-Y dump in a text editor.

The most current parameters to check and/or change are:
In the 'Set format specification' area (general description of the structure of the file):
- Specify if you have one 'Single' line or 'Multiple' line per file
- Specify where the general line (reel) header is - most likely 'File' or 'First Tape'.
- You will want to 'Bypass' the integrity check location.
- The **trace sorting code** is the order of the records in the file. Usually CDP ensemble In the 'Set header locations' area, you specify where the information on line name and CDP and shot points (SP) numbers are taken.
- The line name is usually defined by 'User Input' - it will assign

the line name that you have previously defined. However, in particular when multiple lines are in one single SEG-Y file, it might be necessary to get the line name from the 'Trace header' or the 'Binary header'. This should be apparent in the SEG-Y dump file.
- The CDP number is usually taken in the trace header - look in the SEG-Y dump for 'CDP ensemble' or 'CDP trace number'. However, in rare occasions, it might be necessary to define an 'Expression' based on trace number or other factors.
- The SP (shot point) number has pretty much as much chance to be in the 'Trace header' as to have to been defined by an 'Expression'.
- The default values and format for the header locations are often correct - but still need to be compared with the SEG-Y dump file. This is necessary for any of the file name, CDP or SP that are to be found in the 'Trace header'. If you have chosen 'Both' in the loading mode (i.e. loading seismic and navigation data), you also have to make sure that the station locations (X,Y) are pointing to the correct header location.

Defining an expression for CDP and/or SP: select '**Shot point/CDP expressions...**' to pop up the following window (this is a 'condensed' version of the actual window).

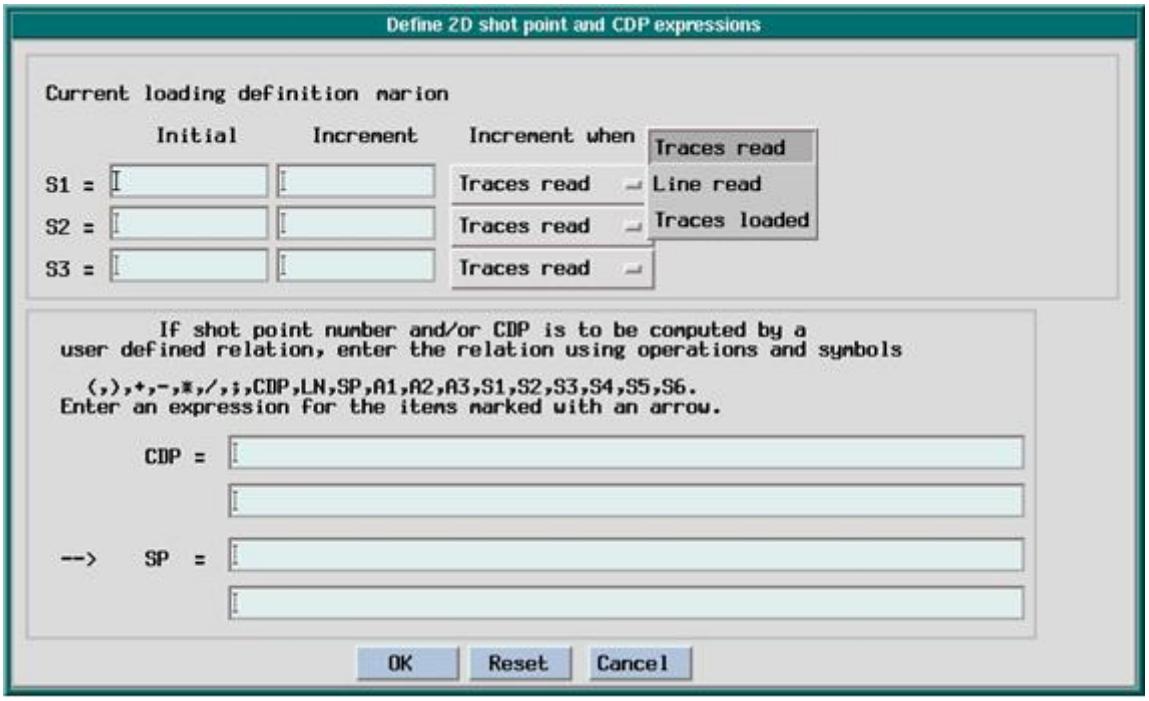

In the most common case, you just have to define an expression for SP as a function of CDP (SP = CDP, or SP=5*CDP+100, ...).

In more exceptional cases, where neither CDP or SP numbers are in the trace header, you have to build the expression from scratch - and use the 'S1','S2',...'S6' variable for this. For instance, if you know that your first CDP number is 1023 and that each trace in the file is a new CDP, you can define:

Initial S1 = 1023 - S1 Increment = 1 - S1 increment when 'Traces loaded' - and CDP = S1.

'OK' when done

If you have additional lines/files to load that were stored in a similar manner, return to the 'Define 2D seismic storage parameters' window, select (highlight) the line you have just defined and press `**Copy...**' to bring up the 'Copy a 2D line' window:

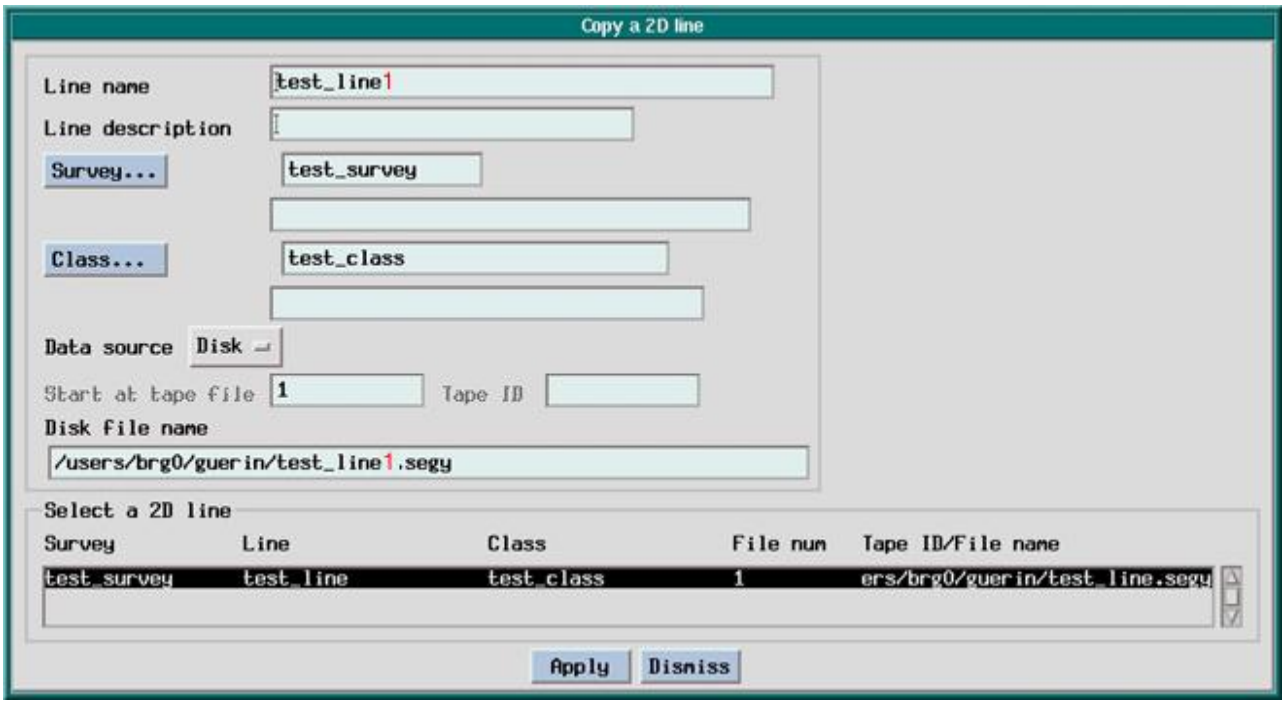

In this example we just change the line name, and the disk file name (changes in red).

'**Dismiss**' when finished.

In the main `Load seismic trace data' window, press `**Load**'. A window will pop up saying the input parameters are OK (or not), and prompt you to continue. Information on the lines being loaded will be displayed on the screen. A message will announce that the loading is finished, but the time clock will continue to run, and the CPU will apparently still be working at full rate. This is a bug in the program, and you can safely close the Load Seismic application at this point.

You don't need to load the navigation data to view your seismic lines - at this stage, it can be useful to start 'Seis2DV' or 'Seis3DV' to visualize your data and make sure that the loading was successful

Loading 3D data

- In the 'Load seismic trace data' window, select '**User defined 3D**' as loading mode, and press `**Define Storage...**' to bring up the 'Define 3D seismic storage parameters' window:

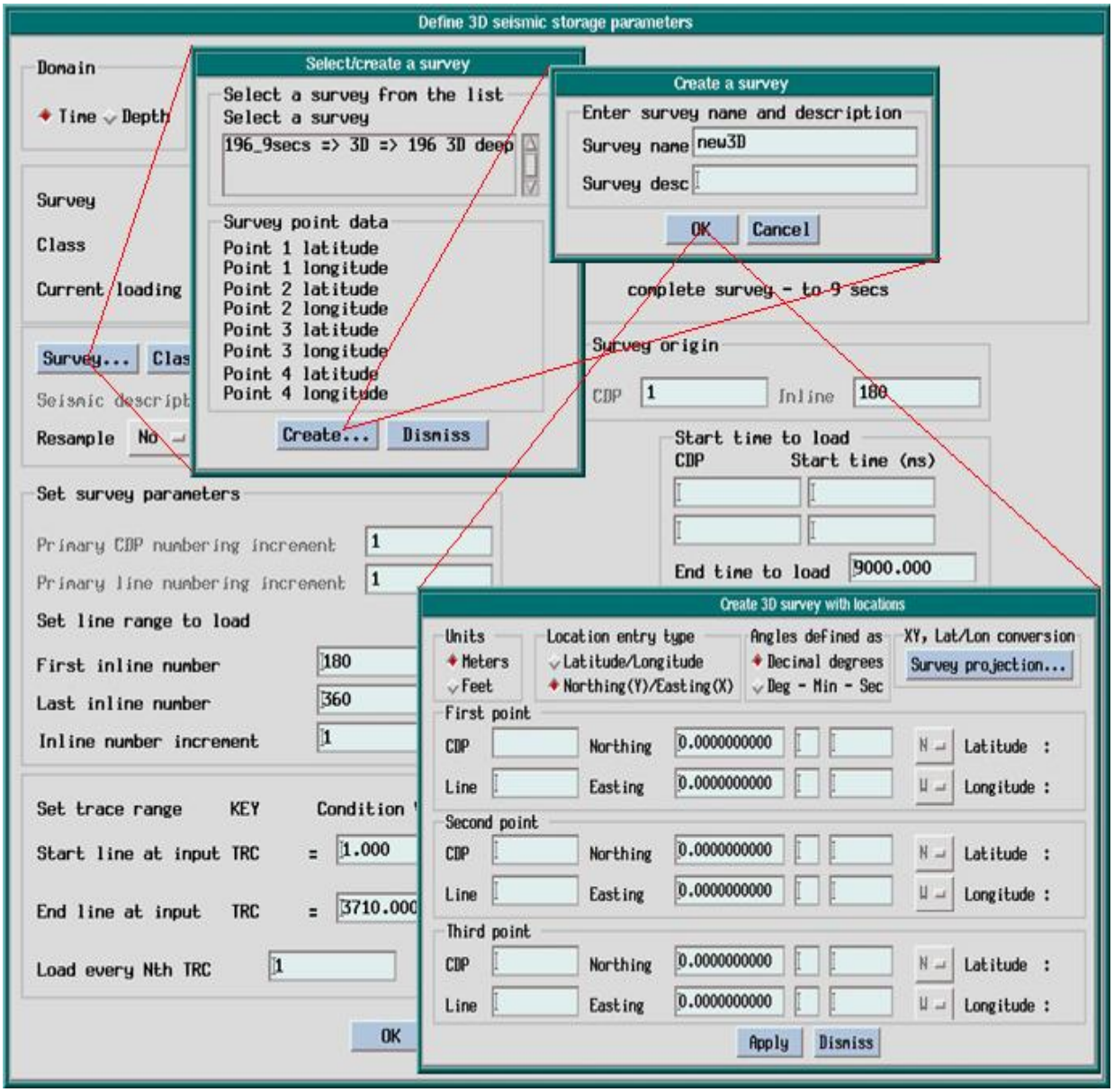

The procedure is very similar to the 2D loading, using a SEG-Y dump to determine the location of the headers. The most significant addition is the requirement to enter the coordinates of three points of the survey. This is shown in the above figure -

clicking 'Survey...' pops up a Select/create survey' window were the coordinates of the 'corners' should appear. For a new survey, there is initially no value - you have to '**create..**' the new survey - give it a name - then '**OK**' to enter the coordinates of the 3 points. In the 'create 3D survey with locations' window, the 'CDP' number is equivalent to crossline number, and the 'Line' number is the inline number.

In the 'Define 3D seismic storage parameters' window, you have to enter the first and last inline numbers, the CDP (crossline) and inline numbers at the origin, the length of the lines (inlines), and eventually a subsampling rate. You can also specify the minimum and maximum time to load, to remove some of the sea and/or the deepest reaches of the survey.

Loading Navigation data

All the lines in the survey can be concatenated in the same file.

- Start up `Load 2D Locations' from the IESX Data Manager:

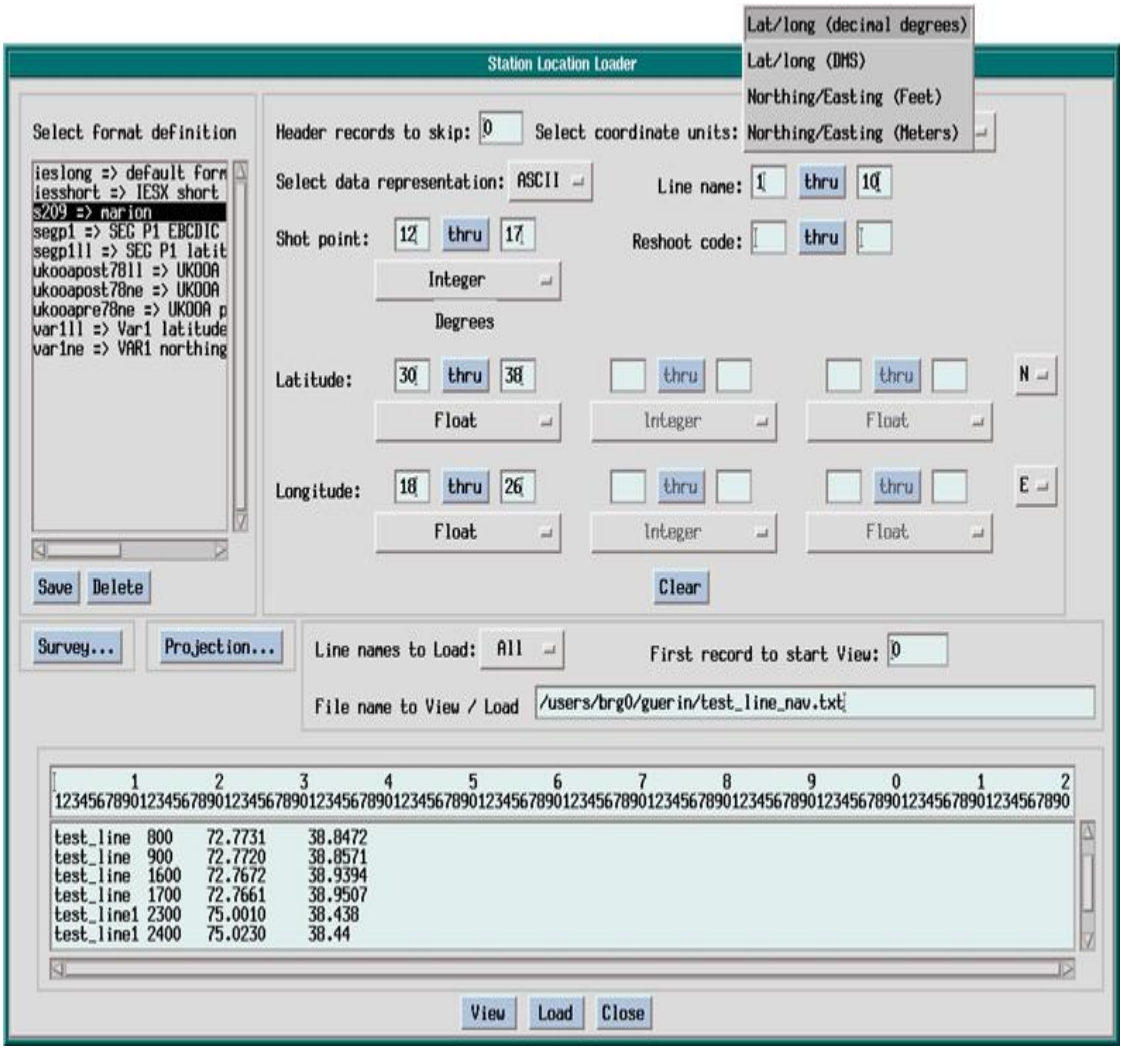

- Enter the full path to the navigation file, and press `**View**' to display it in the lower window. The numbers in this window indicate the column numbers to help describe the structure of the file (the upper row gives the multiple of 10).

- Select the coordinate units system: the most frequent are `Lat/Long (decimal degrees)', and `Lat/Long (DMS - Degrees, Minute, Seconds)'

- Enter the position in the records of the Line Name, Shot Point, Latitude and Longitude. If the coordinates are in DMS (degree, minute, second), you will have to enter also he position of the minutes and seconds.

- Select N/S and E/W. (North and East are positive latitudes and longitudes).

- Press `**Survey...**' and select your survey.
- Press `**Save**', and enter a format definition, to save these parameters that might have to be reused or edited if there is a mistake or a later changes.
- Press '**Load**' - then '**Close**' if successful. You will be able to visualize the navigation in the basemap

Sharing seismic data between projects

In order to save disk space and to avoid loading twice the same data set, it is possible to access seismic data from other projects To do this, select '**Share...**' in the IESX Data Manager to start the 'Share Manager':

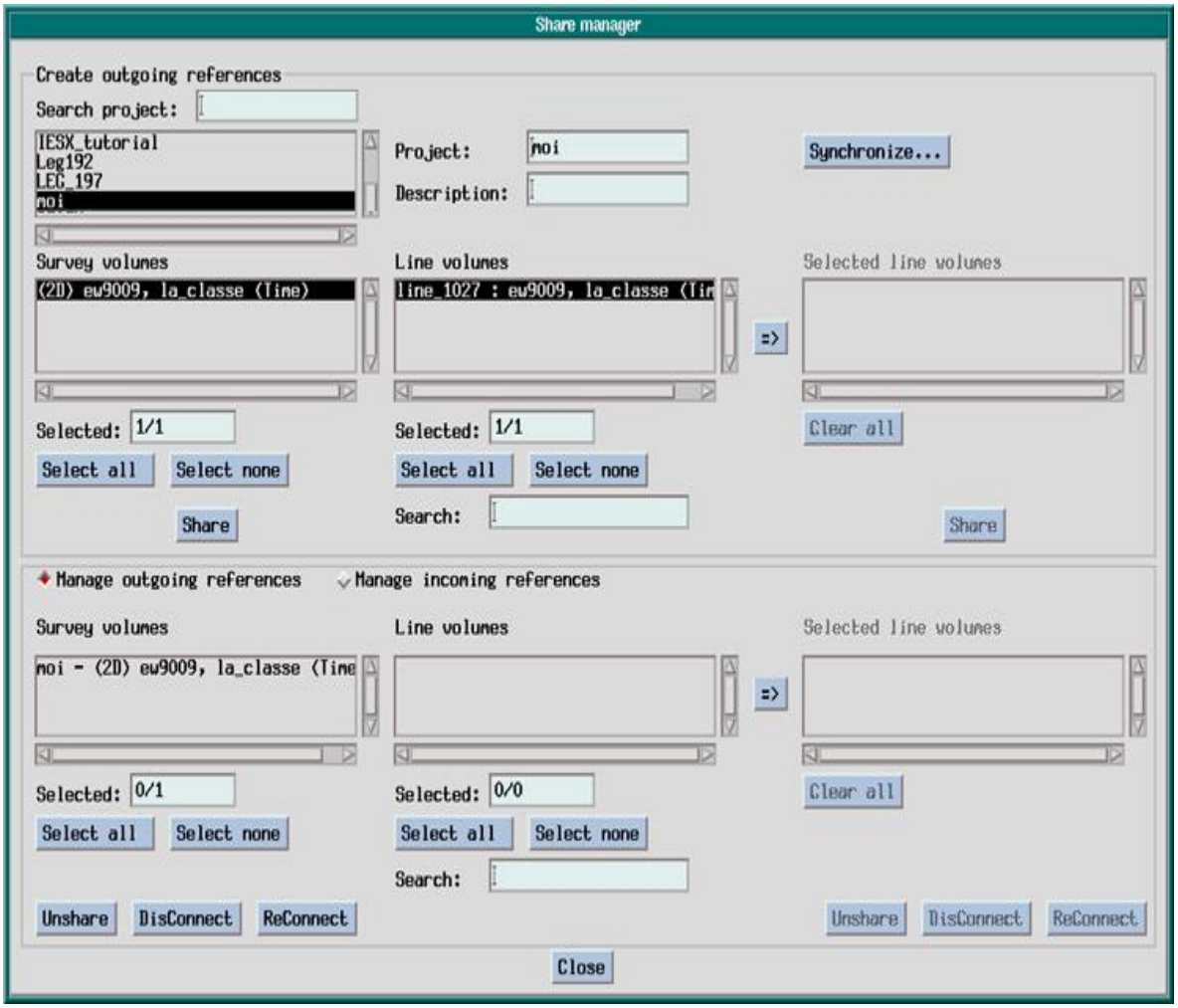

The 'outgoing reference' actually designates data from other projects that you want to access from your project. The list in the upper left corner shows all the project present in the same Oracle database server. When you select one, you are prompted for the password to this project. The survey volumes present in this project will then appear - selecting one will display the seismic line present,...

-> select the items you want to access - and '**Share**'.

This operation can take a while if it's a large data set.

The lower section is for managing shared items - it is used mostly to 'unshare' some items so that they can be deleted. Any shared items cannot be deleted, so you have to unshare it before deletion.

Basemap - viewing the Navigation data

Start Basemap from the applications/Interpretation menu in the IESX Session Manager.

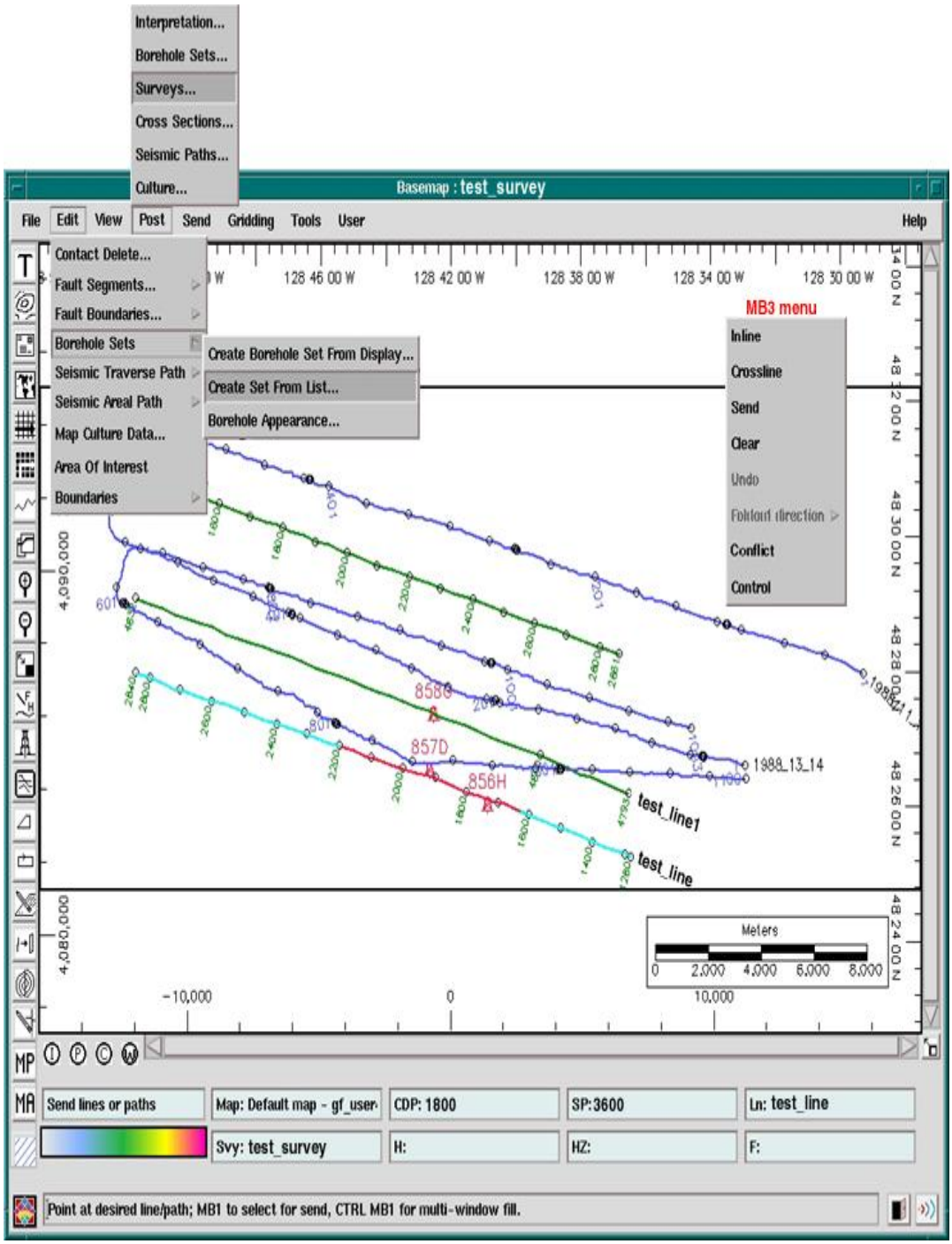

General features

- The first time you start it, navigation data of the last survey that you have just loaded should be the only thing

to appear by default.
- You can then select what survey and what borehole(s) to display.
- Whenever your cursor is on (or close to) a line, this line will be highlighted (here in cyan), and in the bottom message areas you will see the line name, the survey name and the shot point and CDP numbers the closest to your cursor.
- If you have a Seis2DV or seis3DV window opened, the seismic section currently displayed in this window will be highlighted in the basemap (here in red).
- You can define general attributes such as background color, highlight colors, scale location, ticks... under User/Map Annotations.
- When a line is highlighted, **MB3** will popup a menu with several possible actions. The most useful are:
  - **Inline/crossline** : this is mostly useful with 3D surveys - selecting one or the other will define what lines get highlighted when you navigate the map with your cursor.
- You can choose to save any configuration of boreholes/surveys displayed as a 'Map' by selecting '**File/Save as...**' . You will be able later to recover this configuration with **File/Open....**

Posting seismic surveys

If you have multiple surveys, you can choose which one(s) to display - by default only the last one loaded will appear.

To add or remove surveys select '**Post/Surveys...**' to bring up the 'Surveys' manager:

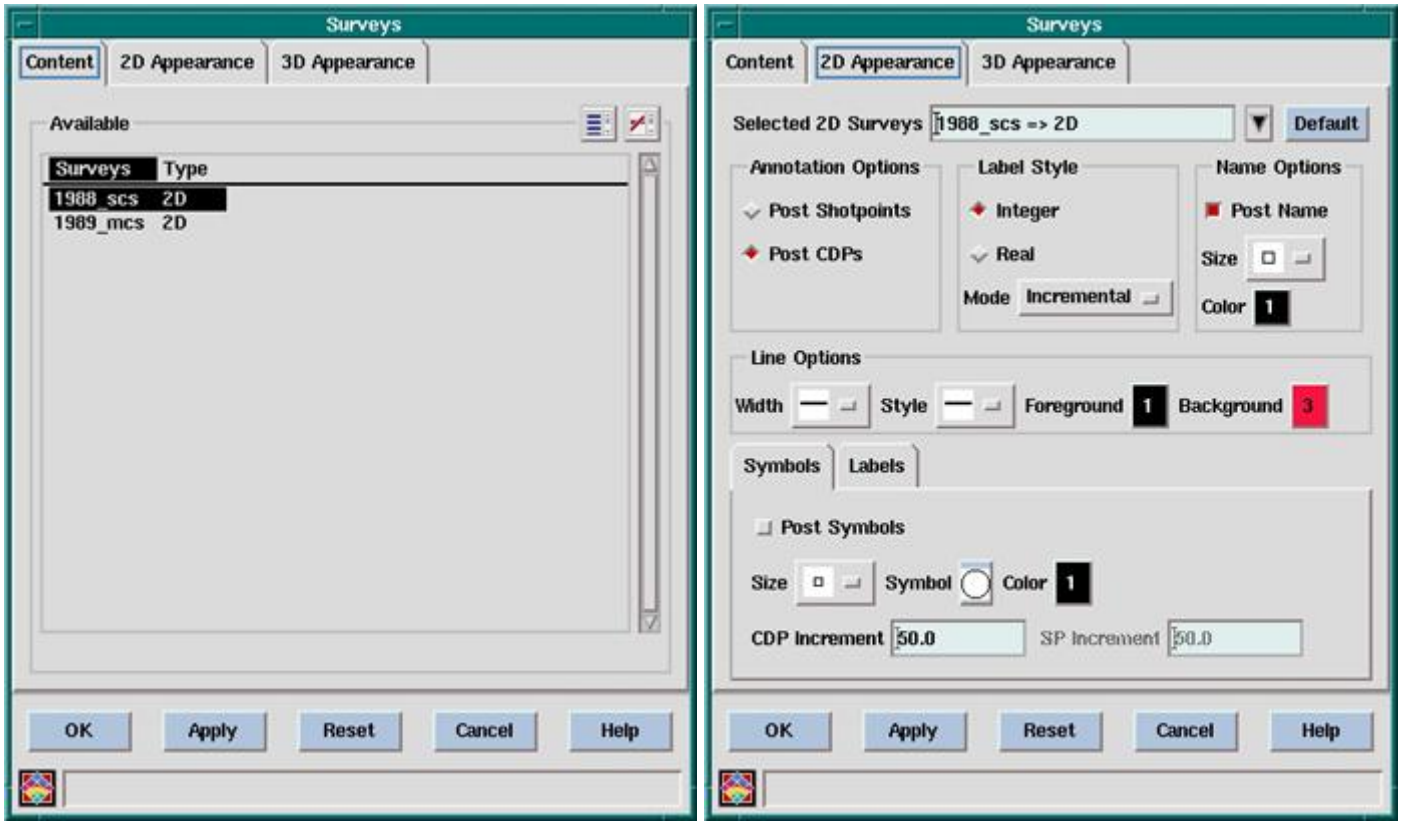

In the 'Content' menu (left), you select the survey(s) to display (press the 'Control' key to select multiple surveys).

In the 2D/3D appearance (right), you define the general appearance of the survey: color, symbols/labels to be displayed

Creating/Editing borehole sets and appearance

To display boreholes, you have to create 'borehole sets', and then 'post' the borehole sets.

A 'borehole set' is a group of boreholes that will have a common 'appearance' - typical borehole sets are holes from the same leg (in the case of multiple legs in one location), or proposed holes vs. actual holes, or whatever grouping is appropriate to the situation.

The same borehole sets are also used in the Seis2DV/Seis3DV applications, and can be edited/created from these applications.

To create a borehole set:

- From Basemap: '**Edit/Borehole sets/Create from list...** to start 'Manage borehole sets' window:
(In Seis2DV and Seis3DV use '**Define/Borehole set...**' for the same purpose)

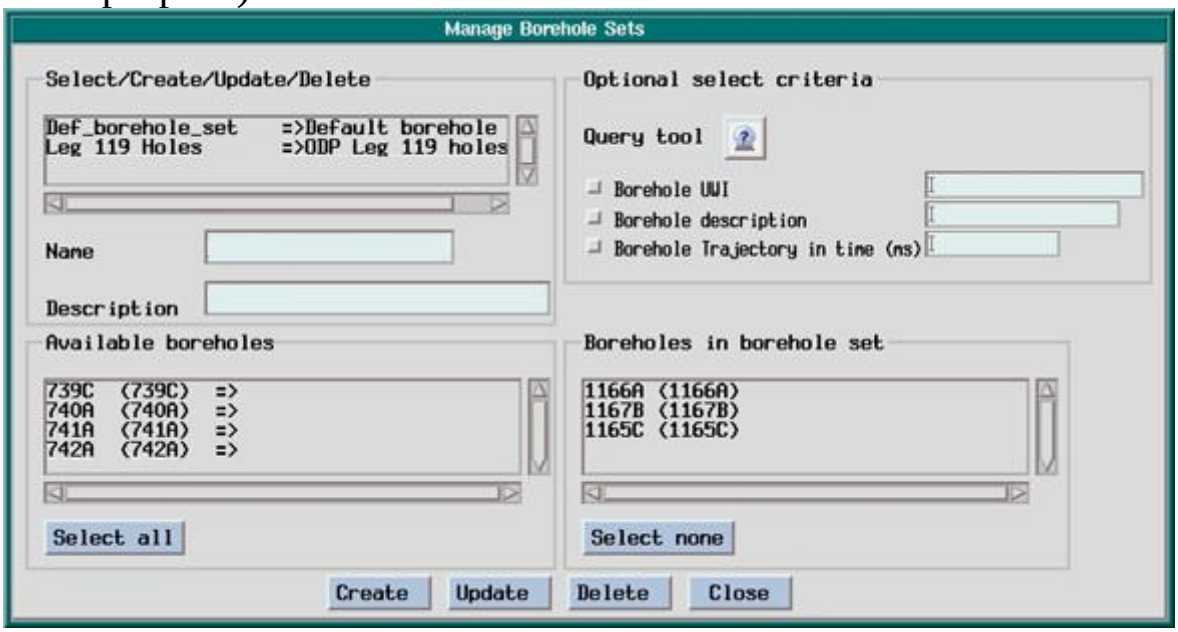

- Choose the boreholes from 'Available boreholes' - they will move to 'Boreholes in borehole set'
- To remove boreholes from a set, select in 'Boreholes in borehole set' and it will move back to 'Available boreholes'.
- Name the set (e.g. Leg_119_holes).
- '**Create**' (if it's the first time) or 'Update' if you are editing an existing set.
->Close

To be able to display a borehole set, you have to define an 'appearance' for it: use '**Edit/Borehole Sets/ Borehole appearance...**' in the basemap:

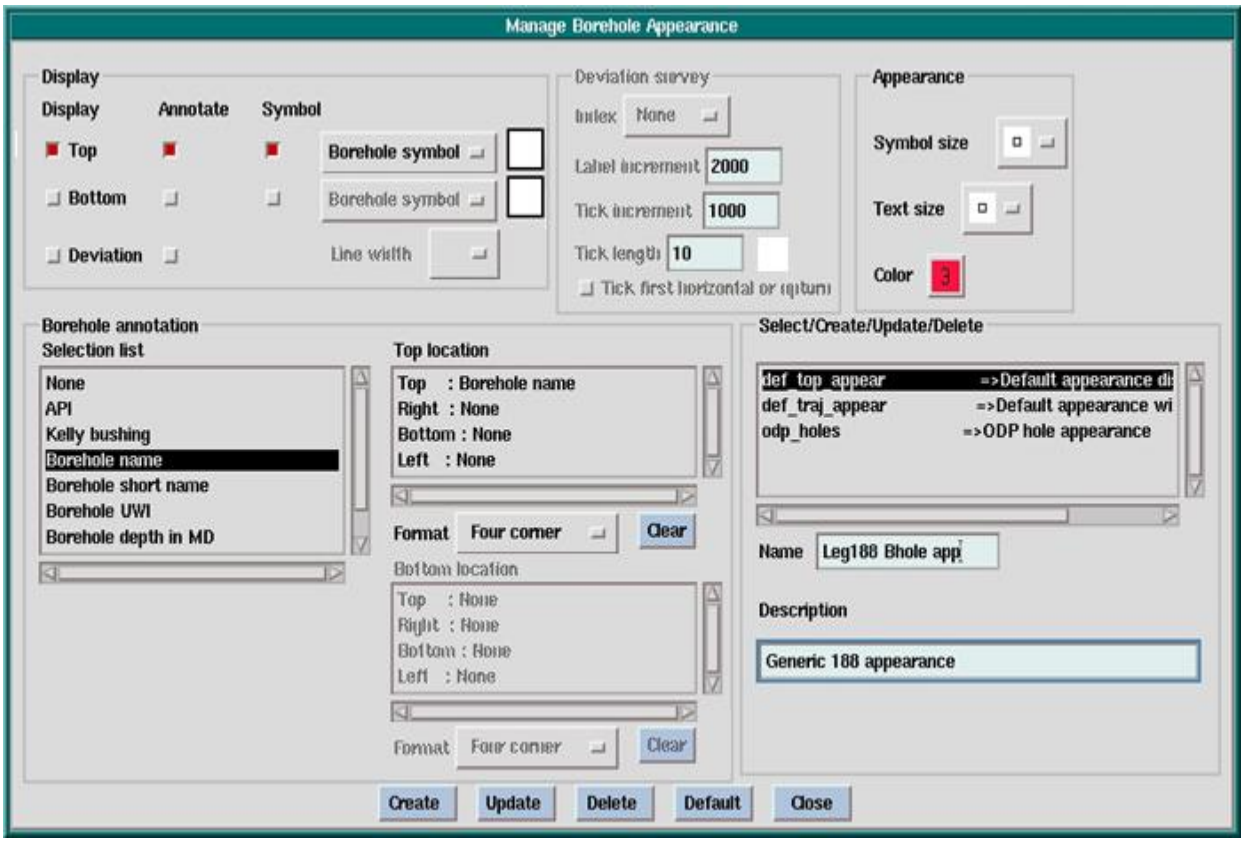

Define the parameters for the appearance (size/color), eventually a symbol, give a name, then 'create' or 'update' (if editing an existing appearance).

To post the boreholes on the map, use '**Post / Borehole Sets**':

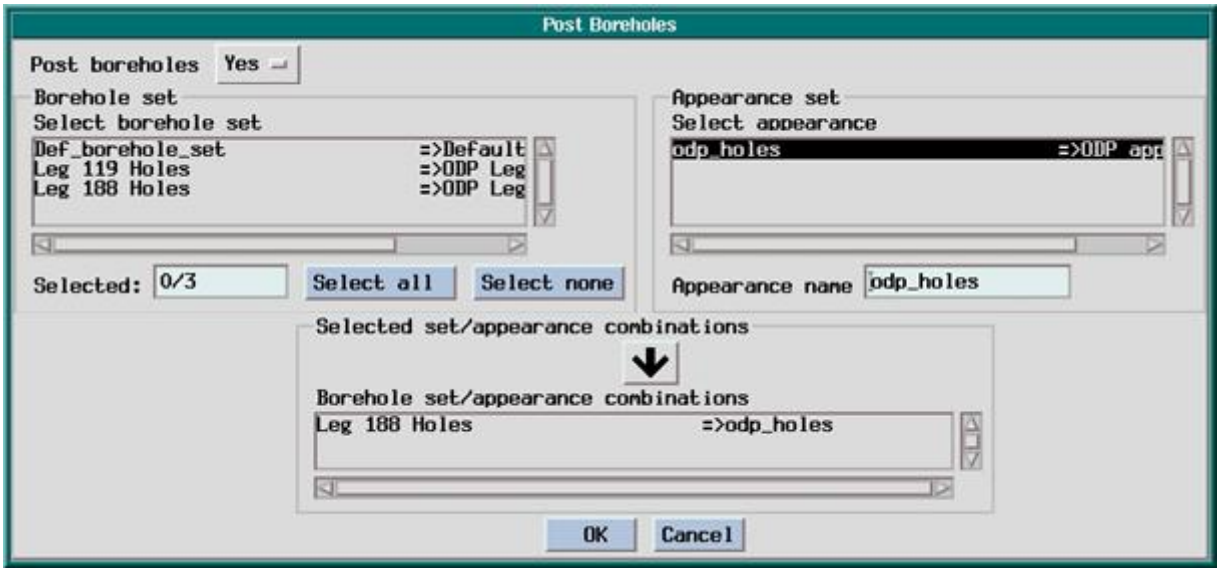

Select the borehole set you want to display and the appearance you have defined, then hit the arrow to make the borehole set and the appearance you have selected appear in the 'Selected set/appearance combinations' area.
-> '**OK**' to apply and close.

5.4 Seis2DV/Seis3DV - viewing and interpreting seismic sections

Viewing seismic lines / general features

Seis2DV/Seis3DV are the applications used to visualize and interpret seismic lines. To start them, select **Application/Interpretation/Seis2DV** (or **Application/Interpretation/Seis3DV**) in the IESX Session Manager:

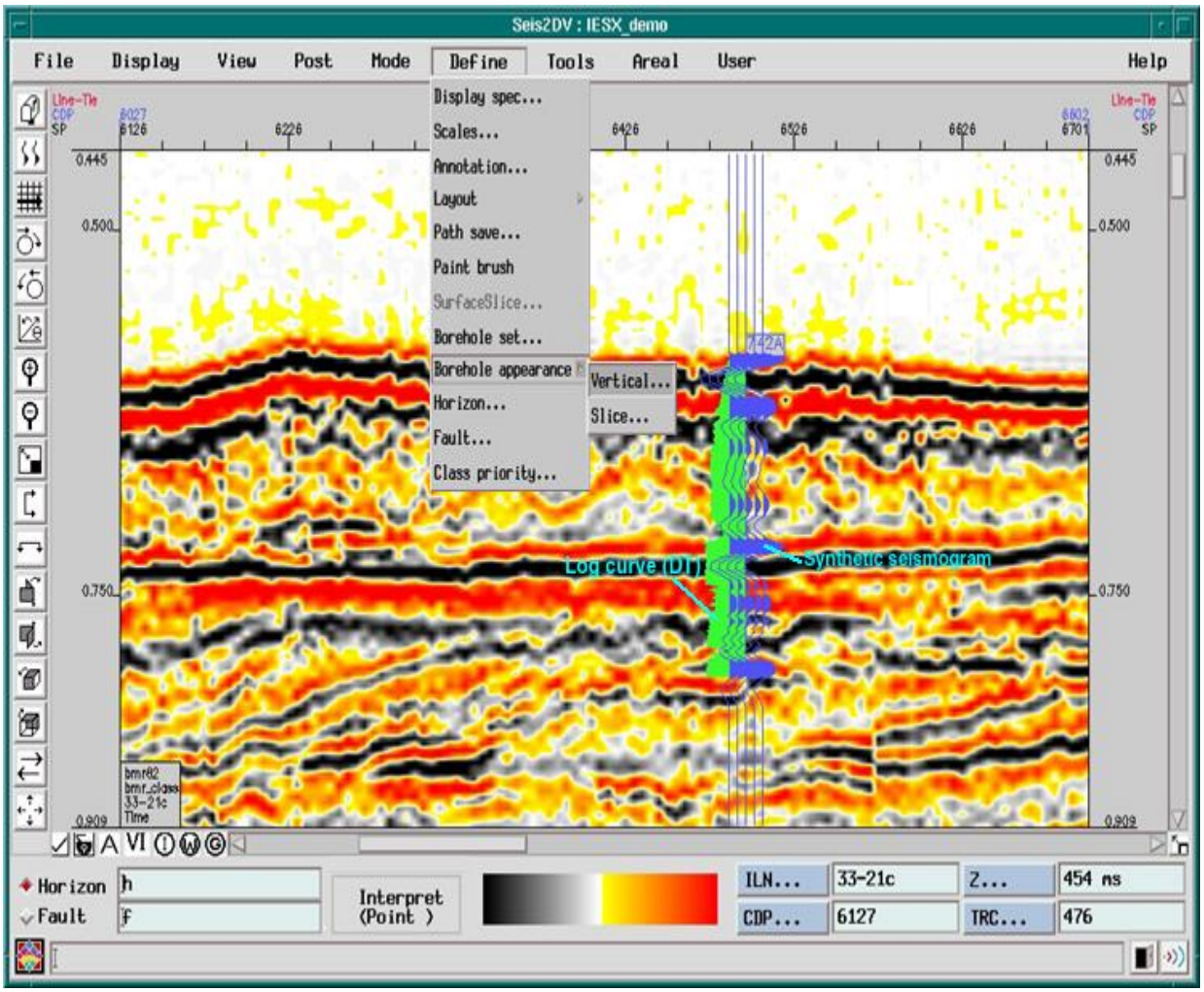

- The application will open with the first seismic data in the list. To change it to the line you want, use Display Menu / Seismic Line, and choose the survey, then the line from the list.
- If you have a basemap opened, you can select the line you want to display in Seis2DV/3DV by selecting it on the basemap. The line will appear highlighted in the basemap (default in yellow), and the section actually displayed will be highlighted in a different color (default red).
- To change the colors, or to change to a `wiggle' display, use the Define Menu / Display spec, and change the Display Style: VI = colors, VA = wiggles. To cycle through the color options, press the color bar at the base of the window. There is also a VI/VA toggle at the base of the window.

- To change the scale, use Define Menu / Scales, and then set the trace decimation, the horizontal scale (traces per inch) and the vertical scale (inches per second).
- Use the magnifying glass icons for zooming in and out.
- As your cursor navigates the window, the message area displays the trace and CDP numbers and the two-way travel time.
- Where two seismic lines cross, you can have a `Foldout' to display the intersection of the lines (use **Display / Fold vertical**).
- To display any two or more seismic lines on the screen at the same time, use **Define / Layout**.

Creating/Editing vertical borehole appearance

- The Borehole sets defined in basemap are also valid in Seis2DV/Seis3DV. New sets can also be created or existing sets can be edited in the same way as described for basemap from **Define/ Borehole Set**.
- Before posting boreholes, you have to define a vertical borehole appearance (like in basemap). To do it, select '**Borehole Appearance/Vertical...**' in the 'Define' menu

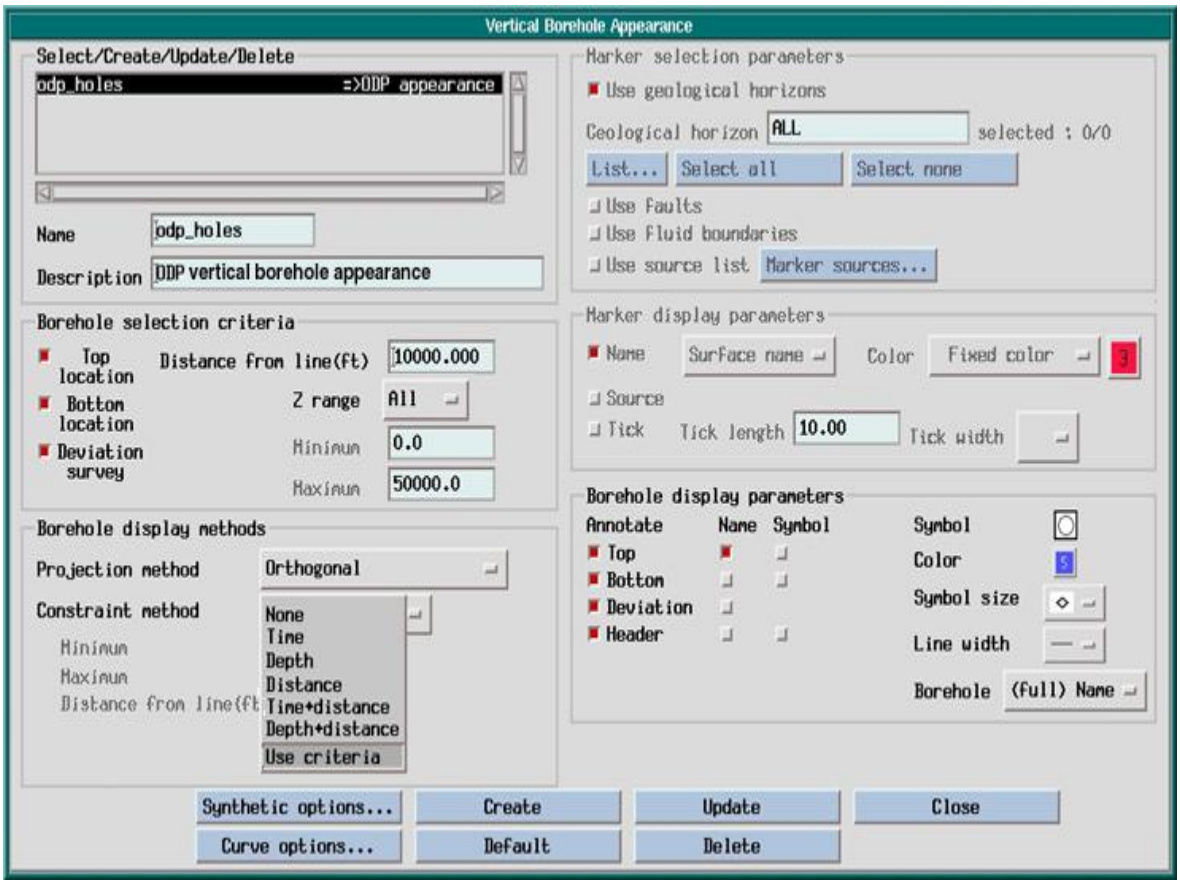

The main parameters to define in this menu are:

- The name of the appearance that you are about to create or edit.
- The maximum distance between a borehole and a seismic line for the borehole to appear in Seis2DV. This distance is defined in the '**Distance from line**' area. From the basemap, you can figure what is the actual distance between wells and lines, and use it for your criteria. Choose '**Use criteria**' as constraint method in the 'Borehole display methods'.

NB: the distance between a well and a line is the shortest distance between the well and the line - i.e. the distance between the well and it's orthogonal projection on the line if you use the orthogonal projection method.

- General display parameters such as symbol, color,

annotations.

- You can choose to display log curves (maximum two logs - one on each side of the trajectory) and/or synthetic seismograms. To do this, select '**Curve options...**' and/or '**Synthetic options...**', respectively.

NB: - if two curves with the same code exit for a borehole (ex: RHOB,...) only the most recently edited will appear.

- IESX recognizes only a limited amount of curve names. Make sure the curve you want to display has such a name.

- To apply your parameters, press 'Create' or 'Update' (whether you are creating or editing an appearance)

-> then 'close' to get back to the Seis2DV display.

- To post the boreholes, the procedure is similar as in basemap: select '**Post/Boreholes...**' to bring up a 'Post Boreholes' window identical to the one in basemap. Select the borehole set(s), the vertical appearance that you have defined, press the arrow to validate your selection - and 'OK' to close.

- Once a well is displayed, you can double click on its label to bring up the 'borehole editor' and change/edit the checkshot survey, reference depth or any other attribute:

- To change the checkshot, select 'Checkshot survey...' to start the 'Select preferred checkshot survey' window, and select the appropriate checkshot. 'Apply' to update the seismic display without closing your window - or 'OK' if you want to close.

- To edit the checkshot, double-click on it in the 'Select preferred checkshot survey' window.

- To define where the borehole label will appear on the seismic line: change the two-way time to the value where you want the label to appear (if the seafloor is at 1 second, you might want to put the label at 0.9 sec). If this first line is (0,0), the label appears at the top of the Seis2DV/Seis3DV window - change the 0 in the two-way time column to where you want the label. If the first value is actually the top of your logged interval, the label will be just at the top of the synthetic/log - in this case, you

have first to 'add a line' at the beginning of the survey, and enter where you want the label to appear - and put '0' in the depth column.

5.4.3 Seismic Interpretation - Picking Horizons/faults.

- **Define / Horizon** will bring up the Horizon Manager. Give the new horizon a name (e.g. top_sand) and a color. Add (or Update if you made changes to an existing horizon).
- Use the items in the Mode menu to define your actions: erase, snap, or smooth a horizon.
- On the seismic, choose `H list' from the right mouse button (MB3) menu, and select the new horizon.
- Pick the horizon point by point on the seismic with the left mouse button. Use Undo from the MB3 menu if you make an error.
- Choose `**Break**' from the **MB3** menu when finished.
- Use **Post / Interpretation** to control which horizons are displayed on the seismic.

Faults work in the same way as horizons.

APPENDIX (B)

Notes on wire line logging

WIRELINE LOGGING

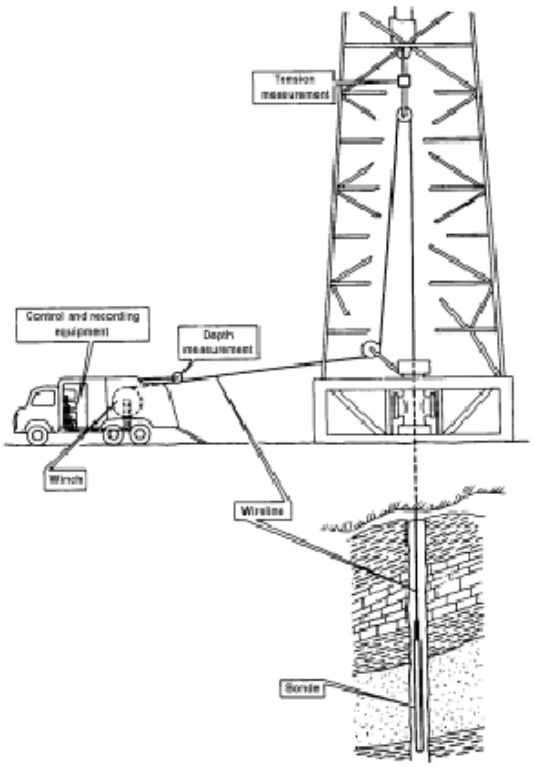

Wireline logging is performed with a ***sonde*** or probe lowered into the borehole or well, usually after the drillstring has been withdrawn.

Openhole logging is based on measurements of the formation's electrical, nuclear and acoustical properties. Other openhole wireline services include formation sampling, fluid sampling and pressure measurements.

Cased-hole logging includes measurement of nuclear, acoustical and magnetic properties. Other cased-hole wireline tools include perforator guns and various production logs.

SP INTERPRETATION

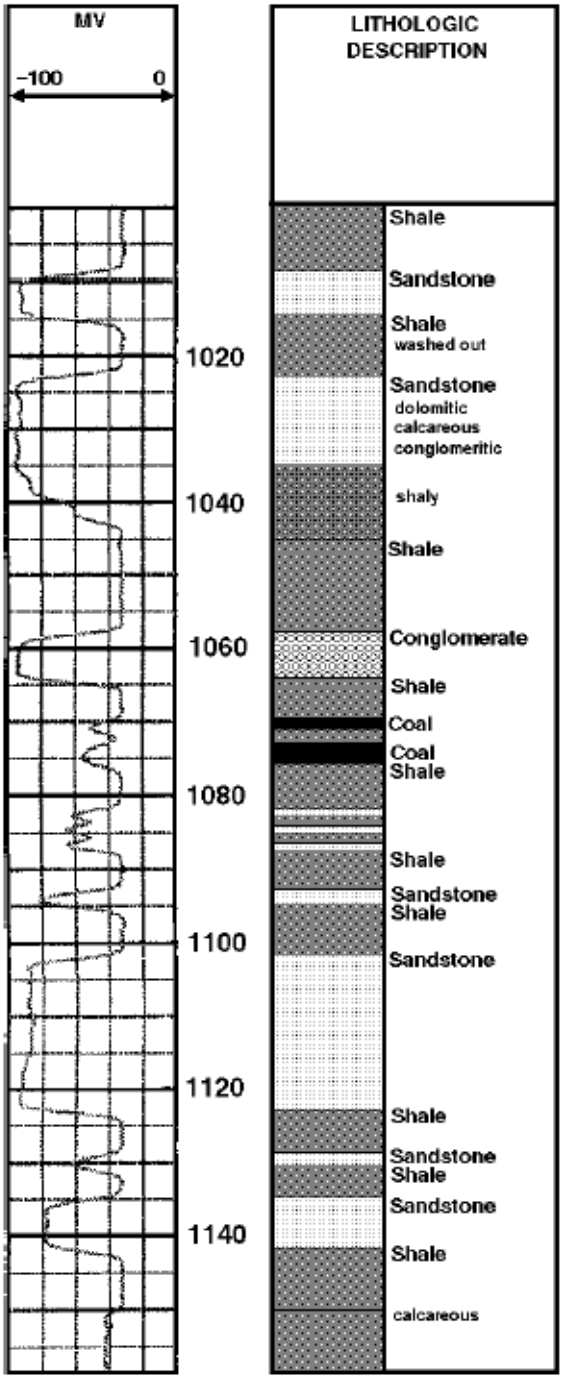

The main use of the SP log is to differentiate between tight, electrically conductive beds (shales) and more permeable, electrically resistive beds (sandstone and carbonate reservoirs).

The magnitude of the SP deflection depends on the resistivity contrast between the mud filtrate and the formation brine.

Permeable beds typically deflect the SP curve to the left (more negative SP).

The rightmost deflection is characteristic of shale. The leftmost deflections indicate clean sands (no fines) or carbonates. Baseline shifts in SP curves are caused by changes in formation fluid salinity. SP curves are also sensitive to bed thickness, the deflection being attenuated in thin beds.

RESISTIVITY LOGS

"Conventional" resistivity logs were made by means of electrodes in contact with the formation through the drilling mud. There were several sondes capable of measuring to different distances (Short Normal, Long Normal and Lateral).

Conventional logs gave good results in soft formations with fresh mud but the quality of results declines in hard formations and carbonates. They have been largely abandoned in favour of modern vertically or spherically focused logs and induction tools.

Guard logs or ***Laterlogs*** produce results that are much less dependent on mud resistivity than conventional logs. These sondes have excellent vertical resolution to identify thin porous layers. The short guard or Laterlog 8 (LL8) is usually combined with the dual induction log.

INDUCTION LOGS

Induction sondes are designed to measure resistivity in wells drilled with non-conductive mud. In addition, they are focused to minimize the effect of the borehole and the invaded zone. Induction logs measure conductivity rather than resistivity.

The DIL (Dual Induction Laterlog) system consists of a deep investigation induction sonde (ILd), a medium range induction sonde (ILm), a Laterlog 8 (LL8) and an SP electrode.

The three focused resistivity readings can be used to accurately determine the true formation resistivity, R_t, even if the invaded zone is extensive.

The formation resistivity is necessary in order to calculate porosity and fluid saturations using other logs.

MICRORESISTIVITY LOGS

Microresistivity logs are recorded on a small volume near a well filled with conductive mud. The aim is to determine the flushed zone resistivity, R_{xo}, and the exact thickness of beds.

The measuring device is mounted on a pad held against the well wall. The Microlog (ML), Microlaterlog (MLL), Proximity Log (PL) and Micro Spherically Focused Log (MSFL) are microresistivity sondes. The sondes are variously affected by factors such as mud cake thickness and the extent of the invaded zone.

Microresistivity logs are not used for correlation but because they focus on very small volumes, they provide a means for the very precise delineation of lithological boundaries. Microresistivity is used to estimate porosity assuming the flushed zone is saturated with mud filtrate.

RESISTIVITY LOG INTERPRETATION

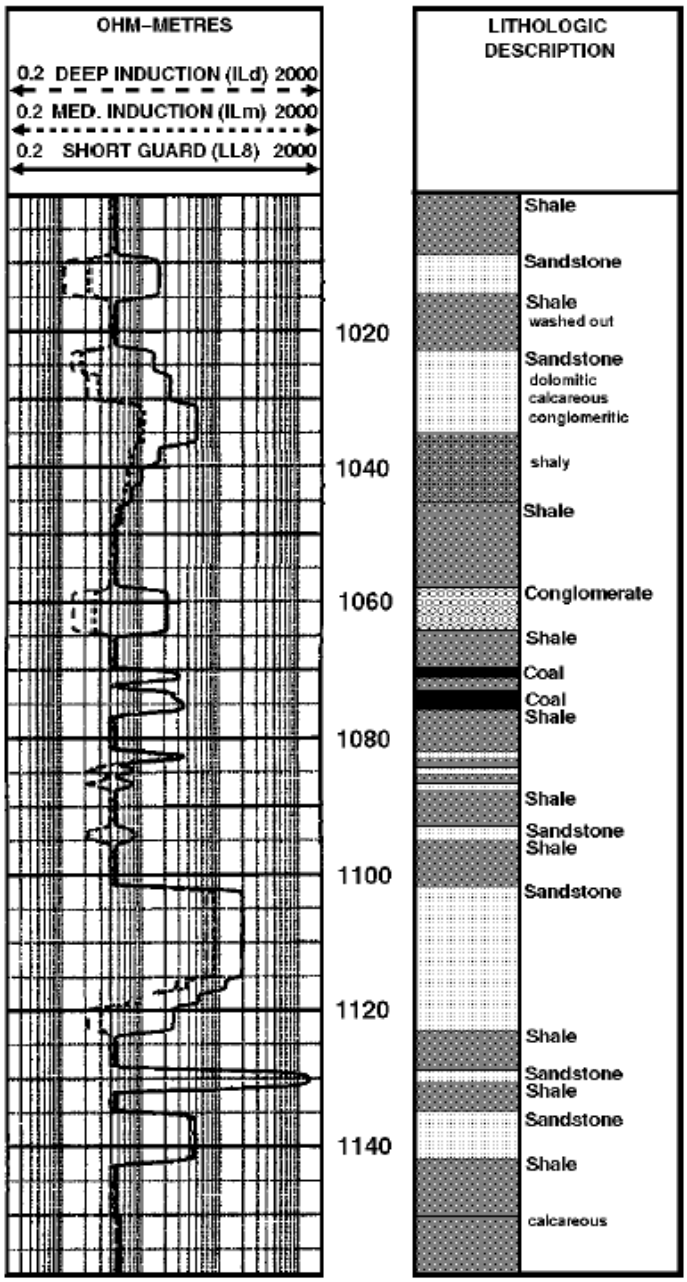

The set of three focused logs shown are produced by the DIL system. All three sondes show a similar response in shales.

The ILd log tends to approximate, R_t, the formation resistivity.

Where the three logs deflect to the right, severe mud filtrate invasion of a reservoir pay zone is indicated.

The shallow guard (LL8) is most affected by mud filtrate invasion and deflects right in all porous formations. Conglomerates with oil saturation may have lower R_t than sands due to lower irreducible water.

ELECTRICAL LOG INTERPRETATION

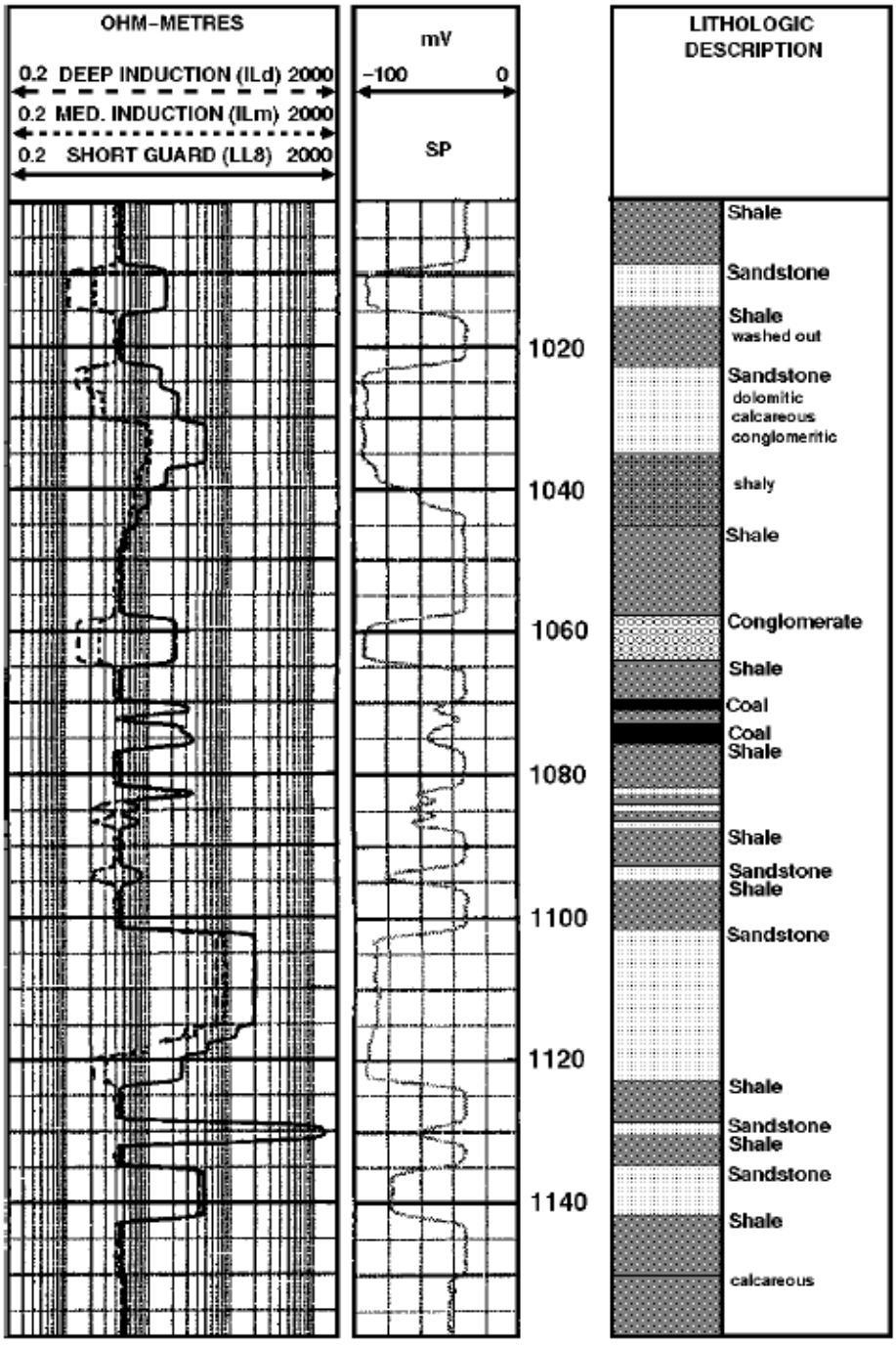

RADIATION

Nuclear logs record radioactivity that may be either naturally emitted or induced by particle bombardment.

Atomic mass is made up by positively charged protons and neutrons. Negative electrons balance the proton charge.

Radioactive materials emit alpha, beta and gamma radiation. Only gamma radiation has sufficient penetrating power to be used in well logging.

Only neutrons are used to excite atoms by bombardment in well logging. They have high penetrating power and are only significantly absorbed by hydrogen atoms.

This is an important property for well logging since the hydrogen atoms in formation fluids (hydrocarbons and water) are very effective in slowing neutrons.

NUCLEAR LOGS

There are a very large number of nuclear well logs. The more common basic logs are:

1. Conventional Natural Gamma Ray (GR)
2. Spectral Gamma Ray (SGR)
3. Formation Density Compensated (FDC)
4. Photoelectric Effect or Litholog (PE)
5. Compensated Neutron (CNL)
6. Sidewall Neutron Porosity (SNP)

Sophisticated nuclear logs now detect particular and measure individual element compositions for C, 0, Cl, H, Si, Ca, Fe, and S. These logs include neutron and gamma spectroscopy and nuclear magnetic resonance (NML) logs.

Examples of the response of natural gamma ray (GR), photoelectric effect (PE), and both compensated density (FDC) and neutron (CNL) logs will be discussed.

NATURAL GAMMA-RAY LOG

Natural radiation is due to disintegration of nuclei in the subsurface. Potassium, Thorium and Uranium are the major decay series that contribute to natural radiation.

In the conventional gamma sonde, a scintillation counter indiscriminately detects total disintegrations from all sources in a radial region close to the hole (150-250 mm).

Because K, Th, U tend to be concentrated in shales and are low or absent in clean sandstones and carbonates, the gamma response is similar to the SP log.

Openhole and cased-hole gamma logs can also be correlated and used to precisely locate pay zones for perforation.

Gamma-ray logs can yield an approximate quantitative estimate of clay content or ***shaliness***.

GAMMA LOG INTERPRETATION

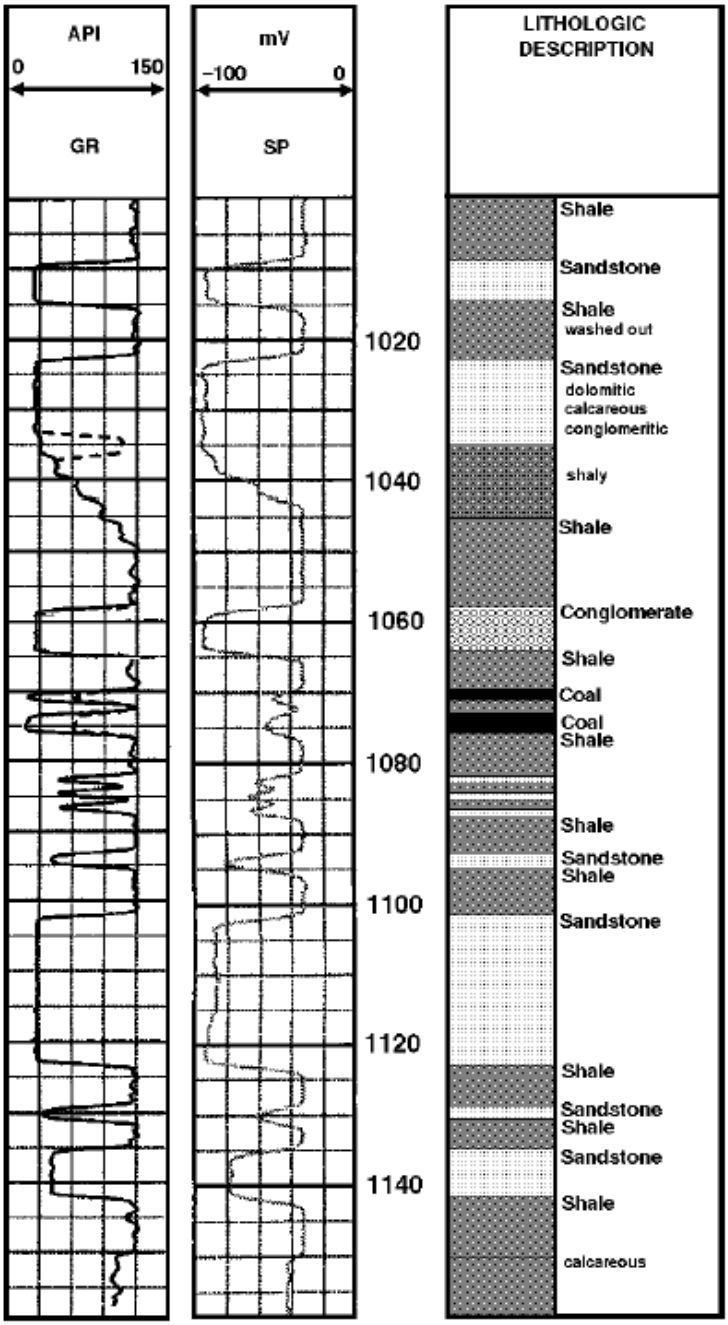

The GR and SP logs show strong correlation. Both deflect to the right for shales and to the left for clean sands.

Notice that the GR response is much less sensitive to bed thickness and that coals produce almost no gamma response.

Because GR is not sensitive to bed thickness and can be run as a cased-hole log, it is used to delineate zones for perforation.

SP is ineffective in salt mud and non-conductive mud. GR is unaffected and is valuable in these situations.

SPECTRAL GAMMA LOG

Spectral gamma logs record individual responses for K-, Th- and U-bearing minerals. The detectors record radiation in several energy windows as GR-K, GR-U, GR-TH.

The main applications of spectral gamma logs are:

1. Clay content evaluation - spectral logs will distinguish between clays and other radioactive minerals such as phosphate.
2. Clay type identification - ratios such as Th:K are used to distinguish particular clay minerals.
3. Source rock potential - there is an empirical relationship between U:K ratios and organic carbon in shales.

Spectral gamma sondes also provide a total GR count that is equivalent to a conventional gamma log.

DIFFUSED GAMMA-RAY LOGS

A gamma source is used to bombard the formation and the scattered energy returning to the wellbore is measured. The source is pressed onto the borehole wall by a pad. Two detectors are used at different distances from the source so that a correction for the effect of mud cake can be made.

Gamma rays react with matter in three ways:

1. Photoelectric absorption occurs for low energy gamma rays. The absorption depends on the atomic number of the nucleus and is the basis for the **litholog** (PE).
2. Compton scattering occurs over the entire energy spectrum and is the basis of the **density log** (FDC).The intensity at the diffused energy at the borehole wall is proportional to the bulk density.
3. Electron-positron pairs are produced at relatively high energy.

LITHOLOGS

The litholog sonde records low energy gamma radiation arriving at the detector. The photoelectric absorption factor depends on the atomic number of the atoms in the formation and the PE log is sensitive to the composition of mineral phases.

Because photoelectric effect is only slightly affected by porosity and variations in fluid content, the PE log provides a direct indication of lithology.

Photoelectric absorption factors (P_e) for common sedimentary minerals are as follows:

Mineral	P_e
Quartz	**1.81**
Kaolinite	1.83
Montmorillonite	2.04
Dolomite	**3.14**
Illite	3.45
Halite	4.65
Anhydrite	5.05
Calcite	**5.08**
Chlorite	6.30

LITHOLOG INTERPRETATION

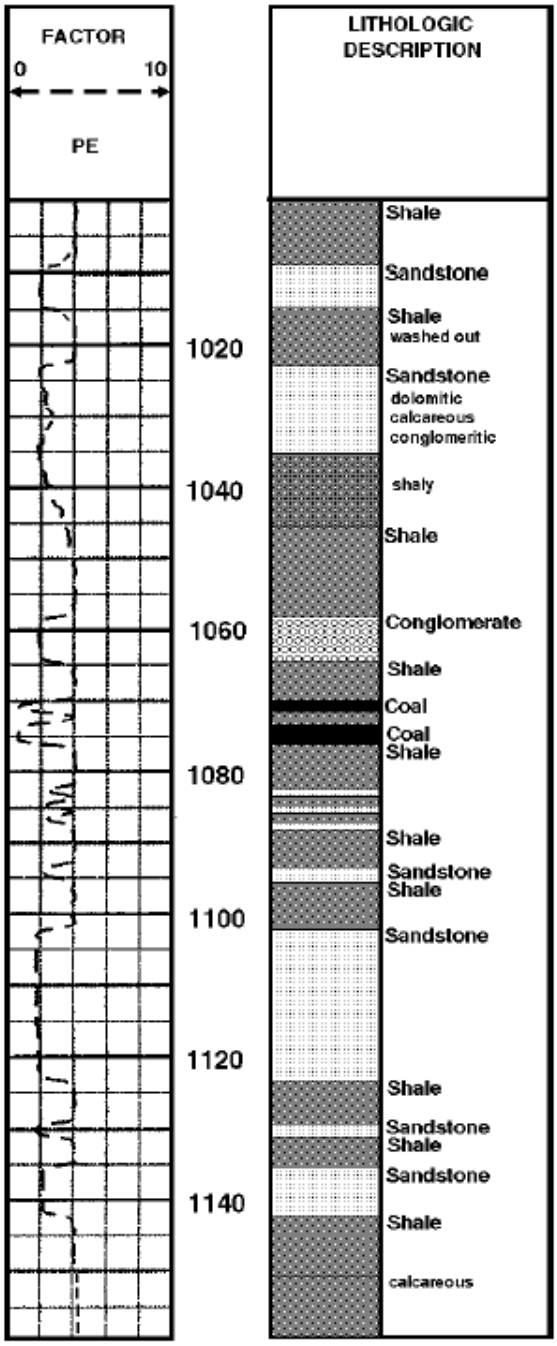

The photoelectric absorption factor is typically about 2 for sandstones and 4 for shales.

In the simple clastic section, coal shows a very low PE factor since carbon has a relatively low atomic number.

Notice the increase in the PE factor in the calcareous units where the log values are influenced by the calcite ($P_e \approx 5$) and the lower deflection for the dolomitic bed ($P_e \approx 3$).

In common with the GR log, PE is not strongly affected by bed thickness so the thin coals and sandstone units are relatively well resolved.

Small quantities of siderite, pyrite and especially barite can produced very high PE log values.

DENSITY LOG

If the grain density and the density of the mud filtrate are known, density logs give direct estimates of porosity (n). Mud filtrate has a density from 1.0 to 1.1 Mg/m^3.

$$n = (\rho_g - \rho_b) / (\rho_g - \rho_f)$$

It is usual to calculate two porosities, one using the grain density of quartz (2.65 Mg/m^3) and another using the density of calcite (2.71 Mg/m^3). Dolomite has an even higher density (2.85 Mg/m^3). Shale grain densities are in the range 2.4 to 2.6 Mg/m^3.

Assume the density log (FDC) indicates a bulk density of 2.2 Mg/m^3 with a mud filtrate density of 1.1 Mg/m^3, then for sand and lime:

$$\mathbf{n_{sand} = (2.65 - 2.2) / (2.65 - 1.1) = 0.45 / 1.55 = 0.290}$$
$$\mathbf{n_{lime} = (2.71 - 2.2) / (2.71 - 1.1) = 0.51 / 1.61 = 0.317}$$

If the formation is gas-saturated (porosity calculated from density logs give anomalously high values since ρ_f for gas is 0.1 to 0.3 Mg/m^3 and 1.0 to 1.1 was assumed.

NEUTRON LOGS

Fast neutrons are emitted by a source in the sonde and travel through the formation where they are slowed mainly by collision with hydrogen atoms. Slow neutrons are captured by atoms with the emission of a gamma ray. Various logs detect:

1. Capture gamma rays
2. Slow (thermal) neutrons
3. Partly slowed (epithermal) neutrons

The Compensated Neutron Log (CNL) tool has two detector spacings and is sensitive to slow neutrons. The Dual Porosity CNL tool has two sets of detectors for both thermal and epithermal neutrons. CNL logs can be run in liquid-filled openholes and cased-holes.

In addition, there are several single-detector, pad-type neutron tools that use epithermal detectors. These include the Sidewall Neutron Porosity (SNP).

POROSITY LOGS

Neutron logs respond to hydrogen ion content and hence to the fluids occupying porosity. Since both oil and water have roughly the same hydrogen ion content per unit volume, calibrations for oil and water saturation are very similar.

Hydrocarbon gas has a much lower hydrogen ion content per unit volume and neutron porosity logs underestimate gas filled porosity.

On the other hand, porosities derived from density logs overestimate gas filled porosity. The density and neutron porosity exhibit a diagnostic cross-over in gas-saturated formations.

Because neutron porosity logs respond to hydrogen ions, minerals containing H in the structure (e.g. gypsum, clays) can be responsible anomalously high apparent porosities.

POROSITY LOG INTERPRETATION

The porosity logs shown are calibrated for sandstone based on density (FDC) and neutron (CNL) logs. The SP log is also shown to indicate lithology.

At 1020m, the porosity is overestimated where the shale "wash out" has occurred.

Between 1040 and 1058m, the density and neutron logs show separation as shaliness increases.

At about 1105m, the two porosity logs cross-over indicating a clean gas zone in the sandstone reservoir.

At 1130m, a very low porosity is indicated in a tight sandstone layer.

Where the two porosity logs agree at 1135 to 1142m, a clean sandstone is indicated.

APPENDIX (C)

Time-Sampled listing of calibrated log data of well (35)

Time – Sampled Listing of Calibrated Log Data

Well Name: HEGLIG- 35

Key

T1 - Two-Way Travel Time (ms below SRD)
Z2 - Vertical Depth (m below KB)
Z1 - Vertical Depth (m below SRD)
INTV - Interval Velocity (m/s)
AVGV - Average Velocity (m/s)
RMSV - RMS Velocity (m/s)
RHOZ - Density (kg/m^3)
DT - Velocity (us/ft)

T1	Z2	Z1	INTV	AVGV	RMSV	DT	ZDEN
ms	mKB	mSRD	m/s	m/s	m/s	us/ft	g/cc
481.0	524.7	516.1	2114.5	2114.5	2114.5	296.7	2.08
483.0	525.7	517.1	1018.1	2110.0	2111.1	303.3	2.11
485.0	526.8	518.2	1016.8	2105.4	2107.8	283.1	2.16
487.0	527.9	519.3	1099.9	2101.3	2104.6	296.8	2.20
489.0	528.9	520.3	1073.4	2097.1	2101.4	270.1	2.34
491.0	530.0	521.4	1094.7	2093.0	2098.3	276.2	2.22
493.0	531.1	522.5	1090.5	2088.9	2095.2	277.7	2.24
495.0	532.2	523.6	1107.3	2085.0	2092.2	271.7	2.31
497.0	533.3	524.7	1073.3	2080.9	2089.0	287.9	2.16
499.0	534.4	525.8	1096.9	2077.0	2086.0	283.5	2.20
501.0	535.4	526.8	1045.4	2072.8	2082.9	289.3	2.16
503.0	536.5	527.9	1063.5	2068.8	2079.8	278.7	2.26
505.0	537.6	529.0	1076.8	2064.9	2076.8	289.1	2.18
507.0	538.6	530.0	1057.1	2060.9	2073.8	289.5	2.05
509.0	539.7	531.1	1077.5	2057.0	2070.8	288.4	2.14
511.0	540.8	532.2	1056.3	2053.1	2067.8	282.9	2.17
513.0	541.8	533.2	1082.1	2049.3	2064.8	277.9	2.17
515.0	543.0	534.4	1134.0	2045.8	2062.0	238.3	2.07
517.0	544.3	535.7	1304.0	2042.9	2059.6	227.4	2.13
519.0	545.6	537.0	1330.4	2040.2	2057.3	229.6	2.11
521.0	546.9	538.3	1333.2	2037.4	2055.0	226.9	2.10
523.0	548.3	539.7	1301.9	2034.6	2052.7	242.2	2.02
525.0	549.5	540.9	1276.4	2031.7	2050.3	239.2	2.04
527.0	550.8	542.2	1312.6	2029.0	2048.0	228.9	2.11

T1	Z2	Z1	INTV	AVGV	RMSV	DT	ZDEN
ms	mKB	mSRD	m/s	m/s	m/s	us/ft	g/cc
529.0	552.2	543.6	1314.4	2026.3	2045.7	233.3	1.97
531.0	553.5	544.9	1295.4	2023.5	2043.4	232.3	2.06
533.0	554.8	546.2	1315.4	2020.9	2041.1	228.4	2.12
535.0	556.1	547.5	1329.0	2018.3	2038.9	230.5	2.06
537.0	557.4	548.8	1346.3	2015.8	2036.8	223.9	2.11
539.0	558.9	550.3	1469.0	2013.8	2035.0	96.8	2.12
541.0	561.7	553.1	2755.0	2016.5	2038.1	112.7	1.99
543.0	564.4	555.8	2735.5	2019.2	2041.1	109.1	2.04
545.0	567.2	558.6	2801.4	2022.0	2044.4	111.5	2.07
547.0	570.0	561.4	2782.8	2024.8	2047.6	111.5	2.02
549.0	572.8	564.2	2812.1	2027.7	2050.9	110.9	2.11
551.0	575.7	567.1	2864.8	2030.7	2054.5	110.0	2.04
553.0	578.5	569.9	2846.1	2033.7	2057.9	109.1	2.10
555.0	581.3	572.7	2816.4	2036.5	2061.1	112.9	2.05
557.0	584.1	575.5	2767.7	2039.1	2064.1	107.4	2.07
559.0	586.9	578.3	2822.4	2041.9	2067.3	107.2	2.03
561.0	589.6	581.0	2729.9	2044.4	2070.0	110.0	2.12
563.0	592.5	583.9	2855.6	2047.3	2073.4	112.7	2.06
565.0	595.3	586.7	2836.6	2050.1	2076.6	110.2	2.05
567.0	598.1	589.5	2756.6	2052.6	2079.3	109.6	2.04
569.0	600.9	592.3	2759.7	2055.0	2082.1	111.7	2.03
571.0	603.7	595.1	2799.0	2057.7	2085.1	97.9	2.10
573.0	606.7	598.1	3007.5	2061.0	2089.0	103.3	2.03
575.0	609.6	601.0	2959.3	2064.1	2092.7	103.5	2.12
577.0	612.5	603.9	2910.0	2067.0	2096.0	111.6	2.03
579.0	615.3	606.7	2767.5	2069.5	2098.7	111.0	2.11
581.0	618.2	609.6	2916.9	2072.4	2102.1	105.3	2.09
583.0	621.1	612.5	2930.7	2075.3	2105.5	102.8	2.06
585.0	624.2	615.6	3045.7	2078.6	2109.4	90.5	2.08
587.0	627.3	618.7	3073.4	2082.0	2113.5	98.0	2.31
589.0	630.4	621.8	3155.3	2085.7	2117.9	93.3	2.19
591.0	633.5	624.9	3111.5	2089.1	2122.0	96.3	2.06
593.0	636.5	627.9	2976.6	2092.1	2125.5	104.8	2.29
595.0	639.6	631.0	3061.9	2095.4	2129.3	101.9	2.37
597.0	642.5	633.9	2883.5	2098.0	2132.3	108.2	2.11
599.0	645.3	636.7	2892.3	2100.7	2135.3	101.0	2.17
601.0	648.3	639.7	2958.0	2103.6	2138.6	102.3	2.12
603.0	651.3	642.7	3023.0	2106.6	2142.1	98.2	2.15
605.0	654.4	645.8	3056.9	2109.8	2145.8	95.2	2.10

T1	Z2	Z1	INTV	AVGV	RMSV	DT	ZDEN
ms	mKB	mSRD	m/s	m/s	m/s	us/ft	g/cc
607.0	657.4	648.8	2990.3	2112.7	2149.1	107.3	2.20
609.0	660.2	651.6	2802.0	2114.9	2151.6	112.7	2.15
611.0	663.1	654.5	2919.1	2117.6	2154.5	98.8	2.16
613.0	666.0	657.4	2951.1	2120.3	2157.6	107.8	2.06
615.0	669.0	660.4	3000.5	2123.1	2160.9	104.4	2.17
617.0	672.1	663.5	3069.9	2126.2	2164.5	102.2	2.10
619.0	675.2	666.6	3041.1	2129.2	2167.9	98.4	2.14
621.0	678.1	669.5	2983.7	2131.9	2171.0	108.6	1.86
623.0	681.1	672.5	2967.3	2134.6	2174.0	106.7	2.06
625.0	684.1	675.5	2961.3	2137.3	2177.0	94.4	1.54
627.0	687.2	678.6	3118.8	2140.4	2180.6	94.1	2.12
629.0	690.2	681.6	3046.0	2143.3	2183.9	95.4	2.16
631.0	693.3	684.7	3079.1	2146.2	2187.3	96.2	2.22
633.0	696.3	687.7	3038.1	2149.1	2190.6	100.8	1.61
635.0	699.3	690.7	2937.2	2151.5	2193.3	108.8	1.54
637.0	702.4	693.8	3103.7	2154.5	2196.8	102.9	1.37
639.0	705.5	696.9	3100.3	2157.5	2200.2	86.3	2.15
641.0	708.6	700.0	3144.1	2160.6	2203.7	121.8	2.15
643.0	710.9	702.3	2310.1	2161.0	2204.1	132.3	2.15
645.0	713.2	704.6	2265.7	2161.4	2204.3	136.8	2.14
647.0	715.5	706.9	2251.0	2161.6	2204.4	138.4	2.13
649.0	717.7	709.1	2236.4	2161.9	2204.5	131.2	2.12
651.0	720.0	711.4	2293.7	2162.3	2204.8	137.1	2.07
653.0	722.3	713.7	2318.8	2162.8	2205.2	126.9	2.18
655.0	724.7	716.1	2414.0	2163.5	2205.8	132.2	2.19
657.0	727.1	718.5	2345.7	2164.1	2206.3	127.4	2.19
659.0	729.5	720.9	2401.5	2164.8	2206.9	132.6	2.17
661.0	731.8	723.2	2372.0	2165.4	2207.4	122.4	2.22
663.0	734.3	725.7	2457.9	2166.3	2208.2	131.0	2.20
665.0	736.6	728.0	2300.3	2166.7	2208.5	131.1	2.19
667.0	738.9	730.3	2304.2	2167.1	2208.8	133.0	2.04
669.0	741.2	732.6	2342.0	2167.6	2209.2	126.8	2.22
671.0	743.6	735.0	2328.6	2168.1	2209.6	133.9	2.11
673.0	745.9	737.3	2274.9	2168.4	2209.8	133.4	2.15
675.0	748.1	739.5	2291.8	2168.8	2210.0	134.7	1.98
677.0	750.5	741.9	2309.5	2169.2	2210.3	129.5	2.17
679.0	752.8	744.2	2352.2	2169.8	2210.7	129.4	2.18
681.0	755.2	746.6	2379.0	2170.4	2211.2	128.1	2.18
683.0	757.6	749.0	2390.2	2171.0	2211.8	131.0	2.15

T1	Z2	Z1	INTV	AVGV	RMSV	DT	ZDEN
ms	mKB	mSRD	m/s	m/s	m/s	us/ft	g/cc
685.0	759.9	751.3	2289.3	2171.4	2212.0	123.8	2.15
687.0	762.4	753.8	2525.2	2172.4	2213.0	115.5	2.21
689.0	765.0	756.4	2624.1	2173.7	2214.3	114.9	2.17
691.0	767.5	758.9	2520.0	2174.7	2215.3	123.1	2.13
693.0	770.0	761.4	2449.2	2175.5	2216.0	121.4	2.17
695.0	772.5	763.9	2519.9	2176.5	2216.9	121.3	2.13
697.0	775.0	766.4	2462.9	2177.3	2217.6	124.7	2.11
699.0	777.4	768.8	2433.2	2178.1	2218.3	127.1	2.09
701.0	779.9	771.3	2479.2	2178.9	2219.1	121.3	2.35
703.0	782.5	773.9	2611.3	2180.1	2220.3	86.3	2.99
705.0	785.3	776.7	2818.9	2182.0	2222.2	103.9	2.12
707.0	788.4	779.8	3044.6	2184.4	2225.0	97.0	2.23
709.0	791.3	782.7	2993.5	2186.7	2227.5	104.6	2.07
711.0	794.3	785.7	2993.6	2189.0	2230.0	103.8	2.02
713.0	797.3	788.7	2997.1	2191.2	2232.6	99.8	2.03
715.0	800.5	791.9	3175.9	2194.0	2235.8	101.3	2.14
717.0	803.8	795.2	3265.9	2197.0	2239.3	91.7	2.36
719.0	807.1	798.5	3280.4	2200.0	2242.9	100.4	2.26
721.0	809.8	801.2	2781.2	2201.6	2244.5	135.6	2.05
723.0	812.2	803.6	2378.6	2202.1	2244.9	126.5	2.10
725.0	814.7	806.1	2445.7	2202.8	2245.5	136.9	1.95
727.0	817.0	808.4	2377.7	2203.2	2245.9	124.7	2.11
729.0	819.6	811.0	2542.6	2204.2	2246.7	130.8	2.05
731.0	822.1	813.5	2521.3	2205.0	2247.5	123.6	2.10
733.0	824.7	816.1	2575.5	2206.1	2248.5	119.0	2.18
735.0	827.1	818.5	2443.1	2206.7	2249.1	122.4	2.23
737.0	829.6	821.0	2457.7	2207.4	2249.6	119.4	2.34
739.0	832.1	823.5	2484.4	2208.1	2250.3	144.6	2.26
741.0	834.6	826.0	2487.8	2208.9	2251.0	111.0	2.29
743.0	837.2	828.6	2693.9	2210.2	2252.3	116.7	2.08
745.0	840.1	831.5	2811.1	2211.8	2254.0	108.2	2.32
747.0	842.8	834.2	2745.7	2213.2	2255.4	117.5	2.33
749.0	845.4	836.8	2554.6	2214.2	2256.3	127.5	2.04
751.0	847.8	839.2	2423.7	2214.7	2256.8	123.0	2.01
753.0	850.3	841.7	2467.2	2215.4	2257.3	120.4	2.04
755.0	852.7	844.1	2458.8	2216.0	2257.9	118.4	2.05
757.0	855.2	846.6	2462.5	2216.7	2258.5	124.7	2.01
759.0	857.6	849.0	2433.1	2217.2	2258.9	126.7	2.12
761.0	859.6	851.0	1968.4	2216.6	2258.2	184.8	2.04

T1	Z2	Z1	INTV	AVGV	RMSV	DT	ZDEN
ms	mKB	mSRD	m/s	m/s	m/s	us/ft	g/cc
763.0	861.2	852.6	1660.0	2215.1	2256.9	178.8	2.01
765.0	862.9	854.3	1690.5	2213.8	2255.6	178.3	2.05
767.0	864.7	856.1	1729.7	2212.5	2254.4	181.1	2.21
769.0	866.9	858.3	2218.1	2212.5	2254.3	130.2	2.17
771.0	869.1	860.5	2267.2	2212.7	2254.3	131.0	2.24
773.0	871.4	862.8	2293.9	2212.9	2254.4	142.0	2.18
775.0	873.7	865.1	2301.4	2213.1	2254.5	134.9	2.20
777.0	876.0	867.4	2252.1	2213.2	2254.5	148.6	2.14
779.0	878.2	869.6	2221.9	2213.2	2254.4	141.4	2.17
781.0	880.5	871.9	2244.2	2213.3	2254.4	123.5	2.22
783.0	882.9	874.3	2424.4	2213.8	2254.9	122.6	2.18
785.0	885.3	876.7	2439.1	2214.4	2255.4	124.7	2.10
787.0	887.7	879.1	2427.8	2215.0	2255.8	127.4	2.15
789.0	890.2	881.6	2428.5	2215.5	2256.3	127.0	1.95
791.0	892.7	884.1	2563.3	2216.4	2257.1	120.4	2.05
793.0	895.2	886.6	2422.1	2216.9	2257.5	130.3	2.03
795.0	897.4	888.8	2239.3	2216.9	2257.5	132.6	2.19
797.0	899.8	891.2	2372.8	2217.3	2257.8	131.9	2.14
799.0	902.1	893.5	2365.9	2217.7	2258.1	124.3	2.16
801.0	904.6	896.0	2438.5	2218.3	2258.5	117.8	2.12
803.0	907.0	898.4	2467.9	2218.9	2259.1	121.5	2.17
805.0	909.8	901.2	2747.3	2220.2	2260.4	106.5	2.23
807.0	912.7	904.1	2891.5	2221.9	2262.2	113.4	2.15
809.0	915.4	906.8	2692.6	2223.0	2263.4	115.6	2.10
811.0	918.0	909.4	2586.3	2223.9	2264.2	132.9	2.10
813.0	920.2	911.6	2195.7	2223.9	2264.0	135.5	2.14
815.0	922.6	914.0	2486.2	2224.5	2264.6	125.9	2.09
817.0	925.0	916.4	2394.8	2224.9	2264.9	124.6	2.20
819.0	927.5	918.9	2494.3	2225.6	2265.5	119.8	2.19
821.0	930.3	921.7	2744.9	2226.8	2266.8	123.9	2.17
823.0	932.9	924.3	2619.5	2227.8	2267.8	112.2	2.20
825.0	935.3	926.7	2423.1	2228.3	2268.1	128.9	2.06
827.0	937.6	929.0	2275.9	2228.4	2268.2	135.7	2.01
829.0	939.7	931.1	2140.6	2228.2	2267.9	156.5	2.11
831.0	941.8	933.2	2050.8	2227.7	2267.4	142.7	2.18
833.0	944.1	935.5	2295.2	2227.9	2267.4	119.2	2.16
835.0	946.5	937.9	2405.4	2228.3	2267.8	126.8	2.10
837.0	949.1	940.5	2569.6	2229.1	2268.5	126.8	2.12
839.0	951.4	942.8	2354.2	2229.4	2268.7	132.5	2.09

T1	Z2	Z1	INTV	AVGV	RMSV	DT	ZDEN
ms	mKB	mSRD	m/s	m/s	m/s	us/ft	g/cc
841.0	953.8	945.2	2431.1	2229.9	2269.1	122.4	2.21
843.0	956.2	947.6	2391.5	2230.3	2269.4	132.8	2.08
845.0	958.6	950.0	2330.8	2230.5	2269.6	131.5	2.04
847.0	961.1	952.5	2538.6	2231.3	2270.3	114.8	2.17
849.0	963.7	955.1	2610.9	2232.2	2271.1	116.3	2.16
851.0	966.3	957.7	2556.9	2232.9	2271.8	117.3	2.13
853.0	968.9	960.3	2589.6	2233.8	2272.6	110.4	2.12
855.0	971.5	962.9	2661.0	2234.8	2273.6	119.2	2.09
857.0	974.0	965.4	2481.9	2235.3	2274.1	124.5	2.03
859.0	976.5	967.9	2529.4	2236.0	2274.8	122.9	2.08
861.0	979.1	970.5	2584.0	2236.8	2275.5	113.7	2.08
863.0	981.7	973.1	2632.6	2237.8	2276.4	120.4	2.09
865.0	984.3	975.7	2570.8	2238.5	2277.1	112.9	2.20
867.0	986.9	978.3	2598.2	2239.4	2277.9	117.6	2.12
869.0	989.8	981.2	2856.6	2240.8	2279.4	111.6	2.17
871.0	992.4	983.8	2668.4	2241.8	2280.4	108.8	2.22
873.0	995.6	987.0	3192.5	2243.9	2282.9	123.7	2.11
875.0	998.1	989.5	2492.0	2244.5	2283.4	118.6	2.13
877.0	1000.6	992.0	2516.8	2245.1	2284.0	120.3	2.21
879.0	1003.1	994.5	2484.4	2245.7	2284.5	123.1	2.14
881.0	1005.6	997.0	2455.4	2246.2	2284.9	137.3	2.16
883.0	1007.9	999.3	2288.7	2246.2	2284.9	137.4	2.21
885.0	1010.3	1001.7	2392.5	2246.6	2285.1	125.1	2.15
887.0	1012.7	1004.1	2436.2	2247.0	2285.5	127.2	2.19
889.0	1015.3	1006.7	2581.3	2247.8	2286.2	123.2	2.09
891.0	1017.8	1009.2	2535.0	2248.4	2286.8	122.0	2.09
893.0	1020.4	1011.8	2591.4	2249.2	2287.5	104.5	2.38
895.0	1022.9	1014.3	2534.8	2249.8	2288.1	126.3	2.17
897.0	1025.5	1016.9	2563.4	2250.5	2288.7	120.3	2.16
899.0	1028.0	1019.4	2501.8	2251.1	2289.2	125.0	2.10
901.0	1030.5	1021.9	2499.0	2251.6	2289.7	122.1	2.13
903.0	1033.1	1024.5	2592.6	2252.4	2290.4	114.3	2.25
905.0	1035.8	1027.2	2720.9	2253.4	2291.5	112.4	2.17
907.0	1038.5	1029.9	2651.2	2254.3	2292.3	113.0	2.14
909.0	1041.2	1032.6	2684.5	2255.2	2293.3	114.7	2.12
911.0	1043.8	1035.2	2687.0	2256.2	2294.2	117.2	2.15
913.0	1046.5	1037.9	2667.3	2257.1	2295.1	115.3	2.18
915.0	1049.0	1040.4	2521.8	2257.7	2295.6	119.0	2.15
917.0	1051.7	1043.1	2636.0	2258.5	2296.4	111.6	2.12

T1	Z2	Z1	INTV	AVGV	RMSV	DT	ZDEN
ms	mKB	mSRD	m/s	m/s	m/s	us/ft	g/cc
919.0	1054.3	1045.7	2618.5	2259.3	2297.2	119.8	2.14
921.0	1056.7	1048.1	2398.2	2259.6	2297.4	126.1	2.24
923.0	1059.4	1050.8	2693.2	2260.5	2298.3	100.7	2.27
925.0	1062.3	1053.7	2902.5	2261.9	2299.8	110.6	2.30
927.0	1065.5	1056.9	3185.6	2263.9	2302.1	91.6	2.27
929.0	1068.7	1060.1	3265.5	2266.1	2304.6	95.5	2.26
931.0	1072.0	1063.4	3233.3	2268.1	2307.0	95.6	2.26
933.0	1075.1	1066.5	3172.8	2270.1	2309.2	95.2	2.28
935.0	1078.3	1069.7	3202.9	2272.1	2311.5	90.7	2.27
937.0	1081.7	1073.1	3354.8	2274.4	2314.2	80.3	2.20
939.0	1084.7	1076.1	2963.0	2275.8	2315.8	154.1	2.22
941.0	1086.7	1078.1	1998.6	2275.3	2315.1	150.6	2.26
943.0	1088.6	1080.0	1981.7	2274.6	2314.5	164.9	2.28
945.0	1090.6	1082.0	1915.2	2273.9	2313.7	155.9	2.28
947.0	1092.5	1083.9	1938.2	2273.2	2313.0	174.4	2.32
949.0	1094.2	1085.6	1720.5	2272.0	2311.9	155.8	2.25
951.0	1096.2	1087.6	1996.2	2271.4	2311.3	176.6	2.21
953.0	1098.1	1089.5	1905.1	2270.7	2310.5	154.9	2.17
955.0	1100.1	1091.5	1979.0	2270.0	2309.8	154.6	2.24
957.0	1102.1	1093.5	1963.2	2269.4	2309.2	155.4	2.23
959.0	1103.9	1095.3	1852.2	2268.5	2308.3	163.3	2.12
961.0	1105.8	1097.2	1940.4	2267.8	2307.6	157.3	2.22
963.0	1107.8	1099.2	1958.8	2267.2	2306.9	157.6	2.23
965.0	1110.4	1101.8	2592.7	2267.9	2307.6	95.9	2.15
967.0	1113.5	1104.9	3058.4	2269.5	2309.4	100.9	2.15
969.0	1116.4	1107.8	2892.4	2270.8	2310.7	118.5	2.17
971.0	1119.2	1110.6	2849.2	2272.0	2312.0	107.9	2.25
973.0	1121.9	1113.3	2727.5	2272.9	2312.9	103.2	2.11
975.0	1124.9	1116.3	2949.1	2274.3	2314.4	104.8	2.22
977.0	1127.9	1119.3	3034.0	2275.9	2316.1	102.6	2.17
979.0	1131.0	1122.4	3090.2	2277.5	2317.9	98.5	2.13
981.0	1134.1	1125.5	3140.9	2279.3	2319.9	104.5	2.16
983.0	1137.0	1128.4	2905.4	2280.6	2321.2	102.6	2.17
985.0	1139.9	1131.3	2847.6	2281.7	2322.4	107.4	2.16
987.0	1142.5	1133.9	2650.1	2282.5	2323.1	128.0	2.17
989.0	1145.2	1136.6	2663.5	2283.2	2323.9	94.9	2.35
991.0	1148.1	1139.5	2886.9	2284.5	2325.2	106.3	2.14
993.0	1150.7	1142.1	2643.6	2285.2	2325.8	106.3	2.22
995.0	1153.6	1145.0	2837.4	2286.3	2327.0	105.4	2.18

T1	Z2	Z1	INTV	AVGV	RMSV	DT	ZDEN
ms	mKB	mSRD	m/s	m/s	m/s	us/ft	g/cc
1075.0	1261.1	1252.5	2083.0	2316.2	2356.6	145.1	2.25
1077.0	1263.4	1254.8	2252.1	2316.1	2356.4	134.7	2.19
1079.0	1265.6	1257.0	2258.1	2316.0	2356.2	131.5	2.29
1081.0	1268.0	1259.4	2380.3	2316.1	2356.3	135.4	2.22
1083.0	1270.3	1261.7	2292.7	2316.1	2356.2	129.6	2.29
1085.0	1272.6	1264.0	2339.1	2316.1	2356.1	135.0	2.29
1087.0	1275.0	1266.4	2350.0	2316.2	2356.1	126.3	2.26
1089.0	1277.4	1268.8	2375.2	2316.3	2356.1	129.0	2.28
1091.0	1279.8	1271.2	2408.6	2316.5	2356.2	123.0	2.26
1093.0	1282.0	1273.4	2240.5	2316.3	2356.0	121.2	2.37
1095.0	1284.6	1276.0	2640.8	2316.9	2356.6	114.1	2.33
1097.0	1287.3	1278.7	2665.7	2317.5	2357.2	109.1	2.30
1099.0	1290.0	1281.4	2717.1	2318.3	2357.9	114.5	2.34
1101.0	1292.6	1284.0	2608.8	2318.8	2358.4	116.5	2.35
1103.0	1295.3	1286.7	2696.3	2319.5	2359.0	126.3	2.30
1105.0	1298.0	1289.4	2699.1	2320.2	2359.7	105.0	2.17
1107.0	1300.8	1292.2	2799.2	2321.0	2360.6	111.6	2.20
1109.0	1303.5	1294.9	2641.5	2321.6	2361.1	120.6	2.26
1111.0	1306.0	1297.4	2554.0	2322.0	2361.5	104.8	2.18
1113.0	1308.8	1300.2	2805.9	2322.9	2362.3	103.1	2.21
1115.0	1311.8	1303.2	2973.4	2324.1	2363.6	102.0	2.20
1117.0	1314.7	1306.1	2885.8	2325.1	2364.6	108.5	2.27
1119.0	1317.5	1308.9	2842.4	2326.0	2365.6	106.4	2.34
1121.0	1320.0	1311.4	2477.7	2326.3	2365.8	140.7	2.23
1123.0	1322.4	1313.8	2338.0	2326.3	2365.7	126.3	2.27
1125.0	1324.7	1316.1	2349.4	2326.3	2365.7	116.5	2.35
1127.0	1327.4	1318.8	2670.2	2327.0	2366.3	116.5	2.37
1129.0	1329.9	1321.3	2571.7	2327.4	2366.6	119.2	2.33
1131.0	1332.6	1324.0	2631.6	2327.9	2367.1	113.6	2.28
1133.0	1335.4	1326.8	2804.1	2328.8	2368.0	97.8	2.25
1135.0	1338.3	1329.7	2889.0	2329.8	2369.0	105.4	2.17
1137.0	1341.1	1332.5	2819.9	2330.6	2369.9	107.8	2.39
1139.0	1344.0	1335.4	2865.7	2331.6	2370.8	106.0	2.20
1141.0	1346.8	1338.2	2892.5	2332.5	2371.8	103.8	2.16
1143.0	1349.8	1341.2	2952.3	2333.6	2373.0	106.2	2.19
1145.0	1352.7	1344.1	2941.7	2334.7	2374.1	98.6	2.25
1147.0	1355.7	1347.1	2957.2	2335.8	2375.2	108.2	2.14
1149.0	1358.5	1349.9	2840.7	2336.6	2376.1	103.4	2.23
1151.0	1361.5	1352.9	2988.7	2337.8	2377.3	102.6	2.11

T1	Z2	Z1	INTV	AVGV	RMSV	DT	ZDEN
ms	mKB	mSRD	m/s	m/s	m/s	us/ft	g/cc
1231.0	1465.8	1457.2	2776.0	2355.3	2394.1	104.4	2.39
1233.0	1468.7	1460.1	2877.2	2356.1	2395.0	110.8	2.37
1235.0	1471.4	1462.8	2747.0	2356.8	2395.6	112.1	2.38
1237.0	1474.1	1465.5	2707.4	2357.3	2396.1	127.5	2.27
1239.0	1476.8	1468.2	2643.2	2357.8	2396.6	105.5	2.35
1241.0	1479.6	1471.0	2806.1	2358.5	2397.3	110.2	2.35
1243.0	1482.3	1473.7	2652.4	2359.0	2397.7	119.8	2.28
1245.0	1484.7	1476.1	2434.9	2359.1	2397.8	125.3	2.31
1247.0	1487.2	1478.6	2479.5	2359.3	2397.9	123.3	2.33
1249.0	1489.6	1481.0	2445.0	2359.5	2398.0	120.7	2.29
1251.0	1491.8	1483.2	2213.8	2359.2	2397.7	133.3	2.18
1253.0	1494.2	1485.6	2415.1	2359.3	2397.7	113.9	2.31
1255.0	1496.9	1488.3	2618.8	2359.7	2398.1	108.2	2.35
1257.0	1499.8	1491.2	2974.5	2360.7	2399.1	99.0	2.36
1259.0	1502.8	1494.2	3003.6	2361.7	2400.2	107.1	2.32
1261.0	1505.3	1496.7	2501.4	2361.9	2400.4	136.4	2.19
1263.0	1507.7	1499.1	2360.9	2361.9	2400.3	133.2	2.19
1265.0	1510.0	1501.4	2306.7	2361.9	2400.2	135.3	2.22
1267.0	1512.2	1503.6	2234.7	2361.7	2399.9	135.9	2.23
1269.0	1514.5	1505.9	2284.8	2361.5	2399.7	129.6	2.25
1271.0	1516.8	1508.2	2283.2	2361.4	2399.5	135.1	2.21
1273.0	1519.0	1510.4	2227.6	2361.2	2399.3	137.9	2.15
1275.0	1521.2	1512.6	2171.5	2360.9	2398.9	143.9	2.18
1277.0	1523.4	1514.8	2190.6	2360.6	2398.6	139.1	2.19
1279.0	1525.9	1517.3	2452.3	2360.8	2398.7	122.2	2.28
1281.0	1528.5	1519.9	2690.2	2361.3	2399.2	97.8	2.40
1283.0	1531.1	1522.5	2601.7	2361.7	2399.5	132.3	2.19
1285.0	1533.6	1525.0	2436.3	2361.8	2399.6	127.0	2.18
1287.0	1536.0	1527.4	2395.2	2361.8	2399.6	130.8	2.20
1289.0	1538.3	1529.7	2335.2	2361.8	2399.5	126.2	2.24
1291.0	1540.7	1532.1	2350.6	2361.8	2399.4	130.5	2.21
1293.0	1543.0	1534.4	2340.0	2361.7	2399.3	131.5	2.22
1295.0	1545.3	1536.7	2340.7	2361.7	2399.2	131.3	2.25
1297.0	1547.8	1539.2	2416.7	2361.8	2399.3	133.2	2.22
1299.0	1549.9	1541.3	2142.6	2361.5	2398.9	141.8	2.14
1301.0	1552.1	1543.5	2165.3	2361.2	2398.5	144.4	2.15
1303.0	1554.3	1545.7	2192.5	2360.9	2398.2	143.1	2.16
1305.0	1556.5	1547.9	2211.7	2360.7	2398.0	137.1	2.21
1307.0	1558.8	1550.2	2320.7	2360.6	2397.8	138.3	2.17

T1	Z2	Z1	INTV	AVGV	RMSV	DT	ZDEN
ms	mKB	mSRD	m/s	m/s	m/s	us/ft	g/cc
1309.0	1561.1	1552.5	2297.6	2360.5	2397.7	133.2	2.18
1311.0	1563.4	1554.8	2324.7	2360.5	2397.6	127.6	2.21
1313.0	1565.8	1557.2	2428.5	2360.6	2397.6	129.1	2.16
1315.0	1568.2	1559.6	2382.1	2360.6	2397.6	126.4	2.23
1317.0	1570.7	1562.1	2496.7	2360.8	2397.8	122.0	2.24
1319.0	1573.2	1564.6	2488.1	2361.0	2397.9	130.5	2.21
1321.0	1575.5	1566.9	2328.5	2360.9	2397.8	134.2	2.20
1323.0	1577.9	1569.3	2375.3	2361.0	2397.8	128.2	2.19
1325.0	1580.4	1571.8	2463.2	2361.1	2397.9	109.0	2.36
1327.0	1583.1	1574.5	2686.3	2361.6	2398.3	110.6	2.34
1329.0	1585.4	1576.8	2313.5	2361.5	2398.2	135.6	2.36
1331.0	1587.5	1578.9	2119.4	2361.2	2397.8	150.8	2.25
1333.0	1589.4	1580.8	1948.8	2360.6	2397.2	149.5	2.31
1335.0	1591.5	1582.9	2081.0	2360.1	2396.8	145.6	2.27
1337.0	1593.6	1585.0	2073.4	2359.7	2396.3	140.1	2.30
1339.0	1595.8	1587.2	2233.7	2359.5	2396.1	131.9	2.36
1341.0	1598.2	1589.6	2359.3	2359.5	2396.0	120.5	2.39
1343.0	1600.8	1592.2	2575.6	2359.8	2396.3	111.6	2.41
1345.0	1603.4	1594.8	2625.3	2360.2	2396.6	127.7	2.40
1347.0	1605.9	1597.3	2463.2	2360.4	2396.7	139.2	2.37
1349.0	1608.4	1599.8	2504.8	2360.6	2396.9	131.3	2.41
1351.0	1612.3	1603.7	3940.7	2362.9	2399.9	77.7	2.42
1353.0	1615.7	1607.1	3426.8	2364.5	2401.8	85.0	2.39
1355.0	1619.6	1611.0	3878.2	2366.8	2404.6	71.0	2.46
1357.0	1624.2	1615.6	4597.8	2370.0	2409.3	85.8	2.35
1359.0	1627.7	1619.1	3522.0	2371.7	2411.3	75.8	2.47
1361.0	1631.9	1623.3	4209.4	2374.4	2415.0	48.2	2.56
1363.0	1634.4	1625.8	2510.8	2374.6	2415.1	270.0	2.57
1365.0	1635.6	1627.0	1117.5	2372.8	2413.7	273.2	2.54
1367.0	1636.7	1628.1	1121.2	2371.0	2412.3	272.0	2.56
1369.0	1637.8	1629.2	1125.2	2369.1	2411.0	270.6	2.57
1371.0	1638.9	1630.3	1123.3	2367.3	2409.6	268.3	2.54
1373.0	1641.3	1632.7	2330.0	2367.3	2409.5	121.3	2.36
1375.0	1643.8	1635.2	2545.6	2367.5	2409.7	122.3	2.28
1377.0	1646.3	1637.7	2503.3	2367.7	2409.8	122.8	2.25
1379.0	1648.8	1640.2	2494.4	2367.9	2409.9	122.6	2.25
1381.0	1651.4	1642.8	2549.8	2368.2	2410.1	119.5	2.20
1383.0	1653.9	1645.3	2570.1	2368.5	2410.4	116.5	2.24
1385.0	1656.5	1647.9	2580.4	2368.8	2410.6	119.7	2.29

T1	Z2	Z1	INTV	AVGV	RMSV	DT	ZDEN
ms	mKB	mSRD	m/s	m/s	m/s	us/ft	g/cc
1387.0	1659.2	1650.6	2679.1	2369.2	2411.0	90.6	2.34
1389.0	1662.3	1653.7	3099.2	2370.3	2412.2	106.3	2.16
1391.0	1665.5	1656.9	3166.9	2371.4	2413.4	101.1	2.25
1393.0	1668.7	1660.1	3212.3	2372.6	2414.8	89.0	2.30
1395.0	1671.8	1663.2	3166.7	2373.8	2416.0	94.4	2.22
1397.0	1675.0	1666.4	3192.8	2374.9	2417.3	89.6	2.29
1399.0	1678.2	1669.6	3220.7	2376.1	2418.6	98.0	2.19
1401.0	1681.4	1672.8	3125.0	2377.2	2419.8	99.2	2.60
1403.0	1684.8	1676.2	3389.5	2378.7	2421.5	75.9	2.59
1405.0	1688.7	1680.1	3980.6	2380.9	2424.4	73.7	2.35
1407.0	1692.8	1684.2	4024.2	2383.3	2427.4	82.8	2.29
1409.0	1696.3	1687.7	3584.2	2385.0	2429.4	89.4	2.19
1411.0	1700.1	1691.5	3752.9	2386.9	2431.8	74.5	2.54
1413.0	1703.7	1695.1	3557.9	2388.6	2433.8	88.6	2.23
1415.0	1707.5	1698.9	3821.5	2390.6	2436.3	78.4	2.60
1417.0	1711.5	1702.9	4019.1	2392.9	2439.3	83.3	2.38
1419.0	1715.0	1706.4	3469.2	2394.4	2441.0	92.1	2.24
1421.0	1718.5	1709.9	3524.7	2396.0	2442.9	82.7	2.35
1423.0	1722.1	1713.5	3562.7	2397.7	2444.8	84.4	2.33
1425.0	1725.2	1716.6	3165.9	2398.7	2446.0	101.3	2.49
1427.0	1728.2	1719.6	2973.4	2399.5	2446.8	106.4	2.48
1429.0	1730.9	1722.3	2684.7	2399.9	2447.2	109.5	2.41
1431.0	1733.8	1725.2	2884.1	2400.6	2447.8	109.7	2.43
1433.0	1737.4	1728.8	3668.8	2402.4	2450.0	88.1	2.25
1435.0	1740.7	1732.1	3296.1	2403.6	2451.3	90.1	2.30
1437.0	1744.0	1735.4	3304.6	2404.9	2452.7	92.9	2.35
1439.0	1747.5	1738.9	3486.3	2406.4	2454.5	88.8	2.23
1441.0	1751.0	1742.4	3490.5	2407.9	2456.2	87.7	2.28
1443.0	1754.4	1745.8	3422.1	2409.3	2457.8	93.1	2.18
1445.0	1757.8	1749.2	3414.8	2410.7	2459.4	91.0	2.24
1447.0	1761.3	1752.7	3479.9	2412.2	2461.1	109.4	2.45
1449.0	1764.8	1756.2	3506.4	2413.7	2462.8	67.4	2.56
1451.0	1768.5	1759.9	3672.5	2415.4	2464.9	86.2	2.32
1453.0	1768.6	1760.0	91.7	2412.2	2463.2	-999.3	-999.25